Individual identification within commingled remains using CT and DEXA scans

Martijn Bastiaans
s1622552@vuw.leidenuniv.nl
06-81848038

Individual identification within commingled remains using CT and DEXA scans

Figure: CT-scan of the left femur of MB11S051V0059

Martijn Bastiaans
s1622552
Archaeology
University Leiden, Master of Science, Human Osteoarchaeology
Dr. S.A. Schrader and Dr. E.M. Winter
Leiden, 19-7-2021, final version

Table of Content

Abstract

CT-scanning has been applied much more to archaeological materials over the past few years and DEXA-scans have also made an introduction in the field of archaeology. This thesis tried to use these two types of scans to find a way to reassociate commingled remains from archaeological contexts. For this the CT-scans and DEXA-scans of a small portion of the Middenbeemster collection were used. Bone mineral density, which was measured using the DEXA-scans, and cortical indices, which were measured using the CT-scans, were calculated for the humeri and femora of these individuals. Regression models were made to see if there was a usable relation between the BMDs or cortical indices of different bones and to find a way to match the values of different bones to each other. Most of the regression models indicated that there were indeed usable relations between the different bones for most of their combinations. The values of each bone were recalculated to match the other types of bones, so that neighbourhood analyses could be performed to try and reassociate these bones. The neighbourhood analysis looks for the distance to the closest neighbour for each of the bones. This was compared to the distance between the bones of the individuals to see how much percent of the time the closest bone was indeed the bone of the same individual. These neighbourhood analyses were performed on different groups sizes for each of the combinations of bones. The groups of five, which are the smallest groups, gave the most results above the 33,33% marker that was used in this thesis. (This marker was used to indicate if the amount of accurately reassociated bones was high enough for the neighbourhood analysis to be applicable to commingles remains.) The left to right femur combinations also scored above this marker for their groups of ten.

After these neighbourhood analyses were preformed, the two variables were rescaled to the same scale and combined to see if their combinations would result in more accurate reassociations. The neighbourhood analyses performed on the groups of five with both combinations all scored above the 33,33% marker, with the femur-to-femur combinations scored a percentage of accuracy of 76%. More combinations of bone also scored above the marker for their groups of ten and the femur-to-femur combinations even scored above the 33.33% accuracy for their groups of fifteen.

Whilst some combinations of bones scored promising levels of accuracy, the applicability

of the BMDs and cortical indices to commingled remains is still limited. The group size of individuals needs to be small, not all bones can be measured, both types of measurement are not always available, and the results are highly dependent on the individuals that are present. Future research is, thus, still needed, but the bone mineral density and cortical index could, in some situations, be used to reassemble the bones of commingled remains.

Acknowledgements

This thesis was made possible by the scans that were performed at the LUMC (Leids universitair medisch centrum). My gratitude goes out to P. Dibbets-Schnieder, L.J. van Schaik, T. Boxmeer and the volunteers from the LUMC that helped with performing these scans. I also would like to thank S.A. Schrader and E.M. Winter for supervising this thesis.

1. Introduction

Commingled remains are often found in archaeological contexts. They can originate from cultural practices, like the long-term burial chambers from the Bronze Age (Osterholtz et al. 2013a, 35). They can originate from natural disasters, like the mass graves resulting from the Black Death (Lütgert 2000, 255). Lastly, they can be the result of natural processes, like the burrowing of animals, that mix different graves (De Groote et al. 2020, 144). The analysis of the populations associated with these remains is made more difficult by the commingling. It is difficult to estimate how many people are buried in commingled graves. There are, therefore, some techniques developed to make estimations of the number of individuals that are buried, but they mainly calculate the minimum number or the most likely number. These techniques also do not or barely help with associating the bones of individuals with each other (Adams and Konigsberg 2004, 141; Lyman 1994, 289).

There are techniques that can be used to identify individuals from forensic contexts. These techniques often use pre-existing radiographic images, like dental records or CT-scans. Once a person dies in a modern-day mass disaster, like a plane crash, then the individual may be identified by comparing the pre-existing images with images made postmortem. CT-scanning can also help with identifying individuals via traits, such as sex and disease. This was, for example, used to identify the people that died in the fires that devastated the state of Victoria in Australia. CT-scanning helped with the identification of 161 of the 163 missing people (O'Donnell et al. 2011, 15). The scans were primarily used to identify diseases, teeth, age, sex, and possible personal items that were on the remains. When teeth were identified, they were compared to the records of dentists to find similarities in cavities, wear, missing teeth, and other dental traits. The age, sex and disease traits that could be identified using CT-scans were more used to help with the profile than to actually identify the victims (O'Donnell et al. 2011, 15-16).

The application of radiographic imaging to commingled remains in archaeological contexts is extremely limited, since there is hardly ever a record of the pathology of those individuals nor are there pre-existing images to compare to. The application of radiographic imaging to archaeological commingled remains has, therefore, been limited to identifying pathological conditions amongst these remains, or identifying age related

traits of skeletal elements. This thesis will look at the possibility of applying radiographic imaging to archaeologic commingled remains in order to reassociate bones of individuals within those remains.
Commingled remains are primarily only sorted by looking at sex, age, and size. The sorting of the commingled remains is a way of making analysis of these individuals more approachable, but the ideal is to identify individuals within a commingled assemblage. There is much more that can be said when studying remains of singular individuals, like activity, but it also helps with putting certainty behind sex and age and it helps with identifying certain pathological elements. In addition, being able to reassociate the bones of a singular individual creates the possibility of ethically re uniting the body of those people. These CT and DEXA-scans will, therefore, hopefully, help with finding a way to identify individuals within commingled assemblages.

1.1 Research questions

This thesis will look at the possible application of two types of scans for the identification of commingled remains in an archaeological context. The type of scans used are computerized tomography or CT-scanning and dual energy X-ray absorptiometry or DEXA/DXA-scanning. CT-scanning is a technique primarily used in the medical field that allows the inside of a body to be studied without damaging it. CT-scanning uses multiple X-ray measurements taken at different angles to create images of the body. DEXA-scanning is a technique that is also primarily used in the medical field. It uses two different X-ray energies to measure the mineral density of bone.
Both of these types of scans will be used to look at the bone mineral density (BMD) of skeletal remains from the Middenbeemster collection. The Middenbeemster skeleton collection or MB11 is currently housed at the osteology department of the faculty of archaeology of Leiden University. A part of this collection will be scanned using both a CT-scanner and a DEXA-scanner at the Leids Universitair Medisch Centrum (LUMC). This creates the possibility of looking at CT-scans and the bone mineral density (BMD) of these skeletons and the possibility of reassociating individuals based on those scans.
The main research question will be:

- Can CT and/or DEXA-scans be used to identify individuals from archaeological commingled remains?

The following questions will be used to answer the main research question:

- Can a consistency in bone mineral density between sides of a skeleton be found using DEXA-scanning?
- Is there a relation in bone mineral density between different bones of an individual?
- Is there a consistency between sides of a skeleton and cortical bone loss, that can be found using CT-scanning?
- Is there a relation in cortical bone loss between different bones of an individual?
- Can bone mineral density and/or cortical bone loss be used to sort out individuals from commingled remains?

The goal of this thesis is to find a relation between the BMD of bones of a single individual that differs enough from other skeletal remains. This relation could, ideally, be a way to sort individuals from commingled remains based on their BMD, but it is also possible that BMD could be used to differentiate groups within a commingled assemblage. Therefore, depending on whether there are positive results from this research, the relation between BMD of bones within a skeleton will lead to a technique that can be used to identify which bones from a mixed assemblage belong to the same person or to a technique that will help more accurately estimating the minimum number of people that are present in said mixed assemblage.

1.2 Hypothesis

A few correlations and differences have to be present for this thesis to have a positive result. Firstly, the differences in BMD between bones from a singular individual should not be significant. A study performed by McClanahan et all. (2002), however, found that athletic activities had influence in the bone mineral density of young adults. They discovered a bone mineral density difference between the upper limbs in both men and women that played sports like golf, basketball, and soccer, but this difference was even more pronounced in tennis and baseball. They also found that there was less often a difference between the lower limbs. The only sports that created a measurable difference for men were football and tennis, whilst women sports showed no significant differences at all (McClanahan et al 2002, 586 and 589).

This research suggests that differences in types of activities already create a difference in BMD per side within the upper limbs. The lower limbs, on the other hand, mostly seem to have similar BMD values. This means that it is more likely for the femora to be associated with each other, than for the humeri.
The larger difference in BMD between upper limbs described above does not exclude the possibility of reassociating the humeri of individuals. For this, the difference within a singular person needs to be smaller than the difference in BMD between individuals. This is also needed for reassociating the femora, but the smaller difference within singular individuals means that the difference between individuals needs to be less big. The results from the study be Curate et all. (2013) suggest that there most likely is a measurable difference in BMD between individuals for the femoral necks, but that this difference not only results from age differences, but also from other factors, like activity. Curate et all. (2013) looked at the possibility of creating an age-at-death estimation technique based on BMD values measured with a DEXA-scanner. The skeletons had a known sex and age, and the BMD values were measured at the femoral necks of the left femora. The age-at-death estimation technique that resulted from this study was described as usable, but with a high standard deviation between 6.2 and 10.4 years (Curate et all. 2013, 296.e1-296.e3).
In all, this means that it is likely that the femora of individuals can be reassociated with the help of BMD measurements. The same type of measurements performed on the humeri could also lead to a way to reassociate the bones with the individual, but the outcome is harder to predict, since there has been less research into the relation of BMD of the humeri between individuals.

Bone mineral density might also be observed with the help of proxies, in particular the loss of cortical bone. Ortner (2003) described a way to identify osteoporosis with the use of CT-scans. He found that people with osteoporosis had less cortical bone in the humerus (Ortner 2003, 414). Mays (1999) found that osteoporosis was associated with low BMD in past populations (Mays 1999, 72 and 74). These two studies do not directly relate BMD with cortical bone loss, but there might be a correlation between them, since they both have a clear relation to osteoporosis. Looking at this proxy might, therefore, give similar findings as bone mineral density, concerning the reassociation of

bones from commingled remains to individuals.
The hypothesis for this thesis is, therefore, as follows:

- There will be a correlation between the BMD values of bones from different sides of the skeleton. This relation will be more prominent in the lower limbs (femoral neck) than in the upper limbs.
- The relation in BMD between different bones of an individual will most likely not be one on one. However, age will, hopefully, have more impact on the BMD values than other factors, which might mean that a different relation in BMD between different bones of an individual might be present.
- Assuming that osteoporosis is strongly related to cortical bone loss, as suggested by Ortner (2003) and bone mineral density, as suggested by Mays (1999), then the relations of cortical bone loss between different bones of an individual will be similar to those of BMD (Ortner 2003, 414; Mays 1999, 72 and 74). These relations will most likely have more variation, since cortical bone loss is not directly related BMD and are more varied between individuals (Ortner 2003, 414).
- The levels of bone mineral density and cortical bone loss between bones of an individual will differ from those of other individuals. This means that these two characteristics can, most likely be used to sort out individuals from commingled remains. The sorting will vary depending on the size of the commingled assemblage. Smaller assemblages may result in individuals being identified, but larger assemblages will more likely result in groups of individuals with similar levels of BMD and cortical bone loss. These groups will, however, still be useful for estimating how many individuals are present within the assemblage.

In the Background chapter the existing techniques for dealing with commingled remains will be discussed, after which the history and application of CT-scanning and DEXA-scanning to archaeological remains will be summarized. The chapter Materials and Methods will look at the background of the skeletal collection used, at the process of scanning the remains and at the analytical process applied to the resulting scans. The chapter Results will look at the scans that were performed and at the outcome of the analytical processes and the chapter Discussion will interpret these findings. This thesis

will finish with a chapter Conclusion that will shortly state the findings of the discussion, the possible applications, and the ideas for future research.

2. Background

This chapter will start with describing the current techniques used for analysing commingled remains. These techniques used on commingled remains focus on the estimation of the number of individuals present in the assemblage. After discussing these techniques this chapter will shortly describe the history of the CT-scanner and the DEXA-scanner and this chapter will finish with describing the application of these two scanners to archaeological remains up to now.

2.1 Commingled remains

Commingled burials generally originate from one of two ways. The first originates from long term use of a burial site. This, for example, occurred in Tell Abrad. This Tell contains a burial tomb that was used between 2100 and 2000 BC. The placement of remains in this tomb mixed up previously buried individuals, which ultimately resulted in a tomb filled with commingled remains, except for one later burial of an articulated skeleton that was placed amongst these commingled remains. This burial is believed to be the last burial in this tomb, after which it was closed off by settlement debris and sand (Osterholtz et al. 2013, 2-5; Osterholtz et al. 2013a, 35-36; Ubelaker and Rife 2008, 99-100).

The other type originates from singular mass disasters, like a plague, war, or natural disaster (Mundorff 2008, 123; Osterholtz et al. 2013, 5). The excavations at the Holy Ghost Hospital at Lubeck, Germany, for example, has multiple commingled assemblages from singular events. The four mass graves date back to around the fourteenth century, during which there were multiple Black Death outbreaks. Two off the mass graves found at this site are believed to be linked to the outbreak of 1350. The other two mass graves are believed to contain victims of other later outbreaks. In the two mass graves linked to the outbreak of 1350, 696 individuals were discovered, even though one of these mass graves could partially not be excavated. The two mass graves with victims of later outbreaks contained 87 and 33 individuals. Only a few thin layers of dirt were found between the layers of skeletons, which corresponds with the idea that these graves were used for individuals from a singular plague outbreak, since reopening the graves would result in either thicker layers of soil or more commingling of the bones (Lütgert

2000, 255-258).

The burials of multiple individuals can also become commingled by processes that are not part of the burial practice. It is, for example, possible that remains get commingled by natural processes, such as the burrowing animals or the washing away of sediments by large quantities of precipitation. These processes can transport and mix the bones. This happened at the burial site in Scladina, where multiple individuals were buried in a cave. Many of the remains were transported out of the cave and down the slope of the hill (De Groote et al. 2020, 144-145).

Lastly, there is a possibility that bones get commingled during an excavation or post excavation. This happened to the North American Midwestern skeletal collection housed at the University of Chicago. The collection was subdivided and housed in multiple institutions when the subsidies for maintaining the collection stopped. During the transport of the collection many notes and materials were misplaced or damaged. Good documentation can often help with finding the bones that are associated and photos from the field can help finding the individual whose bone was misplaced (Osterholtz et al. 2013, 5; Sullivan and Childs 2003, 58-59).

Analysing a commingled assemblage can be difficult, since it is not clear which bones belonged to the same person and since there is no guarantee that the assemblage is complete (Ubelaker and Rife 2008, 97). Calculating the minimum number of individuals for an assemblage can help with analysing the remains. The MNI of a commingled assemblage is calculated by looking for characteristics that can distinguish individuals from each other. Size, age, sex, and side are the most commonly used. The bones in the assemblage are separated based on these parameters. There has to be certainty that bones do not belong together, because a small humerus and a medium femur could still belong to the same person. The MNI is then calculated by counting the minimum number of different individuals present. If there are, for example, a humerus from a child whose age-at-death was estimated between three and four, two female right ilia and one left male Os coxa, then the MNI becomes four. This becomes more difficult once there are more bones present. Other techniques used to calculate the MNI include the shape of the bone, like the overall shape of the Os coxae, and pathological conditions, like rickets (Herrmann and Devlin 2008, 257; Osterholtz et al. 2013a, 39).

The MNI only measures the number of individuals of whom can be stated that they are present with certainty. This means that individuals present in the assemblage that cannot be identified with certainty will not be counted in this estimation. The MNI is, therefore, usually lower than the actual number of individuals. The most likely number of individuals (MLNI) can be calculated to get a more accurate estimation of the amount of people that are present in the assemblage. The MLNI can be calculated with the following formula according to Adams and Konigsberg, 2004:

$$N = \left\lfloor \frac{(L+1)(R+1)}{(P+1)} - 1 \right\rfloor$$

In this formula the N stands for the number of individuals, L stands for the number of a certain element from the left side, R stands for the number of the same element from the right side and P stands for the number of pairs. The brackets mean that the number should be rounded off to a whole number. The formula results in a higher MLNI when there are relatively few pairs, because it is more likely that many individuals were lost if only singular bones remain and the formula results in a lower MLNI when there are relatively many pairs, because it is less likely that many individuals were lost if both bones of individuals were discovered (Adams and Konigsberg 2004, 141).

There is also a technique that does not count the MNI, but the minimum number of elements (MNE). When calculating the MNE, every element of a skeleton is counted separately. If you, for example, look at the right tibiae, then all the right tibia fragments are separated and counted. If there are two proximal ends, one distal end and one whole tibia, and the proximal and distal ends do not overlap, then the MNE for the right tibiae is three. This can then be repeated for every type of bone present in an assemblage (Lyman 1994, 289).

The exact number of individuals present in an archaeological assemblage is hard to determine. The MNI and MNE both measure a minimum amount and the MLNI only makes an estimation. The use of radiographic imaging in archaeology has come a long way and it may also help with the study of commingled remains.

Other researchers have also tried to reassemble commingled human remains with the use of osteometrics. Byrd and LeGarde (2014), for example, used measurements on multiple bones to try and reassociate them. They ended up with and accuracy of 74% up

to 85% (Byrd and LeGarde 2014, 167). When their technique was, however, tested on different populations by Bertsatos and Chovalopoulou (2019) the same measurements resulted in much lower accuracies, ranging between 4,8% and 71,7% accuracy (Bertsatos and Chovalopoulou 2019, 256). Others, like Vickers et al. 2015, made similar techniques for reassembling individuals based on bone sizes, but they are troubled by the size of the commingled assemblage and the difference in bone size of the individuals within that assemblage (Byrd and LeGarde 2018, 348).

The next part of this chapter will, therefore, discuss the history of the CT-scanner and DEXA-scanner and their application to archaeological human remains.

2.2 CT-scanning and DEXA-scanning

The first CT-scanner that was used in a clinical setting was an X-ray CT-scanner. It was introduced in the 1970's and it was used for diagnostic imaging. Previously, the only ways of diagnostic imaging were with regular X-ray or other two-dimensional imaging techniques. The X-ray CT-scanner was, therefore, a big step forward, since it could result in three dimensional images (Hughes 2011, 58).

This type of CT-scanner worked by emitting X-rays from one point and measuring the results on the other side of the scanned element in the form of an arch. The X-ray source and measuring points than turned around the object in a circle, until it was measured from all sides. This would form one image. For the next image, the object would be moved a set distance into the machine, after which the measuring process would start again (Hughes 2011, 58-59).

In 1989 a new type of CT-scanner was introduced: the spiral CT-scanner. In this type of scanner, the subject moves continuously through the machine, whilst the machine rotates around the subject and creates the images. This type of scanner is, therefore, also much faster than the previous type of CT-scanner. Later the multi-detector spiral CT-scanner, or the MSCT, was invented. This type works similar to the spiral CT-scanner, except that it uses more rows of detectors, which makes the MSCT even faster (Hughes 2011, 59).

The dual-energy X-ray absorptiometry scanner, or DEXA/DXA scanner, was first introduced in 1987. This type of scanner was used to measure the bone mineral density

(BMD) of an individual (Blake and Fogelman 2007, 509). The DEXA scanners are used to identify osteoporosis. This is correlated with a higher risk of bone fractures. BMD measurements are not only used for diagnosis, but they are also used to examine the effectiveness of treatments (Blake and Fogelman 2007, 509; Maghraoui and Roux 2008, 605).

There is a small variety of DEXA scanners, but they all work in a similar fashion. Two sources of different X-ray energies and two radiation detectors are placed opposite of each other, one above and one below. The patient or subject is then placed on a table in between the sources and the detectors. The scanner will then measure the X-rays that reach the detectors across the region of the patient or subject that is to be scanned. The lessening of the radiation can then be translated into the BMD for that region (Maghraoui and Roux 2008, 606).

2.2.1 CT-scanning and DEXA-scanning in archaeology

The first CT-scans that were made of archaeological remains, were made of mummies. The use of the CT-scanner gave researchers the possibility to closely examine the insides of mummified remains, without damaging them. The main goals of researchers were to discover pathological conditions, to find age-at-death and sex indicators and to figure out the post-mortem alterations that were made to the remains.

The very first CT-scan of archaeological remains was performed in 1977 on two Egyptian mummies (Hughes 2011, 60). The first scan was of the brain of a fourteen-year-old Egyptian male from around 1200 B.C. (Figure 2.1). The body was not mummified, but merely wrapped in linen, which meant that the brain was not tampered with post-mortem. Both brain hemispheres had already been removed by previous researchers. There were faint outlines of the different types of brain matter. They did not discover any pathological conditions, but they did describe areas that were denser, which they labelled as post-mortem artefacts (Harwood-Nash 1979, 768-770).

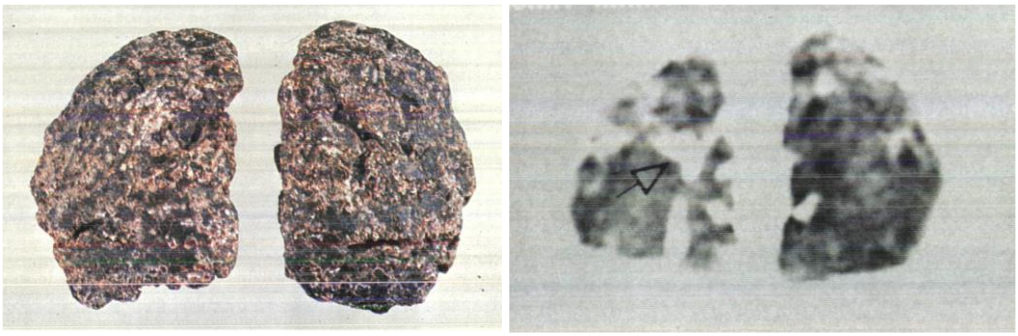

Figure 2.1: Left: Both hemispheres from the fourteen-year-old Egyptian male. Right: The CT-scan of both hemispheres. The arrow points towards the ventricle of the left hemisphere. There translucent parts are believed to be the post-mortem artefacts. The article also states that there are differences between white and grey matter present (Harwood-Nash 1979, 769).

The other mummy that was scanned during this research was a young female from around 850 B.C. The scans showed that her entrails had been removed through an incision on the side of her body. Her brains were removed via the ethmoid and the nose with the use of a trocar. The entrails were then wrapped and placed back into the body via the same incision on the side, together with wax, mud, and sawdust. Wax, mud, and sawdust were also placed in other parts of the body to presumably try and embalm the rest of the body. The incision on the side was then covered with a metal plate. The outside of the body was covered with salts and ornaments, after which it was wrapped in bandages and placed in a stiffened canvas (Harwood-Nash 1979, 770).

The CT-scans of the second skeleton showed the wrapped entrails, the ornaments and in some placed the mud within the mummy. Several untouched organs could also be recognized together with many of the bones. In the skull the path of the trocar could also be seen (Figure 2.2) (Harwood-Nash 1979, 770-773).

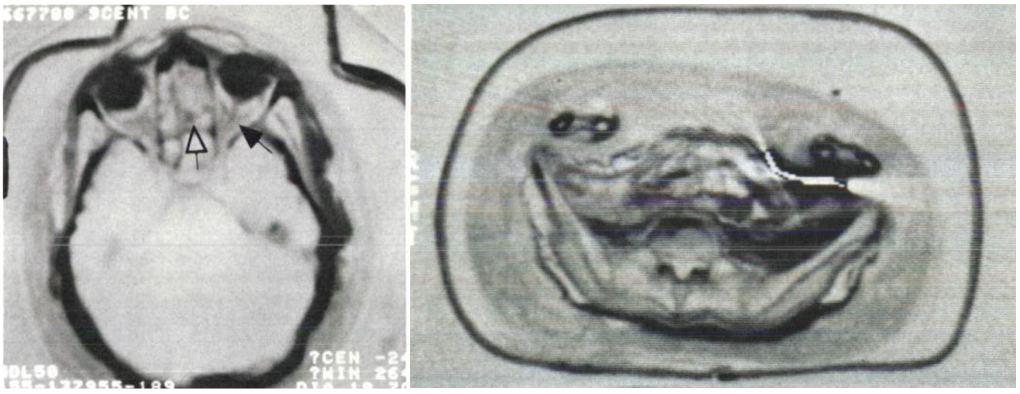

Figure 2.2: Left: A CT cross-section of the head. The white arrow points to the path that the trocar took whilst extracting the brain matter. The black arrow points towards a well-preserved optic nerve. Right: A CT cross-section of the lower abdomen. The white plaque is the piece of metal that was used to close off the incision (Harwood-Nash 1979, 771-772).

The results of these two scans proved that CT-scanning was a very useful non-invasive way of examining mummies and many other mummies were scanned in the next few years (Hughes 2011, 60).

Over the next few decades, CT-scanners and the application of CT-scanning to archaeological remains were improved. Faster and more detailed CT-scanners made scanning more accessible and more data about the insides and structures could be extracted from those scans.

One more notable mummy that was examined using both early and improved CT-scanning was Otzi the ice man. The original CT-scans that were performed in 1991 were primarily focused on the skull. The researchers found fractures in the left maxilla and flattening on the left side of the face. This was most likely caused by the pressure created by the ice that covered the mummy (Nedden et al. 1994, 269-272).

Many more scans were made of the ice man in the following years. With the help of the improved CT-scanning, combined with radiographic imaging, researchers were able to determine much about Otzi (Murphy et al. 2003, 615-616).

The CT-scans showed that Otzi's brain has shrunken and is positioned towards the posterior side of the skull. The different parts of the brain, meaning the hemispheres, brain stem and spinal cord, could still be distinguished, but the difference between white and grey matter could not be observed (Murphy et al. 2003, 616).

The skull itself has a lot of small cracks and fractures. Some of the sutures also appear to

be pushed partially open. These cracks and the state of the sutures are hypothesized to be the result of thawing and freezing of the skull. Water inside the skull would have caused the cranial vault to be pushed open. One of the nasal bones also seems to be broken and placed in a weird angulation towards the inferior side. Researchers believe this to also be a post-mortem fracture caused by the ice pushing down on the skull. Other damage to the mummy from freezing and thawing resulted in translucency in other parts of the skeleton and the crushing of the thorax by ice (Murphy et al. 2003, 617).

Researchers found some mild endplate sclerosis with spurs amongst the lower cervical vertebrae, which is indicative for intervertebral disk disease. There are also signs of healed rib fractures on left fifth to night ribs. These healed fractures are believed to be caused by a singular moment of trauma to the thorax. On the right acetabulum and femoral head, they discovered traces of osteoarthritis and the tibiae showed some Harris lines. The left small toe portrayed signs of arthropathy, which is commonly associated with arthritis, but researchers hypothesized that this could also be a result of frostbite, after considering the absence of arthritic signs in the other digits of the hands and feet (Murphy et al 2003, 618-621).

Most of the organs were hard to be recognized due to the dehydration. Only the brain could be clearly distinguished. There were, however, some calcifications on locations where arteries would be expected, which indicates that Otzi might have had arteriosclerotic cardiovascular disease. An arrowhead was also discovered lodged between the ribcage and the left scapula. Otzi might have died from loss of blood from the arrow wound (Murphy et al. 621-622).

The significant difference in results shows the increase in information that can be extracted from remains with the improvement of the CT-scanners, but the use of CT scans on skeletal material still appears less popular than its use on mummified remains. There are, however, several types of observations that can be made with the use of CT-scanning. Structural changes of the bone can be better analysed via CT-scanning. This is especially useful when looking at diseases that have an effect on these structures, like osteoporosis (Ortner 2003, 521).

Thinning of trabecular bone and cortical bone loss can, for example, be observed via radiographic cross-sections of bones (Crocer et al. 2009, 30; Mays 2001, 36; Ortner

2003, 414). Ortner, 2003, for example, describes a case in which a female skeleton has osteoporosis. Examination of many of the bones had already been performed, but they also made CT-scans of the humeri. The CT cross sections showed that there was thinning of the trabecular bone in the humeral heads and loss of cortical bone throughout the humeri (Ortner 2003, 414).

CT-scanning can also help with identifying pathological lesions that are located within the bones. This can be seen in different case study that was described by Ortner, 2003. CT-scans were made of a male cranium that originated from the Late Prehistoric or Historic period in Tennessee. The skull has multiple osteoblastic lesions, particularly on the occipital bone. The CT-scan of this skull showed that the tumours were also present on the interior of the cranium. On first examination, the growths appeared as benign fibro-osseous tumours with a slow growing rate. The CT images, however, showed that in one area of growth on the anterior aspect of the skull was differently structured. This structure was poorly organized and had no sclerotic margins, in opposition to the other growths that had a more structures appearance, which indicates that this growth might have turned into a malignant tumour (Figure 2.3) (Ortner 2003, 521 and 523).

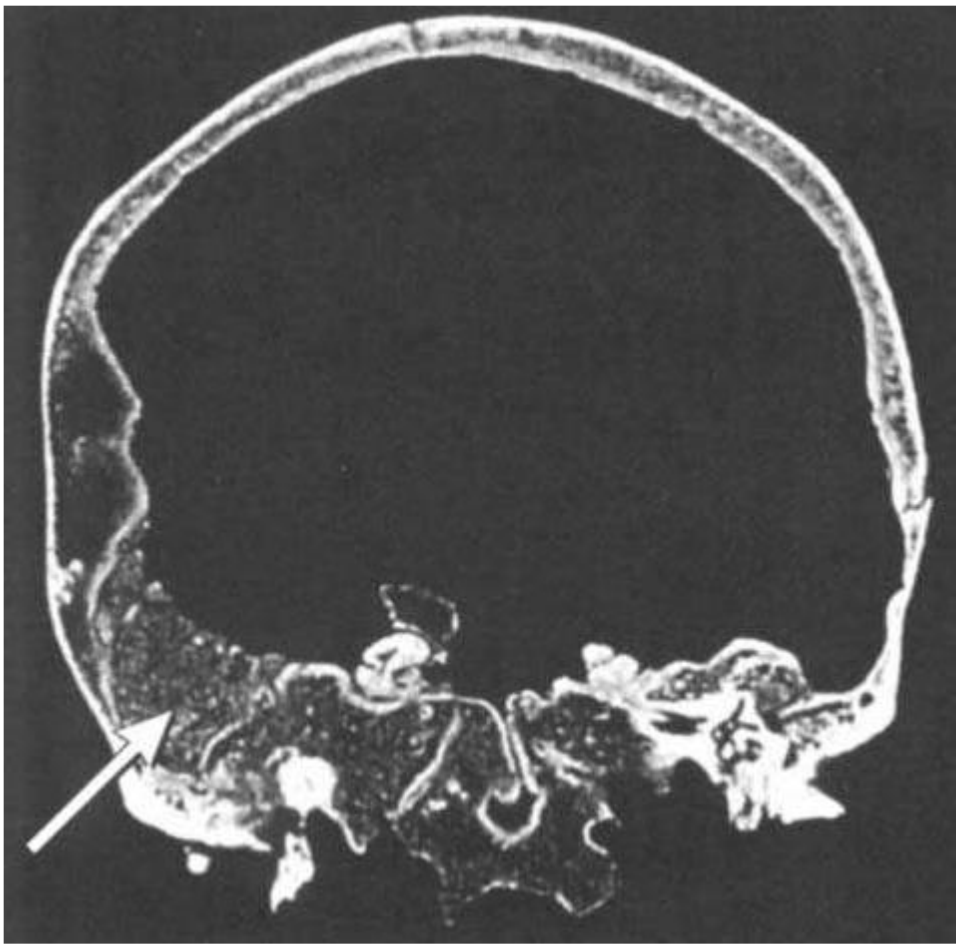

Figure 2.3: The carcinomic growths are clearly visible on this CT-scan. The growth that is believed to be a malignant tumour is shown by the white arrow (Ortner 2003, 522).

CT-scanning of skeletal remains can also help with reconstructing past living situations and events by looking at bone structures and by identifying diseases.

A study by Primeau et al., 2019, for example, used CT-scanning in order to study the effects of two climate events on the contemporary population. They used two skeletal collections from Denmark from the medieval period. These collections were used to look at linear enamel hypoplasia, Harris lines in the tibiae and infectious middle ear disease as proxies for stress and malnourishment. The linear enamel hypoplasia was observed with the naked eye, but the researchers used CT-scanning to look at the Harris lines and infectious middle ear disease (Primeau et al. 2009, 80).

Harris lines are presumably caused by periods of malnutrition, which can cause the growth of the long bones to slow down. The infectious middle ear disease can be seen in the temporal bone. The infection causes a difference in size of the mastoid processes,

differences in mastoid cell structure and sclerosis in the mastoid area. A scan of the temporal bone is needed to see these changes, and even though they used a CT-scan, some other scans, like regular X-ray, can also be used to identify this infection (Primeau et al. 2009, 82-83).

The DEXA-scanner has a smaller range of applications to archaeological materials. These types of scans are solely used to measure the bone mineral density (BMD) for archaeological samples. There has, however, been an increase in the application of DEXA-scanners to archaeological remains in recent years to look at the relation between BMD and sex, age, activity, and other variables (Di Stefano et al. 2012, 232).
Mays et al., 1998, used DEXA-scans to look for age related changes in the bone mineral density. They used a medieval population from England. They divided the population in male and female and subdivided these groups in three age ranges, 18-29, 30-49 and 50+. They then used the DEXA-scanner to measure the BMD in the proximal part of the femur. After comparing the BMD values between the groups, they found that there was no significant difference for the two youngest male groups, but that there was a significant loss of bone mineral density with age for the other groups of both sexes around the femoral neck (Mays et al. 1998, 100-101).
People from the past most likely had similar problems when people suffered from osteoporosis as modern day people. This is, for example, shown by Mays, 1999, who looked for osteoporosis via DEXA-scans from the female skeletons originating from the deserted village of Wharram Percy. He found that the skeletal remains containing compression fractures in the vertebrae and ribs had a lower bone mineral density. Similar fractions in current population can also be traced back to osteoporosis and low bone mineral densities (Mays 1999, 72 and 74).
Kendell and Willey, 2013, also looked at the preservation likeliness of bones compared to their BMD to see if the minimum number of individuals (MNI) calculation should be altered based upon the average BMD of people from a certain age-group. Their hypothesis was that bones with a lower BMD were less likely to preserve, meaning that they would be underrepresented in commingled assemblages. Their study seemed to have positive results, but they did not account for sex differences. They used large age groups and their suggestions for alterations were vague. They suggest that, when

looking for the MNI, researchers should prefer to use bones with a higher BMD, since those bones are more likely to be preserved from each age group, which is difficult to use in practice, where the choice is, most likely, limited by the assemblage (Kendell and Willey 2013, 92-95 and 100-101).

2.3 Conclusion

Commingled remains are studied by measuring the minimum number of individuals or elements present, or by approximating the number of individuals in the commingled assemblage. This helps with studying the associated populations, but it is still limited. The use of CT-scanning in archaeology has grown over the past few decades and DEXA-scanning has also made an introduction. These scans are mainly used for the identification of diseases and changes in bone structure, and for studies associated with these diseases and changes, like the impact of climate events on the contemporary population. CT-scanning and DEXA-scanning have not been applied to commingled remains in large amounts, but they might be usable for identifying individuals based on their bone mineral density and bone structure.

3. Materials and methods

The materials and methods chapter will first describe the skeletal collection that was used for this thesis and give some information about the excavation from which it originated. After this introduction into the materials the chapter will describe the CT-scans that were performed and the measurements that were taken on those CT-scans. Next, the DEXA-scanning will shortly be described. The chapter will finish with presenting the analytical steps taken to examine the data from the CT measurements and from the DEXA-scans, by describing the ways that the resulting data was visualized so it could be interpreted and by describing the way that these outcomes were presented as a possibly applicable way of reassembling commingled remains.

3.1 The Middenbeemster skeleton collection

The grounds adjoining to a Protestant church named the Keyserkerk in Middenbeemster were partially excavated from the 13th of June until the 5th of August 2011. The church was built in the beginning of the 17th century. Burials took place in and around this church from the beginning of the 17th century until the beginning of the 19th century. Excavators, therefore, expected a high number of skeletons to be recovered during the excavation (Hakvoort 2013, 13-14).

The total excavated area covered 440 m^2. The first test pit already uncovered a total of 35 graves, whilst the pit only reached 92 cm below the surface. In the end over 400 burials were discovered during this excavation. When a grave was found, the outline of the grave was first exposed. Afterwards, the remains in the grave were dug out with the use of trowels, wooden sticks, and brushes. Once a grave was fully exposed, the contents were photographed, measured in, documented on a form, and removed to be dried and stored. The orientation, position, additional finds, and missing parts of the skeleton are recorded on the form. The skeletal materials from these burials are currently housed at the faculty of Archaeology of Leiden University (Hakvoort 2013, 19 and 35).

The initial research about the population is based on a subsample of 125 skeletons that was believed to be representative for the population buried next to this church. Out of the 125 skeletons analysed, 54 were adolescent. This is a relatively high number

compared to similar sites. There were many non-adult skeletons aged between the ages of 0 and 3. In the adult population most of the skeletons were aged between 36 and 50. The adult population buried at this cemetery contained 37 females and 34 males (80,3% is determined with certainty). The remains themselves were on average in good conditions and most of the skeletons were mostly complete (64% had a 75-100% completeness). The formulas made by Trotter (1970) were used to estimate height. Most females were estimated to have been between 150 and 169 cm and most males were estimated to have been between 160 and 179 cm (Hakvoort 2013, 40-44).
A lot of pathologies were found in this populations, including various degenerative diseases, deficiencies, and developmental defects. None of the diseases present were very unusual or present in large quantities (Hakvoort 2013, 46 and 51-52).

A total of 50 individuals were scanned using the CT-scanner and DEXA-scanner. The skeletons were selected based on preservation and overall completeness, meaning that sex, age, and pathological conditions were not taken into account. Other individuals from the Middenbeemster collection were still planned to be scanned with these scanners, but due to the deadline for this thesis, only the first 50 scanned individuals could be used. These scans were initially made for other research, but permission was granted to use these scans in this thesis.

3.2 CT-scanning

CT-scans were performed at the Leids Universitair Medisch Centrum (LUMC). These scans were made with a PET-CT Philips Vereos (settings: 64 slice, 140 Kev, 75mAs and slice thickness 1mm). Each skeleton was laid out on a plastic slab in anatomical position. The vertebral column was articulated per vertebrae group (cervical, thoracic, and lumbar) and space was left between them if vertebrae were missing. The skulls and mandible were only scanned if most of the bone was still intact (>50%). The rest of the long bones, and the pelvic girdle were laid out if enough of the bone was intact (pieces bigger than 33%) and small fragments were left out. Lastly, the scapula and clavicle were only scanned for a number of individuals, because there was a limited amount of time to use the CT-scanner.

The cortical bone loss was measured with the use of the cortical bone index described by Mays (2001):

$$CI = \frac{T - M}{T} * 100$$

In this formula CI stands for cortical bone index, T stands for total bone diameter and M stands for the diameter of the medullary cavity (Mays 2001, 36). T and M were measured on established locations using CT-scans. For the femora this correlates to just below the femoral trochanters. The measurements were taken on the CT-slides where the medullary cavity first touched the cortical bone on the superior side. This first occurs on the lateral anterior side of the bone. The T and M were measured from the medial anterior side to the lateral posterior side (just lateral of the linea aspera). The line reached the lateral posterior side on a 90-degree angle (figure 3.1a).
For the humeri the measurements were taken just below the humeral head, on the first CT-slide where over 90% of the medullary cavity touched the cortical bone. The measurements were taken from the must anterior to the most posterior portion of the bone (figure 3.1b). The other bones were excluded.
If these locations were hard to find or on a very different place along the shaft, the location most similar to the examples in figure 3.1 were used. The similarity of location between left and right of one individual were valued higher than the similarity to the

examples.

In some instances, the measurements were hard to take due to, for example, sand inclusions, damage, or possible pathologies. These bones were excluded from the cortical index measurements.

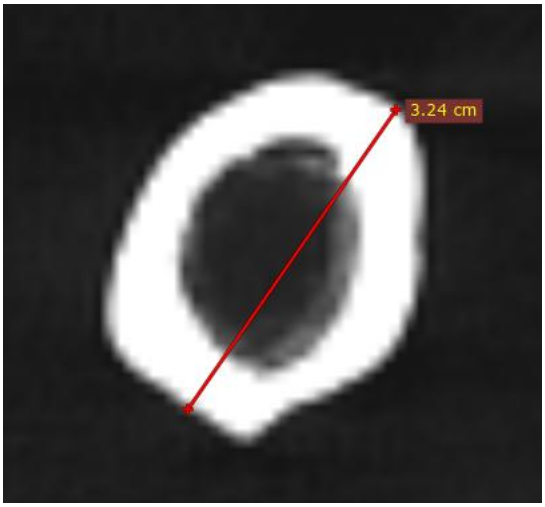

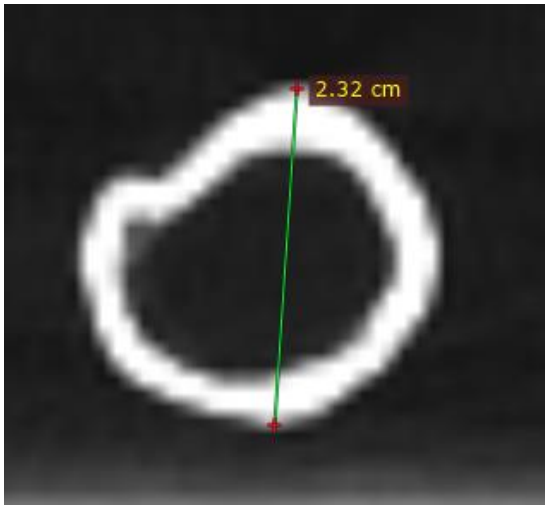

Figure 3.1a (left): A CT cross-section of the right femur of skeleton S045V0055. The red line indicates where the measurements were taken.
Figure 3.1B (right): A CT cross-section of the right humerus of skeleton S045V0055. The green line indicates where the measurements were taken.
(Both the cross-sections are a bottom view, which means that the right lateral side is on the left.)

3.3 The DEXA-scans

The DEXA-scans were also made at the LUMC. They were made with a Hologic Horizon A DEXA-scanner. When scanning with a DEXA-scanner, there is a protocol in the program for each of the bones that are normally measured. This protocol basically instructs the machine to make the scan for that type of bone. The location of a bone where the measurement will be taken is placed under the scanner and the protocol associated with that bone is activated.

For each of the skeletons the humeri, femora, ulnae, radii, and the five lumbar vertebrae were selected. If a bone was damaged in the area where the measurement would be taken, then these bones were not scanned.

The humeri and femora were scanned individually. The scans of the humeri were made with the hip protocol. The bones were positioned as if the individuals were laying on

their backs. Only the proximal ends of the humeri and femora were scanned, since the bone mineral density was measured at the femoral neck and just below the humeral head. The radii and ulnae were measured in articulated position. The measurement of the radii and ulnae was taken around 1/3 onto the shaft from the distal side. The DEXA-scans of these bones are, therefore, from the distal end up to 2/3 of the bones. The lumbar vertebrae were scanned together. They were positioned with their posterior side upwards, since it was easier to stabilize them that way. They were laid down with a small distance between their bodies, which later made it easier to identify them.
In the rest of this thesis, only the BMD measurements of the humerus and femur are used due to the limited time available to do this research.
The bone mineral density measurements were made by P. Dibbets-Schnieder of the LUMC. The software that belongs to the scanner was used to make these measurements. For both the femora and the humeri she positioned the region of interest (ROI), in which the program measures the BMD, on the neck of the bone so that the midline divides the head in two equal parts. This ROI was not allowed to cross the bone in any other region, like the trochanter. The measurements were then performed by the software.
The resulting BMD values were difficult to compare to 'normal' ranges that are found in living individuals. The humerus is normally not scanned with the DEXA-scanner and there are, thus, no 'normal' ranges present for living nor dead individuals. For the femur there are 'normal' ranges for living individuals and ranges that indicate the presence of abnormalities like osteoporosis. The skeletons of the Middenbeemster collection are no longer surrounded by tissue, are dry and have been undergoing taphonomic processes. It is, therefore, uncertain that the 'normal' ranges of living individuals are comparable to the BMD values of these skeletons. Hence, the 'normal' ranges of living individuals are, to avoid confusion, not presented here.

3.4 Statistics

After the measurements of the humeri and femora were taken, they were compared to each other to see if the femora and humeri of individuals could be reassociated.
The measurements showed a difference in value between the bones and a slight difference between sides. For the different bones to be reassociated, the data, thus, had

to be recalculated. Regression models were, therefore, made with the use of excel.
For the bone mineral density values, a regression model was created for each combination of bones using excel. A combination of bones refers to a pair of the four bones that were used in this thesis, namely a pair of the left femur, right femur, left humerus and/or right humerus. For the regression models, the BMD values were paired by the individual to whom these values belong, to create coordinates. A polynomial, logarithmic, linear, exponential, and squared model was created for each of these combinations. Each formula gave similar standard deviations and correlation coefficients per combination. The regression model with the lowest standard deviation was selected for each of the combinations in both directions. (When trying to reassociate bones, bone A could be used to look for bone B, but bone B could also be used to look for bone A. One combination of bones can, thus, be used in two directions.) For example, a regression model for the most likely associated BMD of a right femur for a left humerus was selected, but a different model was also made for estimating the most likely associated BMD of the left humerus for the right femur.
One left humerus had a negative BMD, which is most likely not the natural BMD of this individual, but caused by a fault in measurement, a disease or taphonomic factors. This bone was, therefore, excluded from the regression models.
Regression models were also made for the cortical index of each combination of bones. The five different types of regression models were also created here, but similar to the BMD models, the standard deviations and correlation coefficients were very similar for each type of model per combination. The best fitting models were also selected for the cortical indices.

This neighbourhood analysis was performed in R. A neighbourhood analysis is a function that can be used to look at data point patterns in one or more dimensions. The NNDIST function from the spatstat package in R was used in this thesis (see appendix 1). The default of this specific neighbourhood analysis function looks for the distance between each data point and its closest neighbouring point. The function was slightly altered for the requirements for this thesis. The data was grouped per bone, and later these groups were subdivided to form groups of different sizes. The distance to the nearest neighbouring bone of each bone type was searched. The distance to the nearest

neighbouring searched bone could then be collected and compared to the distance between the bones per individual. The distance between the two bones associated to the same individual was measured with excel, since this is a mere subtraction. If the distance between two bones of an individual were the same as the distance between a bone and its nearest neighbour, the individuals' bones were accurately reassociated. If there was a bone from a different individual closer to the original bone, the individuals' bones would not be accurately reassociated. The percentage of accurately reassociated bones per combination were then calculated for each combination of bones, in both directions, for both the BMDs and the cortical indices.

The process described above was performed on the total number of skeletons, but also on smaller groups of individuals. This was to see if there was a difference in results between large quantities of skeletons and smaller quantities of skeletons.
Firstly, five groups of five were randomly selected out of the total sample. In order to prevent large amounts of overlap the following set of requirements were made for a group:
- A group can have no more than two individuals that are also present together in another group, but it can have singular individuals from the other groups.
- An individual is not used more than two times.
This was performed for each combination of bones for both BMD and cortical index separately. A neighbourhood analysis was then also performed on each of these groups.
After the groups of five, the neighbourhood analysis was also performed on groups of ten. The combinations of bones that had an accuracy below 33,33% for the groups of five were excluded from this step. This is because the accuracy is very unlikely to grow, since larger groups result in more values and, therefore, more overlap between values.
Not enough BMD data was present to make five groups of ten using the set of requirements described above. The maximum number of groups was, therefore, selected. The cortical indices are in large enough number to form five groups for each combination.
Lastly, groups of fifteen were made for the groups of ten that scored above the 33,33% threshold. The same requirements for group formation were also used here, after which neighbourhood analyses were performed on each of those groups.

3.4.1 BMD and cortical index combinations

After the groups of fifteen were finished, a new set of neighbourhood analyses were performed, where both the bone mineral density and cortical indices were used. The bones were selected that had both these values, for each of the combinations.
In order to be able to match the BMD values with the cortical indices the values had to be rescaled. This is because the BMD values (0,3-1,2) are much smaller that the cortical indices (25-70). In order to do this the ranges over which the values were spread, were determined for each of the bones for both variables. These lowest and highest values were rounded off, so the lowest and highest values did not correspond with the end of the ranges, but instead fell within the range. For BMD the ranges were rounded off with 0,05 accuracy just below the lowest value and above the highest value. For the cortical indices the ranges were rounded off in the same way to whole numbers. The values were then recalculated to a range from 0 to 100, so the values could be properly compared.
The distance between the bones of an individual were calculated with the help of Pythagoras, since the bones are now spread over a two-dimensional field. The neighbourhood analyses function in R calculated the distance between the two bones directly.
The first neighbourhood analyses performed on the combinations of bones that combined the BMD values with cortical indices were the total groups. Afterwards five groups of five were formed for each of the combinations. Neighbourhood analyses were then also performed on these groups. The 33,33% boundary was then used to decide for which combinations neighbourhood analyses would be performed for larger groups. Using the same requirements that were used when creating larger groups for the separated variables, the groups of ten, fifteen and twenty were made. Lastly, the neighbourhood analyses were performed on these group sizes.

3.5 Assessment of the neighbourhood analysis results

After these neighbourhood analyses were all finished, the differences between bones that were accurately reassociated were selected for each combination of bones and plotted out against the value of the original bone (the BMD value or cortical index that was not recalculated). This might give an indication if the distance from the average

value has a large influence on the chances of two bones being reassociated with accuracy. These graphs were then compared for the total groups, groups of five, ten and fifteen, to get an indication of how much group size can influence the accuracy of these comparisons.
The inaccurate data was also plotted in the same graphs to see if there is a distribution for the inaccurate data compared to the measurement values.

For the data that combined both variables, 3D graphs were made per group size per combination. One side of the graphs shows the BMD value, the other side of the graph shows the cortical index, and the Y-axis of the graphs show the differences between the two associated bones. In these graphs the plotted bones are divided based on whether or not they were accurately reassociated to their own bone.
These 3D graphs were plotted with the help of the scatterplot3d function in R, which is a function specifically made for creating graphs like the ones described here (see appendix 1).

Another type of graph was made for the neighbourhood analyses that had an accuracy above the threshold. These graphs for the separate variables will show the BMD or cortical index value of the bone on the X-axis and the distances between each bone and its nearest neighbour on the Y-axis. The colour of the point on the plot will indicate if the bone was accurately reassociated or not. These plots will give an indication as to how accurate a reassociation is depending on how close the individual lays to the average, since it will be more likely that two bones with rare values belong to each other than two bones that both have very common values.
Similar graphs will also be made for the combined variables. These 3D graphs will also show the distance to the nearest neighbour and the corresponding values of the bone used. Other than being three dimensional, the function of these 3D graphs will be the same as those made for the separate variables. These graphs will also be made with the use of the scatterplot3d function in R.

3.6 Application and ethics

Lastly, the data was used to create a set of guidelines as to how to use bone mineral density and cortical indices to sort out humeri and femora from commingled remains.

This outline contains the formula to recalculate the measurements to match different bones and variables, and a table that shows which variables result in what percentage of accuracy for each of the combinations.

The research performed in this thesis is solely based on scans of bones, which means that the skeletal material was not harmed during this research. The application of this research to the reassembly of individual will also only use scanning techniques and no other, possibly destructive, methods. The non-destructiveness of this approach should, thus, not cause ethical conflict when it is applied to the remains of individuals, whilst providing researchers with the data needed to analyse the remains (Walker 2000, 24-26). The reassociation of human remains that were commingled is in the eyes of many also a humane way of treating the dead (Anstett and Dreyfus 2015, 109), which means that overall, there are no mayor ethical dilemmas with the research performed here nor with the application of these techniques to commingled remains in the field.

4. Results

This chapter will begin with presenting the results from the DEXA-scans and CT-scans. It will then continue to describe the regression models that were created in order to examine the data that came out of those scans. The rest of the chapter will focus on the neighbourhood analyses that were performed on the data and the visualization of the resulting data.

4.1 Results DEXA-scans

The scans resulted in usable BMDs of 41 left femora, 40 right femora, 24 left humeri and 33 right humeri. The missing values either resulted from missing or damaged bones or from faulty measurements (e.g., BMDs of 0).

The measured bone mineral densities ranged between 0,48 and 1,19 for the femora (figure 4.1a and 4.1b) and between 0,32 and 0,80 for the humeri (figures 4.1c and 4.1d). One left humerus had a BMD of -0,28, which is most likely not the natural bone mineral density of an individual, but instead caused, by disease, taphonomy or a fault in measurement. This humerus was, therefore, excluded from further analysis.

4.2 CT-scan results and cortical indices

A total of 48 skeletons were scanned with the CT-scanner of the LUMC. This resulted in cortical indices for 46 left femora, 45 right femora, 45 left humeri and 44 right humeri. The missing values either resulted from missing bones, sand inclusions that prevented measurement or pathology/taphonomy that prevented measurement.

The cortical indices ranged between 25,08 and 65,69 for the femora (figures 4.2a and 4.2b) and between 19,68 and 54,57 for the humeri (figures 4.2c and 4.2d).

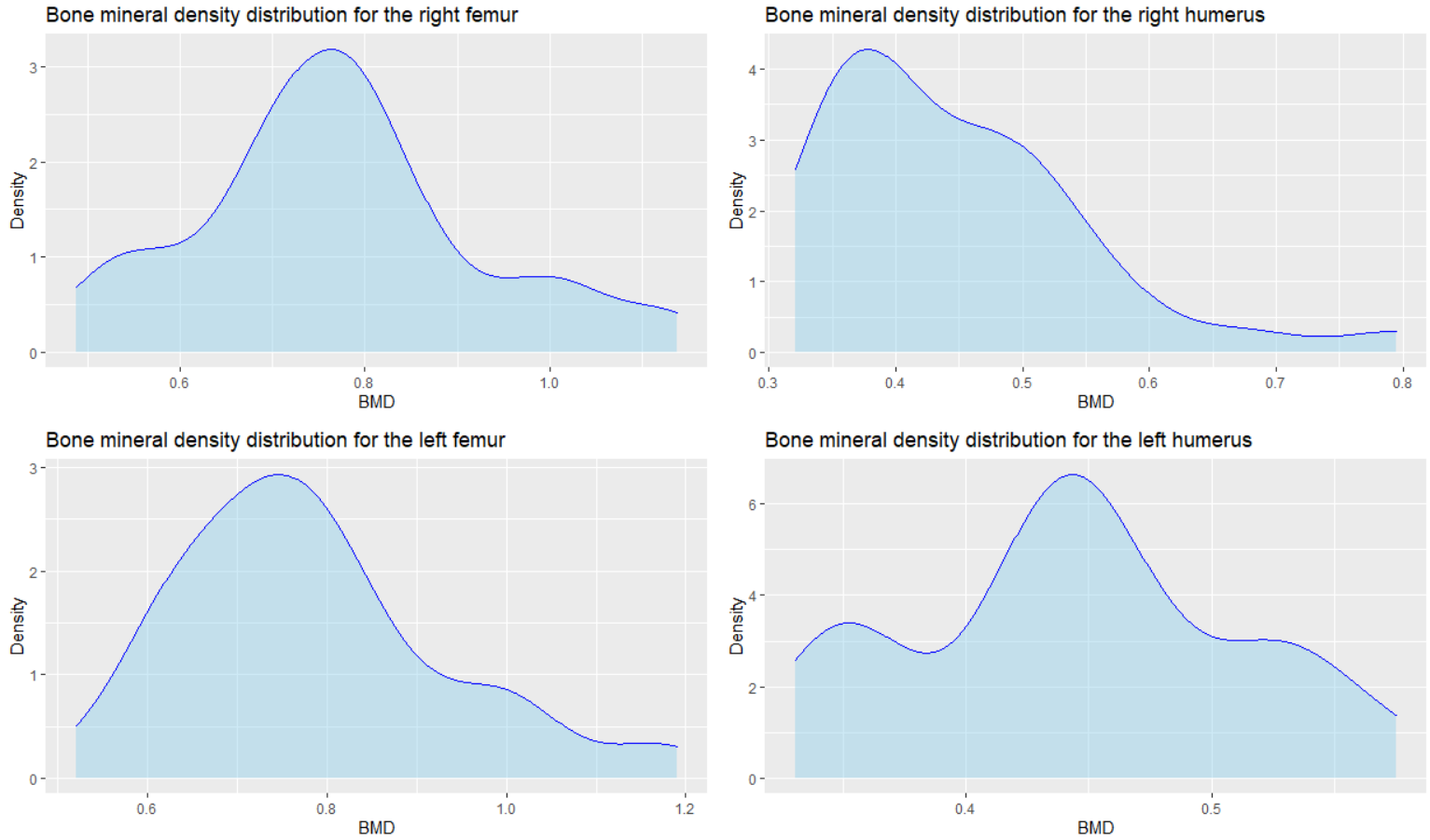

Figure 4.1a (top left): The bone mineral density value distribution for the right femur.
Figure 4.1b (bottom left): The bone mineral density value distribution for the left femur.
Figure 4.1c (top right): The bone mineral density value distribution for the right humerus.
Figure 4.1d (bottom right): The bone mineral density value distribution for the left humerus. The value lower than 0,25 is -0,28.

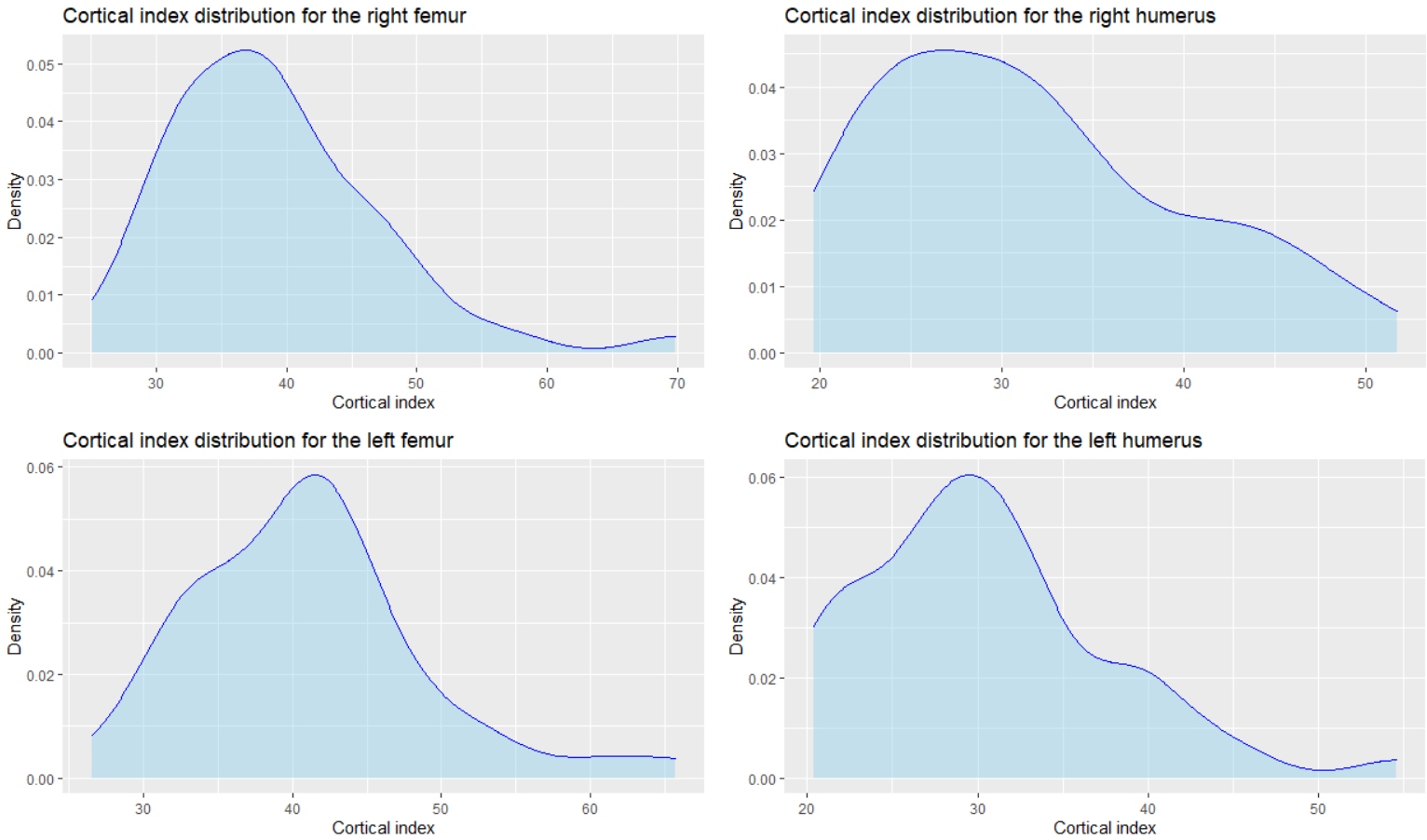

Figure 4.2a (top left): The cortical index distribution for the right femur.
Figure 4.2b (bottom left): The cortical index distribution for the left femur.
Figure 4.2c (top right): The cortical index distribution for the right humerus.
Figure 4.2d (bottom right): The cortical index distribution for the left humerus.

4.3 Regression models

The data resulting from the CT-scans and the DEXA-scans was used to make regression models in order to be able to compare the values of different bones with each other. The standard deviation and correlation coefficient were also calculated for the resulting models.

The individuals that had the values of both bones that were used in a regression model were selected and plotted out to find the formula that best represented the correlation between the two bones.

For example, if the expected bone mineral density of a right humerus has to be calculated when the bone mineral density of a left femur is known, the following model is created (Figure 4.3):

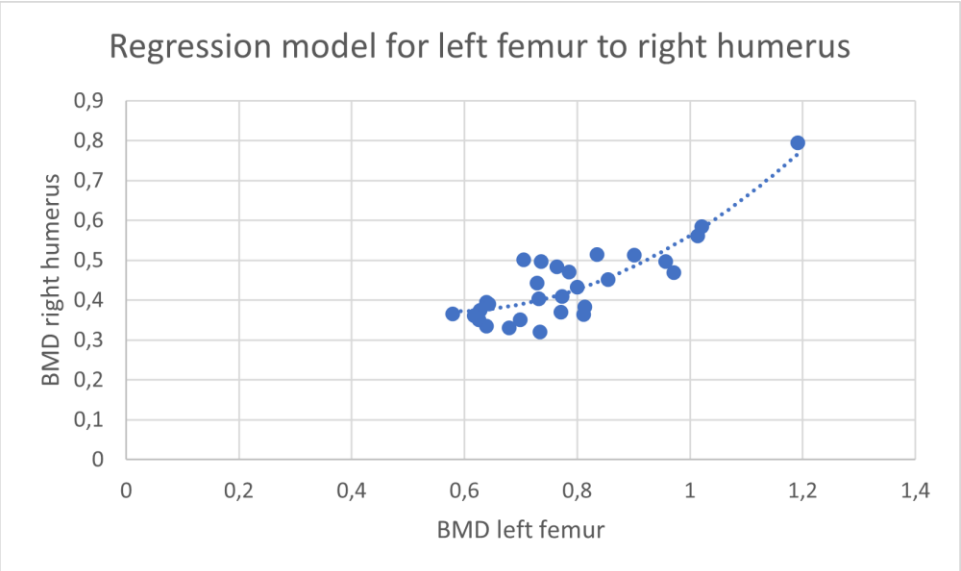

Figure 4.3: Example regression model for the calculation of the expected BMD of right humeri based on the BMD of left femora of the same individuals. The dotted line is the best fitting formula based on the BMD values.

The formula that resulted from this model is:

$$y = 1{,}0039x^2 - 1{,}131x + 0{,}6898$$

In this formula y is the expected BMD of the right humerus and x is the BMD of the left femur. The associated standard deviation of this formula is 0,09768 and the correlation coefficient is 0,8722.

Similar models were created for each combination of bones, meaning for each pair of

the four bones that were used in this thesis, for both the BMD values and the cortical indices (Table 4.1). These formulas were then used to calculate the expected BMD's and cortical indices for all the combinations of bones.

Table 4.1: This table shows the formulas for recalculating bone mineral density and cortical indices to estimate what the values would be of another bone or for the same bone of the other side. The standard deviation and correlation coefficient are also given for each formula.

Bone	Estimated Bone	BMD formula	SD	R	Cortical index formula	SD	R
L Femur	R Femur	$y = 1,0843x^2 - 0,8752x + 0,7894$	0,146755	0,943398	$y = 0,8072x + 9,1528$	7,89393	0,844452
L Femur	L Humerus	$y = 1,847x^{1,0357}$	0,108131	0,826136	$y = 0,4283x + 28,081$	7,757022	0,353412
L Femur	R Humerus	$y = 1,2018x + 0,2535$	0,141336	0,830542	$y = 0,53x + 24,024$	8,026326	0,51049
R Femur	L Femur	$y = -0,011x^2 + 0,9585x + 0,0299$	0,150324	0,91717	$y = 0,8834x + 3,1846$	8,257818	0,844452
R Femur	L Humerus	$y = 4,0836x^2 - 1,7681x + 0,7525$	0,143926	0,853053	$y = 0,6435x + 19,784$	8,229917	0,504777
R Femur	R Humerus	$y = -0,4039x^2 + 1,5661x + 0,1718$	0,138046	0,809568	$y = 0,644x + 19,046$	8,481152	0,596238
L Humerus	L Femur	$y = 0,2455e^{0,7467x}$	0,053981	0,808703	$y = 0,2916x + 18,275$	6,400287	0,353412
L Humerus	R Femur	$y = -0,0029x^2 + 0,367x + 0,1596$	0,057273	0,843742	$y = 0,3959x + 14,677$	6,4557	0,504777
L Humerus	R Humerus	$y = -0,5135x^2 + 0,9288x + 0,1419$	0,061083	0,710493	$y = 0,7403x + 7,4887$	7,322382	0,821279
R Humerus	L Femur	$y = 1,0039x^2 - 1,131x + 0,6898$	0,097678	0,872238	$y = 0,4917x + 11,525$	7,730518	0,51049
R Humerus	R Femur	$y = 1,1226x^2 - 1,249x + 0,7101$	0,09731	0,869713	$y = 0,5521x + 9,68$	7,852347	0,596238
R Humerus	L Humerus	$y = 4,5851x^2 - 2,9244x + 0,8248$	0,114108	0,71854	$y = 0,9111x + 3,5397$	8,123493	0,821279

4.4 Results Neighbourhood analysis

The closest neighbours in regard to BMD value and cortical index were compared to the distance to the bone of the same individual to see how often the bones of individuals are closest to each other. The table 4.2 shows the total number of bones that could be compared per combination of bones and the resulting percentages.

Table 4.2: This table shows the group sizes for the combinations of bones and the percent accuracy of the neighbourhood analysis performed on the total groups.

4.2 Bone	Searched bone	Group size BMD	% BMD	Group size CI	% CI
Left femur	Right femur	37	18,92	43	13,95
Left femur	Left humerus	19	21,05	41	2,44
Left femur	Right humerus	29	6,90	40	7,50
Right femur	Left femur	37	13,52	43	11,63
Right femur	Left humerus	19	5,26	40	0
Right femur	Right humerus	29	13,79	40	7,50
Left humerus	Left femur	19	15,79	41	4,87
Left humerus	Right femur	19	5,26	40	7,50
Left humerus	Right humerus	15	20	40	5
Right humerus	Left femur	29	17,24	40	2,50
Right humerus	Right femur	29	10,34	40	5
Right humerus	Left humerus	15	0	39	7,69

Table 4.2: "Bone" refers to the type of bone whose values were used to find associated bones. "Searched bone" refers to the type of bone that the neighbourhood analysis was looking for. "Group Size BMD" and "Group Size CI" are the total amount of paired bones that were used for each neighbourhood analysis. "%BMD" and "%CI" are the percentage of individuals whose own searched bones were closest to their bones, which translates to the degree of success for the analysis.

4.4.1 Neighbourhood analysis on smaller groups

The neighbourhood analysis was also performed on smaller groups, starting with groups of five. The percentage of individuals whose correct bone was found with the help of the neighbourhood analysis is given in table 4.3.

Table 4.3: This table shows the percent accuracy of the neighbourhood analysis performed on five groups of five.

4.3 Bone	Searched bone	% BMD	% CI
Left femur	Right femur	56	36
Left femur	Left humerus	28	24
Left femur	Right humerus	40	28
Right femur	Left femur	68	44
Right femur	Left humerus	40	28
Right femur	Right humerus	44	48
Left humerus	Left femur	20	36
Left humerus	Right femur	40	28
Left humerus	Right humerus	32	56
Right humerus	Left femur	40	32
Right humerus	Right femur	36	40
Right humerus	Left humerus	24	52

Table 4.3: "Bone" refers to the type of bone whose values were used to find associated bones. "Searched bone" refers to the type of bone that the neighbourhood analysis was looking for. "%BMD" and "%CI" are the percentage of individuals whose own searched bones were closest to their bones, which translates to the degree of success for the analysis.

The neighbourhood analysis was also performed on groups of ten. This was performed on five groups of ten for each of the combinations that had a percent accuracy higher than 33%. Since the amount of BMD data was insufficient to make five groups, the number of groups for BMD was reduced per combination. Table 4 shows the number of groups that could be used and the percentage of accurate reassociated bones per combination.

Table 4.4: This table shows the percent accuracy of the neighbourhood analysis performed on groups of ten.

4.4 Bone	Searched bone	Number of groups	% BMD	Number of groups	% CI
Left femur	Right femur	4	37,50	5	34
Left femur	Left humerus	-	-	-	-
Left femur	Right humerus	3	20	-	-
Right femur	Left femur	4	32,50	5	32
Right femur	Left humerus	2	25	-	-
Right femur	Right humerus	3	26,67	5	20
Left humerus	Left femur	-	-	5	20
Left humerus	Right femur	2	20	-	-
Left humerus	Right humerus	-	-	5	32
Right humerus	Left femur	3	30	-	-
Right humerus	Right femur	3	23,33	5	26
Right humerus	Left humerus	-	-	5	28

Table 4.4: "Bone" refers to the type of bone whose values were used to find associated bones. "Searched bone" refers to the type of bone that the neighbourhood analysis was looking for. "Number of groups" are the total amount of groups that were used for each respective variable. "%BMD" and "%CI" are the percentage of individuals whose own searched bones were closest to their bones, which translates to the degree of success for the analysis.

After the groups of ten were analysed, the same steps were followed to make groups of 15. This meant that only for the left femora, the right femora were searched for both BMD and cortical index. The results and the number of groups are given in table 4.5.

Table 4.5: This table shows the percent accuracy of the neighbourhood analysis performed on groups of fifteen.

4.5 Bone	Searched bone	Number of groups	% BMD	Number of groups	% CI
Left femur	Right femur	2	30	3	24,44

Table 4.5: "Bone" refers to the type of bone whose values were used to find associated bones. "Searched bone" refers to the type of bone that the neighbourhood analysis was looking for. "Number of groups" are the total amount of groups that were used for each respective variable. "%BMD" and "%CI" are the percentage of individuals whose own searched bones were closest to their bones, which translates to the degree of success for the analysis.

After the groups of 15 were finished, the BMD a cortical index data was combined to see if combining the variables would make the reassociation of bones more accurate. The

first set of neighbourhood analyses was performed on the total groups. The group sizes and the percentages of accuracy are presented in table 4.6.

After this, five groups of five were made for each of the combinations of bones for the combined variables. The results are shown in table 4.7. Following the 33,33% boundary, groups of ten were also made, but since every combination had an accuracy above this limit for groups of five, neighbourhood analyses were performed on all the combinations for groups of ten. The results and the number of groups that could be formed per combination are presented in table 4.8. The same boundary was used for groups of fifteen, those accuracies are presented in table 4.9, and for the groups of 20, whose accuracies are presented in table 4.10. For the groups of 20, only the femur-to-femur combinations are given, since they are the only two combinations that scored higher than 33,33% for their groups of fifteen.

Table 4.6: This table shows the percent accuracy of the neighbourhood analysis performed on the total groups that were based on both the BMD values and the cortical indices.

4.6 Bone	Searched bone	Group size	% accurate
Left femur	Right femur	35	22,86
Left femur	Left humerus	19	26,32
Left femur	Right humerus	28	14,29
Right femur	Left femur	35	22,86
Right femur	Left humerus	18	11,11
Right femur	Right humerus	28	17,86
Left humerus	Left femur	19	21,05
Left humerus	Right femur	18	16,67
Left humerus	Right humerus	15	6,67
Right humerus	Left femur	28	7,41
Right humerus	Right femur	28	10,71
Right humerus	Left humerus	15	26,67

Table 4.6: "Bone" refers to the type of bone whose values were used to find associated bones. "Searched bone" refers to the type of bone that the neighbourhood analysis was looking for. "Group Size" refers to the total amount of paired bones that were used for each neighbourhood analysis. "%accurate" refers to the percentage of individuals whose own searched bones were closest to their bones, which translates to the degree of success for the analysis.

Table 4.7: This table shows the percent accuracy of the neighbourhood analysis performed on the five groups of five that were based on both the BMD values and the cortical indices.

4.7 Bone	Searched bone	% accurate
Left femur	Right femur	76
Left femur	Left humerus	44
Left femur	Right humerus	36
Right femur	Left femur	76
Right femur	Left humerus	52
Right femur	Right humerus	36
Left humerus	Left femur	44
Left humerus	Right femur	40
Left humerus	Right humerus	40
Right humerus	Left femur	48
Right humerus	Right femur	36
Right humerus	Left humerus	52

Table 4.8: This table shows the percent accuracy of the neighbourhood analysis performed on the groups of ten that were based on both the BMD values and the cortical indices.

4.8 Bone	Searched bone	Number of groups	% accurate
Left femur	Right femur	4	47,50
Left femur	Left humerus	2	35
Left femur	Right humerus	3	23,33
Right femur	Left femur	4	47,50
Right femur	Left humerus	2	35
Right femur	Right humerus	3	33,33
Left humerus	Left femur	2	25
Left humerus	Right femur	2	25
Left humerus	Right humerus	1	40
Right humerus	Left femur	3	20
Right humerus	Right femur	3	36,67
Right humerus	Left humerus	1	40

Table 4.7 and 4.8: “Bone” refers to the type of bone whose values were used to find associated bones. “Searched bone” refers to the type of bone that the neighbourhood analysis was looking for. “Number of groups” refers to the total amount of groups that were used for the neighbourhood analysis. “%accurate” refers to the percentage of individuals whose own searched bones were closest to their bones, which translates to the degree of success for the analysis.

Table 4.9: This table shows the percent accuracy of the neighbourhood analysis performed on the groups of fifteen that were based on both the BMD values and the cortical indices.

4.9 Bone	Searched bone	Number of groups	% accurate
Left femur	Right femur	2	43,33
Left femur	Left humerus	1	26,67
Left femur	Right humerus	-	-
Right femur	Left femur	2	36,67
Right femur	Left humerus	1	13,33
Right femur	Right humerus	2	20
Left humerus	Left femur	-	-
Left humerus	Right femur	-	-
Left humerus	Right humerus	1	6,67
Right humerus	Left femur	-	-
Right humerus	Right femur	2	20
Right humerus	Left humerus	1	26,67

Table 4.10: This table shows the percent accuracy of the neighbourhood analysis performed on the groups of twenty that were based on both the BMD values and the cortical indices.

4.10 Bone	Searched bone	Number of groups	% accurate
Left femur	Right femur	1	30
Right femur	Left femur	1	20

Table 4.9 and 4.10: "Bone" refers to the type of bone whose values were used to find associated bones. "Searched bone" refers to the type of bone that the neighbourhood analysis was looking for. "Number of groups" refers to the total amount of groups that were used for the neighbourhood analysis. "%accurate" refers to the percentage of individuals whose own searched bones were closest to their bones, which translates to the degree of success for the analysis.

4.5 Assessment of the neighbourhood analysis results

The accurate results and the inaccurate results of the neighbourhood analyses were plotted out against the value of the bone that was not recalculated to see if the distance from the average value has a lot of influence on the chances of a pair of bones being accurately reassociated. The graphs for the left femur to right femur combination are presented below as an example (figure 4.4 to 4.11). The other graphs are presented in appendix 2. The following properties apply to these graphs:

- the X-axis presents the BMD-value or cortical index of the known bone

- the Y-axis represents the absolute difference in BMD value or cortical index of the bones of an individual
- green dots represent individuals whose own bone was reassociated
- red dots represent the individuals whose bones were reassociated with bones of a different individual

After these graphs, the 3D graphs that were made for neighbourhood analyses that used both variables. These 3D graphs can be found in appendix 3. The following properties apply to these graphs:

- the X-axis presents the BMD-value of the known bone
- the Y-axis presents the cortical index of the known bone
- the Z-axis presents the absolute difference between the known bone and the searched bone of that individual
- green dots represent individuals whose own bone was reassociated
- red dots represent the individuals whose bones were reassociated with bones of a different individual

Bone mineral density (BMD)	Cortical index
4.4 Total groups	4.5 Total groups
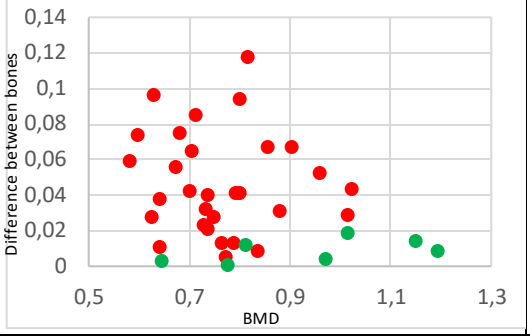	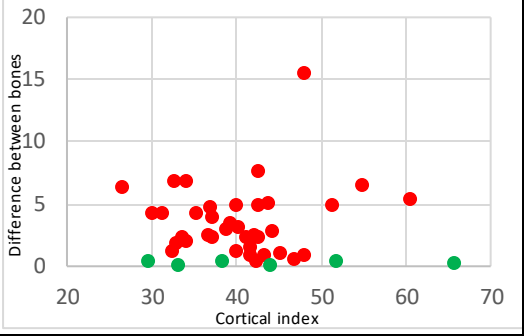
4.6 Groups of five	4.7 Groups of five
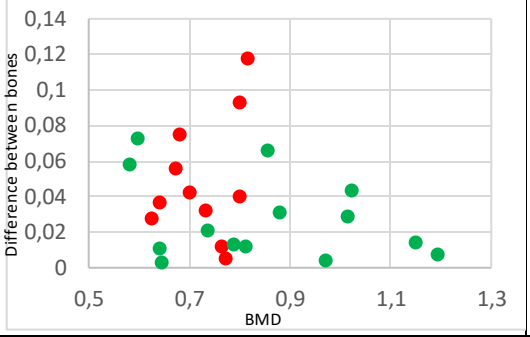	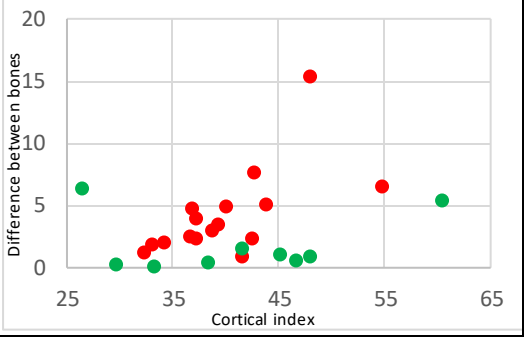
4.8 Groups of ten	4.9 Groups of ten
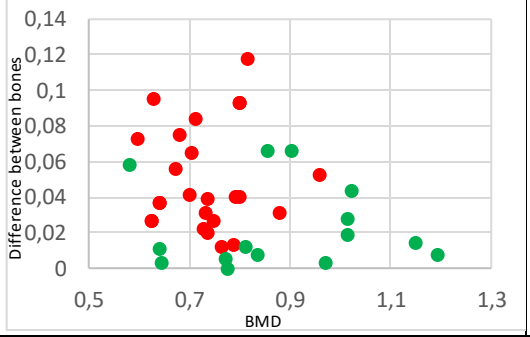	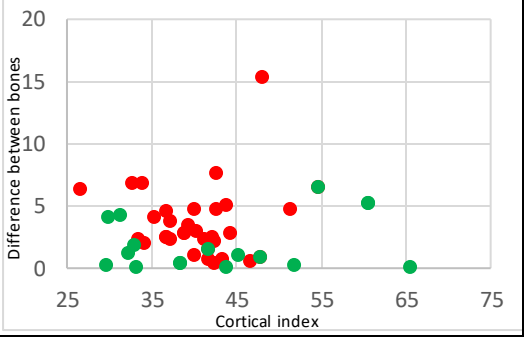
4.10 Groups of fifteen	4.11 Groups of fifteen
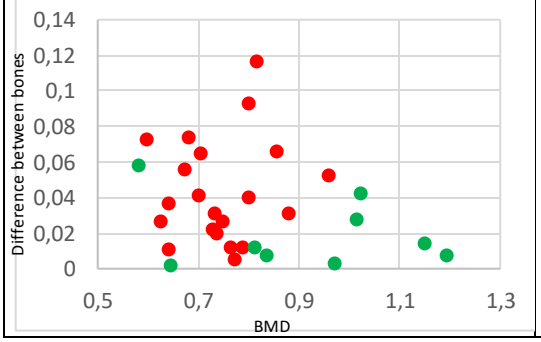	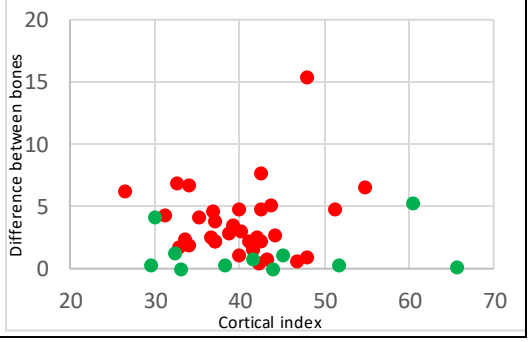

Figure 4.4 to 4.11: The difference between the BMD or cortical index of bones of an individual compared to their respective value for the left femur to right femur combination.
Green dots: accurately reassociated individuals
Red dots: inaccurately reassociated individuals

For each of the neighbourhood analyses that had an accuracy above the 33,33% threshold, a plot was made that show the distance to the nearest neighbour for a bone (Y-axis), compared to the value of the bone (X-axis). For the combined variables, the BMD is given on the X-axis, the cortical index on the Y-axis and the distance to the nearest neighbour on the Z-axis. These graphs were made to give an indication as to how likely it is that two bones that are matched with the neighbourhood analysis actually belong together. The graphs for the left femur to right femur combination are presented below as an example (4.12-4.18). The graphs for the other combinations can be found in appendix 4.

Bone mineral density (BMD) - groups of five

4.12 Left femur to right femur

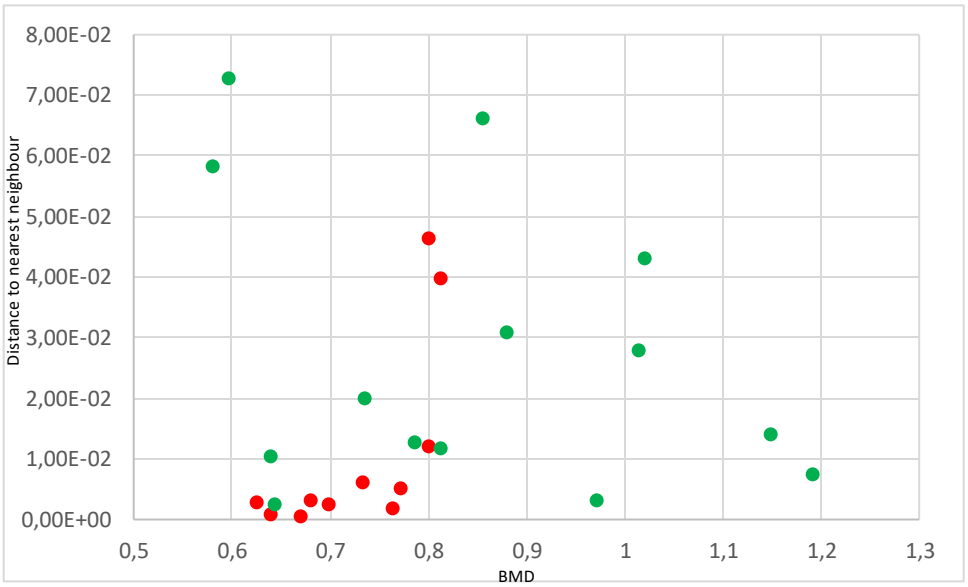

Figure 4.12: The distance from the BMD of a bone to the nearest neighbouring bone.
Green dots: accurately reassociated individuals
Red dots: inaccurately reassociated individuals

Cortical index - groups of five

4.13 Left femur to right femur

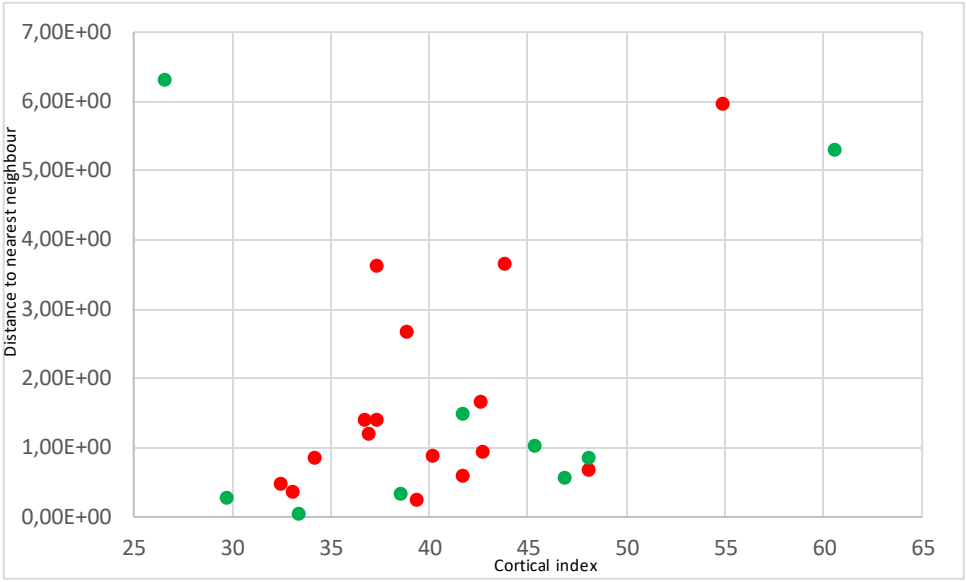

Figure 4.13: The distance from the cortical index of a bone to the nearest neighbouring bone.
Green dots: accurately reassociated individuals
Red dots: inaccurately reassociated individuals

The BMD and cortical index combined- groups of five

4.14 Left femur to right femur

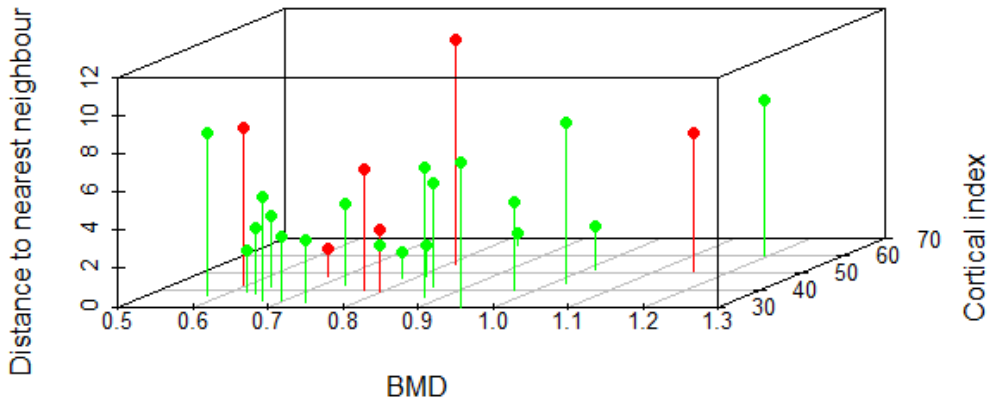

Figure 4.14: The distance from the BMD and cortical index of a bone to the nearest neighbouring bone.
Green dots: accurately reassociated individuals
Red dots: inaccurately reassociated individuals

Bone mineral density (BMD) - groups of ten

4.15 Left femur to right femur

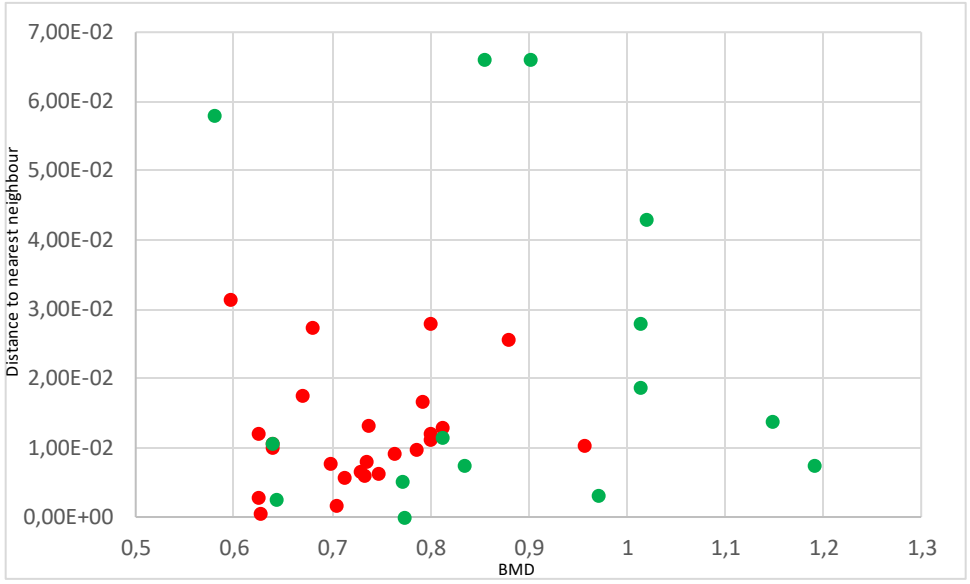

Figure 4.15: The distance from the BMD of a bone to the nearest neighbouring bone.
Green dots: accurately reassociated individuals
Red dots: inaccurately reassociated individuals

Cortical index - groups of ten

4.16 Left femur to right femur

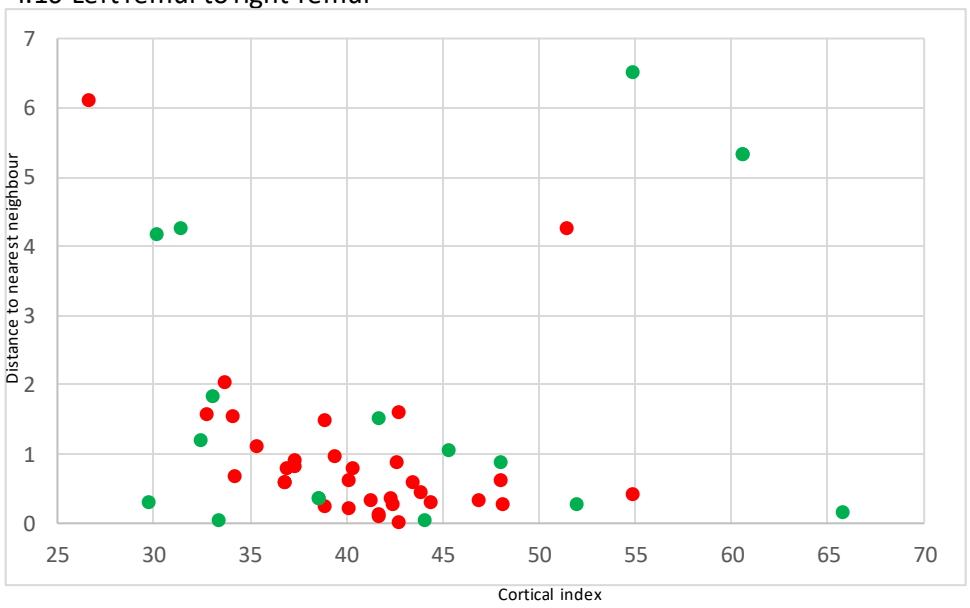

Figure 4.16: The distance from the cortical index of a bone to the nearest neighbouring bone.
Green dots: accurately reassociated individuals
Red dots: inaccurately reassociated individuals

The BMD and cortical index combined- groups of ten

4.17 Left femur to right femur

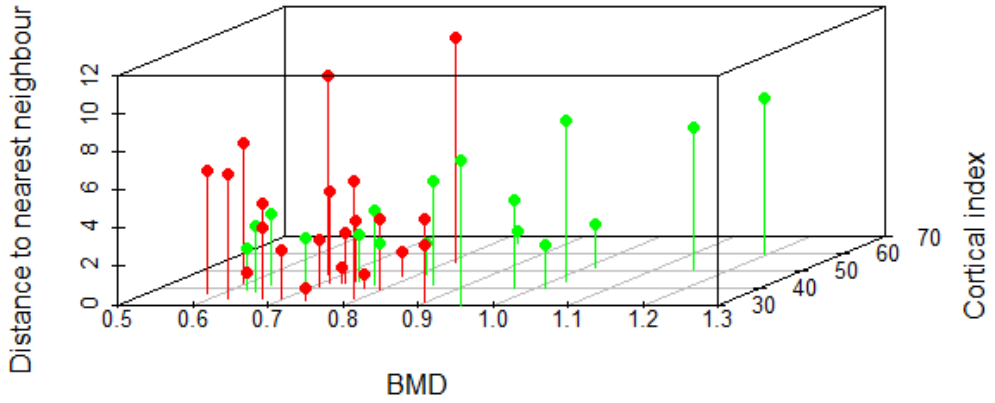

The BMD and cortical index combined- groups of fifteen

4.18 Left femur to right femur

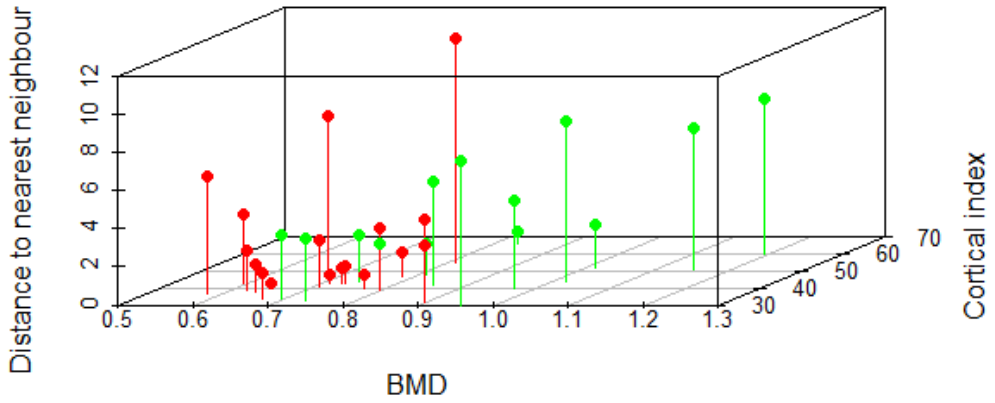

Figure 4.17 and 4.18: The distance from the BMD and cortical index of a bone to the nearest neighbouring bone.
Green dots: accurately reassociated individuals
Red dots: inaccurately reassociated individuals

4.6 A set of guidelines

For the set of guidelines, summarization of some of the data was needed, which is presented in the following tables (table 4.11 to 4.13). Each table shows the accuracies for each variable for one group size. Only the groups that had accuracies above the 33,33% threshold are included, since the use of the groups that scored below the threshold is not advised.

Table 4.11: This table shows the percent accuracy of the neighbourhood analyses performed on the groups of five that were based on both the BMD values, the cortical indices, and the combined variables.

4.11 Bone	Searched bone	% accurate BMD	% accurate cortical index	% accurate combined variables
Left femur	Right femur	56	36	76
Left femur	Left humerus	-	-	44
Left femur	Right humerus	40	-	36
Right femur	Left femur	68	44	76
Right femur	Left humerus	40	-	52
Right femur	Right humerus	44	48	36
Left humerus	Left femur	-	36	44
Left humerus	Right femur	40	-	40
Left humerus	Right humerus	-	56	40
Right humerus	Left femur	40	-	48
Right humerus	Right femur	36	40	36
Right humerus	Left humerus	-	52	52

Table 4.11: "Bone" refers to the type of bone whose values were used to find associated bones. "Searched bone" refers to the type of bone that the neighbourhood analysis was looking for. "%accurate" refers to the percentage of individuals whose own searched bones were closest to their bones for that variable or those variables, which translates to the degree of success for the analysis.

Table 4.12: This table shows the percent accuracy of the neighbourhood analyses performed on the groups of ten that were based on both the BMD values, the cortical indices, and the combined variables.

4.12 Bone	Searched bone	% accurate BMD	% accurate cortical index	% accurate combined variables
Left femur	Right femur	37,50	34	47,50
Left femur	Left humerus	-	-	35
Left femur	Right humerus	-	-	-
Right femur	Left femur	-	-	47,5
Right femur	Left humerus	-	-	35
Right femur	Right humerus	-	-	33,33
Left humerus	Left femur	-	-	-
Left humerus	Right femur	-	-	-
Left humerus	Right humerus	-	-	40
Right humerus	Left femur	-	-	-
Right humerus	Right femur	-	-	36,67
Right humerus	Left humerus	-	-	40

Table 4.13: This table shows the percent accuracy of the neighbourhood analyses performed on the groups of fifteen that were based on both the BMD values, the cortical indices, and the combined variables.

4.13 Bone	Searched bone	% accurate BMD	% accurate cortical index	% accurate combined variables
Left femur	Right femur	-	-	43,33
Right femur	Left femur	-	-	36,67

Table 4.12 and 4.13: "Bone" refers to the type of bone whose values were used to find associated bones. "Searched bone" refers to the type of bone that the neighbourhood analysis was looking for. "%accurate" refers to the percentage of individuals whose own searched bones were closest to their bones for that variable or those variables, which translates to the degree of success for the analysis.

Whilst this chapter has presented the data that came out of this research, the following chapter will provide the interpretation of these results. It will also discuss the applicability of the BMD values and cortical indices to the reassembly of individuals with the use of the data provided here.

5. Discussion

The discussion chapter will begin with interpreting the results from each of the steps taken in this research. These interpretations will, firstly, describe the results in short after which the indicators for relations between bones, usability for reassociation and the differences between variables and group sizes will be given. Afterwards, the research questions will be answered with the use of these interpretation. This chapter will finish with the possible application of the results of this thesis and its limitations, and the future research that is advised based of the outcome of this research.

5.1 The measurement data

The data that resulted from the DEXA-scans and the measurements on the CT-scans was plotted out to see how the data was divided over the range that it occupied. This resulted in a set of graphs that present a normal distribution of the data.

The normal distribution for the BMD values of the femora had a similar shape. They present a large peak between 0,7 and 0,8 and their extension towards the higher end runs a bit further than their extension towards the lower end. The peak of the values for the right femur is higher and thinner than that of the left femur.

The normal distributions for the BMD of the humeri, however, differ from each other and from the distributions of the femora. Their peaks lay around the 0,4 with the peak of the right humerus a bit lower than that of the left humerus. The lower extension of the right humerus is also the smaller one, whilst the higher extension of the left humerus is smaller. Lastly, the peak of the values for the right humerus is higher and thinner than that of the values for the left humerus.

This indicates that for the femora there is a high chance that the bone mineral density values can be used for their reassembly, but that the values of the humeri are more diverse and, therefore, less likely to be successful. When the values of the femora are compared to the values of the humeri it can be seen that the values of the femora are almost twice as high. The decision was therefore made to create regression models for the BMD values for each combination of bones before the neighbourhood analysis was performed.

The normal distributions for the cortical indices for the femora also had similar peaks around 40. Their extensions are both short towards the lower side and they both only have a few values further towards the higher side. The peak of the right femora is slightly lower and wider than that of the left femora.
The distributions for the humeri are similar to those of the femora, except their peaks lay around 30-35 and their extensions towards the higher side are a bit larger. The peak of the right humeri is also slightly lower and wider than that of the left humeri.
The similarity in graphs indicates that the cortical indices are likely useful for the reassociation of bones, since similar values are needed for the reassociation to work.
Since the peaks of the femora and humeri had a slight difference, it was decided that regression models were also to be made for each of the combinations of bones for the cortical indices.

5.2 The regression models

Regression models were created for each of the combinations of bones for both the BMD values and the cortical indices. The models were made in both directions. This was done, because the recalculation from one bone type to another bone type might give a different level of accuracy than the recalculation in the other direction.
The correlation coefficients, which indicate to what degree two variables are related, range between the 0,71 and 0,94 for the bone mineral density models. The highest correlation coefficients, 0,94 and 0,92, come from the models for the relation between the left and right femora. These high correlation coefficients were expected, since similar results were also found in other studies (McClanahan et al 2002, 586; Curate et all. 2013, 296.e1-296.e3).
The correlation coefficients for the combinations of humeri with femora all lay between 0,81 and 0,87. These combinations of bones will, therefore, most likely give similar results when these combinations are used to reassociate bones. The slight difference that was expected between bone combinations from the same side and bone combinations from different sides was not represented in the correlation coefficients, but the standards deviations are slightly higher for the latter combinations.
The lowest correlation coefficients, 0,71 and 0,72, belong to the combinations of the humeri. This might be due to the effect that activity can have on the bone mineral

density of the humerus (McClanahan et al 2002, 586). The reassociation of bones based in the BMD of humeri will, therefore, be less accurate than that of the femora. The correlation coefficients are, however, still high and it is thus possible that the humeri can still be used.

The correlation coefficients for the cortical indices range between 0,35 and 0,84. The highest correlation coefficients range between the 0,82 and 0,84. They are associated with the comparisons between humeri and between femora, with the latter being slightly higher. These correlation coefficients indicate that the cortical indices can reliably be used to reassociate bones, but this should be done with caution. For the femora the BMD's will most likely be more accurate, since those coefficients are higher, but the cortical indices will probably give better results for reassociating humeri.
The combinations with both humeri and femora give a much lower correlation coefficient. For most of them this ranges between 0,50 and 0,60. These combinations are, therefore, not likely to accurately reassociate bones, but they might still be useful to a certain degree. For the combinations of the left femur with the left humeri the correlation coefficients are around 0,35. These combinations will, thus, not be very accurate when they are used to match these bones, but they were included in the rest of the analysis.

5.3 The neighbourhood analyses

With the use of the nndist function in R the nearest neighbours for each bone were identified. The distances to the nearest neighbours were compared to the bones of the same individual. If these two distances are the same, they are considered as a positive reassociation of bones, but if the nearest neighbour is not associated with the original bone, then it is considered as a negative result.
The skeletons for whom both bones of a combination had the needed values were selected and used in the neighbourhood analysis.

5.3.1 Total groups

The first set of neighbourhood analyses were performed on the total amounts of skeletons that had the needed values for a combination. This resulted in groups of very different sizes, especially for the bone mineral density measurements.

The results of these neighbourhood analyses for the BMD values are surprisingly inconsistent. It was expected that combinations of bones would have similar levels of accuracy in both directions, but this was not the case. The only combinations of bones that gave similar results in both directions were the right femur with the left humerus and the right femur with the right humerus, with the latter still having a small difference. This is presumably caused by two factors.

The first and main reason is the group size. Since the number of individuals in the total groups is relatively large in relation to the differences between bones, it is very likely that the number of values that are used in the neighbourhood analysis are creating random accuracies. It becomes more likely that for one pair of bones the reassembly is only accurate in one direction if the concentration of values increases (Figure 5.1).

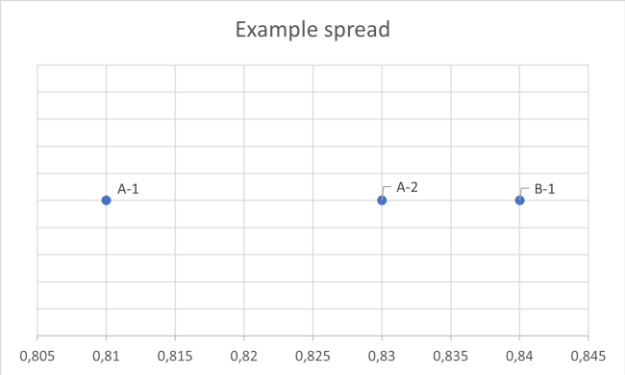

Figure 5.1: This figure contains fake data in order to shows what goes wrong in a neighbourhood analysis of too much data is entered compared to the difference within one individual. In this figure A and B are two different individuals and 1 and 2 are two different bones. If the distance from 1 to 2 are measured, A1 will give a positive outcome, but if the distance from 2 to 1 are measured A2 will give a negative outcome.

Since the percentages of accuracy of the total groups are low it is possible that what is explained in figure 5.1 causes the accuracies to be slightly random. If the group totals would increase further, the accuracies would decrease further, and this randomness would also most likely increase.

The second factor that appears to have had influence on these results is chance. All of the percentages represent only small numbers of combinations that were successful. Most of them range between 0 and 5 successful combinations and only the combination

left femur to right femur reaches 7. It is very likely that many of these combinations are just the few individuals for whom the recalculation formulas work best, or the individuals that have the furthest outlying values, which would decrease the chances of other individuals interfering with their reassociation.

The results of neighbourhood analyses performed on the cortical indices of the total groups have lower levels of percentual accuracy than the BMD values. This is most likely caused by the larger group sizes that were available for the cortical indices. The overlap of pairs has increased with the increase of individuals and, subsequently, this also caused the percentual accuracy to decrease.
The total number of accurate reassociations ranges between 0 and 3 for most of the combinations. The combinations that only include the femur are slightly larger with 5 and 6 accurate pairs. This indicates that the total groups are also too large for the neighbourhood analysis when looking at the cortical index. The values appear a bit more similar than those of the BMD results, when comparing a combination of bones in two directions, but since the percentages are so low it is hard to say if this is an indicator for a pattern or merely a coincidence, similar to what effected the BMD percentages.

5.3.2 Groups of five

In order to see if the results would improve for smaller amounts of individuals, five groups of five were made from random individuals for each of the combinations. The neighbourhood analysis was then performed on each of the groups and the total percentual accuracy was calculated for each combination of bones.
The accuracies for these neighbourhood analyses were much better. For the bone mineral density, the left femur and right femur combinations presented the best results of 56% and 68%. Whilst not being very close to each other, these percentages lay much higher than the other outcomes for groups of five. All the combinations of bones give similar accuracies in both directions, which is more in line with what was expected. Most of them have around 40% accuracy, but as indicated by the regression models for the humeri, their combinations resulted in lower accuracies, namely 32% and 24%. This is thus due to their lower level of correlation. The left femur and left humerus combinations also present lower accuracies, 20% and 28%. These lower percentages were not expected since their regression models indicated that these two bones had a

reasonable relation in terms of BMD value. The reason why this combination of bones had a lower accuracy is uncertain. It might be caused by unfortunate sampling, but for now these two groups, together with the left humerus-right humerus combinations, were excluded from the further analysis.
These groups were excluded from neighbourhood analyses performed on slightly larger groups, since their level of accuracy was lower than 33,33%.

For the groups of five that were based on the cortical indices, the highest levels of accuracy were found for the combinations of the left humerus with the right humerus and vice versa. They had accuracies of 56% and 52% respectively. This is significantly better than the accuracies found for these combinations with the use of the BMD values. For most of the other combinations, this was not the case.
Most of the combinations have similar percentages in both directions. The combinations between the femora give percentages around 40%, which is less accurate than the results of the BMD groups. This was expected, since the correlation coefficients were lower for the cortical indices for these combinations than those of the BMD values.
Most of the other combinations also correlate with their correlation coefficients. The right femur-right humerus combinations result in percentages of 40% and 48% and their correlation coefficients are around 0,6. The right femur-left humerus and the left femur-right humerus combinations have percentages around 28% and their coefficients are around 0,5. The only combinations that give results that are slightly higher and varied than expected are the combination of the left femur with the left humerus and the same combination in the other direction. Their percentages are 24% and 36% respectively, whilst their correlation coefficients are around 0,35. It is, therefore, believed that these higher percentages are caused by similar patterns as the higher percentages found for the total groups, because the relations between the cortical indices between these two bones that were found with the regression models, are not good enough to present these high results.
Nevertheless, the same boundary of 33,33% was used for excluding combinations with low accuracies from neighbourhood analyses of larger groups. The left humerus to left femur combinations was, thus, included, but the results should not be seen as significant.

5.3.3 Groups of ten

For the groups of ten that were created for the BMD values, the percentual accuracies were about half the size of the accuracies of the groups of five. The combinations of bones did still result in similar values for both directions. The only combinations that had a slightly larger percentual difference were the combinations between the left femur and the right humerus, which had a difference of ten percent. Since the difference in number of bones only corresponds to three bones, this difference was written off as insignificant.

The right femur and left femur combinations had slightly higher accuracies, just as their corresponding groups of five individuals had slightly higher accuracies amongst their respective groups. For the groups of ten the left femur to the right femur combination had the highest level of accuracy, which also corresponds with the correlation coefficients found for these combinations. This is, however in contrast with the groups of five, where the reversed combination had higher levels of accuracy. This difference could be caused by the fact that the total number of samples that were used in this analysis were not high enough, which resulted in a small chance factor in the neighbourhood analysis and its outcome.

The 33,33% boundary was also used on the groups of ten, which meant that the neighbourhood analysis was only performed on the left femur to right femur combination for the BMD values.

The accuracy of the groups of ten for the cortical indices was also much lower than that of the corresponding groups of five for most of the combinations. There was a slightly less drastic decrease in accuracy for the right femur to left femur combination and there was barely a change in accuracy for the left femur to right femur combination. These combinations presumably changed less because the two bones are more related to each other in terms of cortical thickness, which could result in larger groups staying more accurate, whilst other combinations of bones decrease faster in accuracy when their group sizes increase. This does, however, not account for the accuracy of the left femur to right femur group staying at a similar level. The reason why this combination of bones only had a percentual decrease of 2% is uncertain.

The 33,33% boundary was also used for these groups, which means that only the left femur to right femur combination is used for the groups of 15.

5.3.4 Groups of fifteen

The left femur to right femur combination had an accuracy of 30% for the bone mineral density groups of 15. This level is somewhat lower than the accuracy of groups of 10, but still much larger than the accuracy of the total group of 37. The results of this neighbourhood analysis are, thus, as expected.

The same combination had an accuracy of 24,44% for the cortical indices groups of 15. This level is lower than the accuracy of the groups of ten, which means that if the level of accuracy indeed stays similar between groups of five and ten, then the line of accuracy does start to lower somewhere between the groups of ten and fifteen.

The accuracy of 24,44% was much closer to the level of accuracy present in the total groups than expected. The total group still has half the level of accuracy but is almost three times as large.

This weird curve for the accuracy levels for the cortical index data is possibly caused by the presence of a few outlying individuals that remain accurately reassociated when the group size increases, combined with the possibility that the random samples taken for the smaller groups had an unfortunate combination of individuals that kept the accuracy on the same level.

5.3.5 Total groups for the BMD-cortical index combination

All the combinations of bones had an increase in accuracy when the two variables were combined, except for the right humerus to the left femur and the left humerus to right humerus combinations. The increase in accuracy also differs per combination. The right humerus to left humerus, for example went from 0% and 7,69% to 26,67%, whilst the left femur to right femur combination went from 18,92% and 13,95 % to 22,86%. Unfortunately, none of these total groups resulted in accuracies above the 33,33% threshold.

For the left femur and right femur combinations the accuracies became more similar in both directions, but for the other combinations the accuracy differences between the directions remained similar or became larger. For the left humerus to right humerus combination the directions even switched in terms of highest and lowest accuracy.

For these total groups the accuracy levels did, thus, get slightly better, but they are still largely influenced by the same factors that influenced the total groups of the BMD-values. Therefore, groups of five were created for each of the combinations to see if the accuracy also increased for that group size.

5.3.6 Groups of five for the BMD-cortical index combination

Combining the two variables had a positive increase in accuracy for some of the combinations of bones, whilst other remained similar in accuracy or even decreased. The combinations of the left femur and right femur increased in accuracy in both direction to 76%. The left femur and left humerus combinations also both increased to an accuracy of 44%. The combination from the right femur to the left humerus got an accuracy of 52%, whilst the combination did not get a better accuracy in the other direction and only got 40% accuracy. Similarly, the right humerus to left femur combination got an accuracy of 48%, whilst the other direction remained in the middle of its BMD and cortical index accuracy for groups of five with 36%.
There was one combination that decreased in accuracy. The right femur to right humerus combination ended up with an accuracy lower than both the accuracies found when looking at the separated variables. The other combinations remained between their accuracies from the groups of five for their BMD's and cortical indices.

The changes in accuracy originate from the relation of the BMD values of an individual's bones with those of the cortical indices of the same bones. If the relation is good, then the bones will become more dispersed when they are plotted out, resulting in relatively smaller differences within an individual and larger differences between individuals. The reassociating of bones for which this is true will become more accurate. If the relation between BMD and cortical index of a bone is less good, then the distance between bones of an individual and the distance between individuals might change, but the amount of accuracy will similar. Lastly, if the relation between the two variables of a bone is bad, then the bones of different individuals will get closer to each other and consequently, the accuracy will also decrease, which is what happened for the combination of the right femur to the right humerus.

5.3.7 Groups of ten for the BMD-cortical index combination

The percentage of accuracy were lower for most of the groups of ten then for the groups of five. The only two combination for whom this was not the case are the left humerus to right humerus combination and the right humerus to right femur combinations. The left to right humerus combination remained the same in accuracy, which could be explained by the low amount of data that is present for this combination (only 15 individuals). Due to this low amount of data, the accuracy could have been tainted by random individuals with similar values and/or by random individuals with uncommon values.

The right humerus to right femur combination had a very small increase in accuracy form 36% for the groups of five to 36,67% for the groups of ten. This very slight increase in accuracy is most likely caused by the need to duplicate a few of the individuals and their data to reach the required number of individuals for three groups. These two duplicated individuals also turned out to be correctly reassociated individuals for their second appearance.

Overall, the results of the combined groups of ten are much better than those of the separate variables. The femur-to-femur combinations even have accuracies of 47,5%. The combinations of humerus to humerus and femur to femur also have the same levels of accuracy in both directions.

There is, however, more variation between the combination of different bones. The combinations of femora with the right humerus have similar accuracies in both directions, but the combinations of femora with the left humerus do not. When the left humerus is used to find these femora, the accuracy is only 25%. These combinations, where the left humerus is used to find other bones, and the combinations between the left femur and right humerus, which were similar in accuracy, but still low, are, thus, excluded from the groups of fifteen.

5.3.8 Groups of fifteen for the BMD-cortical index combination

All the combinations only had enough data to form one or two groups of fifteen. The levels of accuracy will, thus, be more influenced by the individuals that are present, and they will, consequently, be less telling of how accurate the neighbourhood analyses actually are for groups of fifteen. For the two combinations between the humeri, the

total groups were already groups of fifteen. The results are, thus, the same.
The accuracy for all the combinations dropped when the groups were increased to fifteen individuals. The only combinations for whom the accuracy was still above the 33,33% threshold are the combinations of the femora. All of the combinations for which both directions of searching bones, were present, had similar percentages of accuracy and they, at most, only differed two positive reassociations. The only two that do not give similar results are the combinations of the humeri, which were already discussed when the total groups were described.
The only combinations for which the groups of twenty were formed, are the combinations of the femora.

5.3.9 Groups of twenty for the BMD-cortical index combinations

Both of the groups scored below the 33,33% threshold. Both of the directions only had a difference of two correctly reassociated bones, but since there was only enough data to form one group per direction, this meant that they did have an accuracy difference of 10%.
No further groups or larger groups sizes were formed, since both of these groups scored below the threshold.

5.4 Assessment of the neighbourhood analysis results

5.4.1 Graphs of the difference within an individual

Many of the graphs that were made for the results of the neighbourhood analyses performed on the BMD-values, have a similar pattern. The accurately reassociated bones have the smallest difference compared to the other bones of similar BMD values. The bones that have larger differences are generally wrongly reassociated. The bones that lay further away from the average bone mineral densities, often also have a larger difference between the bones, but their chances of being accurately reassociated also increase. This is because, the further away from the average a bone lies, the smaller the chance becomes that the bones of another individual have similar values. This mostly occurs amongst bones that have values higher than the average, most likely because their distance from the average is also larger.
The bones that had a negative result, meaning that they were incorrectly reassociated,

tend to be clustered around the average value. The negative results also tend to have larger distances between their values, than the bones that were accurately reassociated with similar BMD-values.
There seems to be a correlation between the level of accuracy and the degree to which the pattern described above can be seen in the plot. With higher degrees of accuracy, larger distances get more often accurately reassociated, and the distribution of the negative results shrinks towards the average. Consistently, the pattern described above is less visible in plots based on combinations and group sizes that have a low level of accuracy.

The same pattern can be seen amongst the plots made for the cortical index results. The results stray relatively further from the average, and the cluster around the average appears more spread out. The difference between two bones with less common values is often still too large to reassociate the bones accurately.
Thus, whilst the reassociation of bones becomes more accurate with distance from the average when looking at BMD values, this appears to not be the case for the cortical indices. Instead, the cortical indices are mainly dependent on small differences between the bones, independent of their distance from the average cortical index.

When looking at the 3-dimensional plots made for the combined variables, similar patterns appear for most of the groups that have accuracies above the 33,33% threshold. This means that most of the inaccurately reassociated bones are located on the lower portion of the BMD-axis. On the cortical index-axis, the data is more spread out, with sometimes miner clustering around the lower side. For most of the plots based on accuracies below the threshold and some of the plots that lay above it, the distribution of accurately versus inaccurately reassociated bones seems random. For the plots that show accuracy, but no pattern in the distribution, the level of accuracy is most likely caused by the spread of the data within the groups, because the accuracy will be much higher, if the individuals of a groups are spread apart. The spread of the individuals within a group can, thus be very influential on the level of accuracy that comes out of the neighbourhood analyses performed in this thesis, but it will similarly also have much influence on the success of the reassociation of bones found in commingled assemblages.

5.4.2 Graphs of the difference to the nearest neighbour

When looking at the relation between accurate and inaccurate reassociations, the value of the bone, and the distance to the nearest neighbour, no real pattern can be observed amongst all the graphs. For the 2-dimensional plots, many of the points lay in the same range. For the BMD plots, most of the combinations show a severe decrease in inaccurate reassociations with higher values. The only combinations for whom there seems to be no decrease in inaccurate reassociations with higher values, are the combinations involving the left humerus.
The same sort of distribution of accurate and inaccurate reassociated bones can be seen amongst the plots for the cortical indices. Here, the inaccurate and accurate bones lay in the same region, except for when the cortical index increases in value, which is accompanied with a decrease in inaccurate bones. The only plots for whom this does not seem to be the case are the plots with an accuracy below 36%.

When looking at the 3-dimensional plots, that have both variables compared to the distance to the nearest neighbour and the accuracy of reassociation, once again, similar patterns appear. The accurate and inaccurate bones appear in the same region with similar distances to their nearest neighbour, but when the value of the variables increases, the number of inaccurate bones decrease. This seems to be slightly more the case for the BMD values, than for the cortical indices, but it can be seen in both. However, in almost half of the plots this trend cannot be observed. All of the plots in which this cannot be observed, except for one, are based on combinations that involve the left humerus. In some of the plots that involve the right femur, the trend is present, but less obvious.

If bones are to be reassociated with these variables, a reasonable reliability is needed. The reliability increases with higher values if the pattern in present, but if the pattern is not present, the reliability will not be higher than the percentual accuracy of the neighbourhood analysis. The left humerus has, thus, a low level of reliability for reassociation based on the bone mineral density or based on the bone mineral density combined with the cortical index. Similarly, combinations that scored below 36% accuracy when using the cortical index, also don't have a higher reliability for higher values.

For the rest of the combinations, the reliability of an accurate reassociation increases with the value of the bones and this should, therefore, be applicable to commingled remains. But, when the values of the bones are located in the clusters of the lower values, the reliability decreases and it will, thus, become less useful for individuals that have values around the average.

5.5 Answering of the research questions

- Can a consistency in bone mineral density between sides of a skeleton be found using DEXA-scanning?

  The regression models that were made to compare the bone mineral densities of different bones had descent correlation coefficients. For the combinations of bones of the same sides of the skeleton, these correlation coefficients range between 0,81 and 0,87, which means that there is indeed a good relation in BMDs of the same side of an individual. When the bones were compared diagonally, for example when the right femur and the left humerus were compared, the correlation coefficients also ranged between the 0,81 and 0,87. This similarity in range indicates that the relation between bones of the same side of an individual are not better than the relation of bones from different sides of an individual (excluding the relations between the same bones from different sides). There is, thus, not a consistency in BMD between sides of a skeleton, but there is a good relation between the BMD's of humeri and femora in general.
- Is there a relation in bone mineral density between different bones of an individual?

  The relations between different bones of an individual that were found in this research are of sufficient quality to get positive results for some of the combinations of bones. When looking at the correlation coefficients, the femur-to-femur comparisons have the best relation, followed by the combinations between femora and humeri. The combinations of both humeri have the least accurate correlation coefficients of 0,71 and 0,72. The combinations of the left and right humeri and the combinations between the left femur and left humerus are the only ones that did not result in any accuracies above 33,33% and, thus, they are the only combinations for whom the relation in regard to bone mineral density alone was not good enough for the analysis performed for this thesis.
- Is there a consistency between sides of a skeleton and cortical bone loss, that can be found using CT-scanning?

  A cortical bone index was used in order to measure the cortical bone thickness.

The regression models that were made for each of these combinations of bones gave varying correlation coefficients. When the humeri were compared and when the femora were compared, these correlation coefficients were reasonably high (just above 0,8), but when the humeri were compared to the femora, the correlation coefficients only reached 0,6 and lower. The comparisons of the right femur with the right humerus gave the best results, whilst the comparisons between the left femur with the left humerus presented the lowest. There is, thus, a small consistency in cortical bone index for the right side of the skeleton, bust the best relations between bones are found within types of bones.

- Is there a relation in cortical bone loss between different bones of an individual?
  The relations in cortical bones loss between different bones of an individual that were found in this research vary depending on the combination of bones. The relation between the same type of bone of different sides is much better, and thus more useful, than the relation between different bones. Even though the correlation coefficients of bones of the same side were not high, they did give accurate reassociation levels that were just above the 33,33% threshold for some of the combinations when looking at groups of five. In most instances, the relation in cortical index between different bones of an individual is, thus, much less accurate and applicable for reassociating commingled remains than the relation of bone mineral densities. The only bones that have a better relation are the humeri and the combination of the left humerus to the left femur.
- Can bone mineral density and cortical bone loss be used to sort out individuals from commingled remains?
  In this research the two variables were also combined, to see if the number of accurately reassociated bones would improve if both variables were considered. For the total groups, the percentage of accuracy increased, but it did not reach above the 33,33% threshold. Therefore, groups of five were made and, subsequently, larger groups were formed for the combinations for whom the threshold was exceeded.
  In most cases the results from these neighbourhood analyses that use both variables, were better than those of the separate variables. All the combinations

scored above the threshold when looking at groups of 5, with the femur-to-femur combination reaching up to 76% accuracy. These two combinations also scored above the threshold for groups of fifteen. When trying to reassociate bones of commingled individuals, the combined variables are, thus, a better option than the separate variables when looking at accuracy.

The main research question:

- Can CT and/or DEXA-scans be used to identify individuals from archaeological commingled remains?
  Depending on the number of individuals present amongst the commingled remains and the combinations of bones, it is possible to reassociate some of the bones of an individual using CT and DEXA-scans. In most instances the group size can't exceed five individuals for this reassociation to be reliable. The level of accuracy also depends on how different the values of the bones of individuals are from the bones of the other individuals present amongst the commingled remains. The following part of this chapter will discuss the issues that come with this application of cortical indices and BMD's, since there are many factors that limit it.

5.6 The possible application and the limitation

As described above, the application of the cortical indices and BMDs to the reassociation of bones is limited by various factors. Group size, which bones are combined, what variables are used, the individuals that are present amongst the commingled remains are the main ones, but others, like the cost of making these scans, also limit the application.

5.6.1 Group size

When applying BMD's and cortical indices for the reassociation of the bones, the number of individuals that is present is very influential on the accuracy. When only one variable can be used, the group size cannot exceed five individuals, or the accuracy would become too low. Only the left femur to right femur combination has a possible application for groups up to ten.

When the two variables can be combined, the groups size can also increase. Groups of five show high enough accuracies for all the combinations and many of the combinations also have high enough accuracies for groups of ten. The left femur and right femur combinations could possible even be applied to combinations of fifteen. Unfortunately, the exact group size of a set of commingled remains is hardly ever known. The technique described in this thesis, should, therefore, not be used in cases with large numbers of individuals, nor in cases where the number of individuals is estimated with much uncertainty. The reassociation of bones using the BMD and cortical index is only reliable when the group size is small enough.
The same limitation is present with other techniques that try to reassociate individuals. All the techniques based on bone size that were tested by Byrd and LeGarde (2018) had similar issues. They state that the group size is very influential on the accuracy of recombination, but they do not provide the percentage or number of individuals that could be accurately reassociated for different group sizes, which prevents the comparison to this research (Byrd and LeGarde 2018, 345-346).

5.6.2 Combination of bones

The reliability of using the BMD's and cortical indices to reassociate bones is also very dependent on which combination of bones is used and in what direction the search is applied. Most of the combinations of bones have different levels of accuracy. They often also have a difference in accuracy depending on which bone is used to search for the other bone in that combination. If the left femur, for example, is used to search for the right femur in groups of five, meaning that the right femur is recalculated using table 4.1 and the nearest neighbour of the left femur is searched, then the accuracy is much less than when the left femur is recalculated and the right femur is used to search for the associated bone.

The left humerus does not seem to follow the same pattern when bone mineral density is plotted out against the nearest neighbour. This is presumably related to a difference in BMD change between the left humerus and the rest of the body. There are, however, still some combinations that involve the left humerus that have an accuracy above 33,33%. For these combinations the accuracy of reassociation does not increase with the bone mineral density.

When bones are to be reassociated using bone mineral densities or cortical indices, it is, thus, important that the level of accuracy for the combination is checked and that the bones are reassociated using the right direction.

The combination of bones is also a large factor in reassociating bones based on their size. They generally exclude combinations that have different types of bones from different sides, but there already is a large difference in accuracy per side and per bone type. Their humerus to humerus and femur to femur comparisons give better results than their comparisons between the humerus and femur, but the exact level of accuracy is unfortunately not presented in most of these studies. The study by Vickers et al. 2015, did provide levels of accuracy for each of their combinations, but these were later proven to be assemblage specific (meaning that other assemblages had much lower accuracies for this technique) by Byrd and LeGarde 2018 (Bertsatos and Chovalopoulou 2019, 256-256; Byrd and LeGarde 2018, 347; Vickers et al. 2015, 104-105).

5.6.3 Bone mineral density and cortical index availability

Whilst combining both of the variables used in this thesis generally gives the best results, it is not always possible to obtain both of the variables. The bone mineral density could not be measured for many of the bones used here and for a few it was also impossible to measure the cortical index. When this is applied in the field it is, thus, very likely that not all the bones can be measured. The best possible variable or variables should, therefore, be selected for the bones that are supposed to be reassociated. Other ways of reassociating bones, such as shape and size, should also be used to get the best possible results. The bone mineral density and critical index are by far not a miracle solution on their own, nor when they are combined, but they are able to further the process of reassembly.

5.6.4 The individuals amongst the commingled remains

It is always possible that two individuals have very similar bone mineral density values and cortical indices. When multiple bones are measured, they should, therefore, be plotted to see how far apart the bones lay in terms of each variable. If two or more bones lay very close to each other, it is fair to say that a reassociation with the use of that variable will not be very accurate for those bones. Other bones that lay further

apart could still be reassociated with a certain degree of accuracy. The spread of the bones of individuals is largely based on chance, but still a large factor as to how successful the application of a variable is.

This problem will most likely occur to some degree in almost all techniques that aim to reassociate individuals based on numeric variables. There is always a chance that two people are very similar. Hence, this problem is also found by Byrd an LeGarde (2018) when they evaluated some of the techniques that use bone measurements (Byrd and LeGarde 2018, 348). This limitation is hard to avoid when trying to make these techniques, but a user of those techniques should still be made aware of the possibility that two or more similar individuals are present.

5.6.5 Further limitations

Other limitations that also influence the applicability of what is described here are the availability of a CT-scanner and a DEXA-scanner, and the cost that is associated with using them. The inter and intra observer errors, which are not examined in this research, will most likely also have a large effect on the accuracy. Other factors, like taphonomy, race and population, might also influence the accuracy and the applicability of the results of this thesis. Further research is, therefore, still needed in order to see to what degree these limitations influence the reliability of using BMD's and cortical indices to reassociate individuals.

5.6.6 Application

For the bone mineral density and cortical index to be applied to commingled remains, the following steps need to be taken.

Firstly, the assemblage needs to fit within the limited range for which this technique is applicable, meaning that there should not be too many individuals amongst the commingled remains and the remains should be in a good enough state to be measured.

The population on which this research is performed is also a Western European post-medieval population. Other populations have higher BMD's, like the modern African American population, whilst others have lower BMD's, like modern Asian populations (Melton 2001, 180). Since the cortical index is related to the BMD of an individual, it is very likely that they also differ per population. The results of this thesis are, therefore, most likely not useable to these populations, but the variables used in this thesis could

help with the reassociation of bones of individuals belonging to those populations once they have been tested.

Secondly, the measurements need to be taken with the use of DEXA and/or CT-scanning, or a different type of scan on which the cortical index can be measured. Depending on what measurements and which scanners are available, the most accurate variables and directions of bones should be selected for each of the combinations of bones that need to be reassociated using tables 4.11 to 4.13. The measurements should then be recalculated using the regression models presented in table 4.1 in order to be able to match the bones. If only one variable is used, the neighbourhood analyses can then be performed.

If both variables are used, the values should first be recalculated to the same scale. In this thesis the scale of 0 to 100 was used. For the testing of the applicability all the data was placed within these ranges, but when it is applied to actual commingled remains the same scale should be used as in this thesis, which means that some of the individuals might lay outside of this range. By rescaling to the same scale that was used in this thesis, the resulting reassociations can be compared to the spread of accurate and inaccurate reassociations found in this thesis.

Lastly, the resulting reassociation should be interpreted. The reassociations that come out of a neighbourhood analysis are not all correct. The user of this technique needs to plot out the results and see how closely together the bones are located. If all the bones are close to each other, the chances are high that the reassociations are incorrect, but if some of the bones lay further apart their reassociations are more likely to be correct. Afterwards, the location of these bones should be compared to the plots in appendices 2,3 and 4. If a reassociated bone lays in or close to the cluster of inaccurately reassociated bones in the associated plot, then the chances are higher that the two bones belong to two different individuals, even if no other bones are found amongst the commingled remains with similar values. It is possible that not all bones of all the individuals are present or that the right bones could not be measured. The user of this technique, thus, has to figure out how reliable the results are for themselves.

5.7 Future research

Whilst the technique described in this thesis is technically applicable, a lot more

research and testing is still needed. As was described in the limitations section, things like population, taphonomy and observer errors still need to be looked at. For some of the combinations of bones, the groups were also very small. These combinations would also benefit from more data from more individuals.

Other than the improvement of this research, additional research could also be useful. If the bone mineral density and/or cortical index of other bones could also be compared to the humeri and femora, larger parts of the skeleton could possibly be reassociated. Other factors, like the total bone diameter or the trabecular bone loss, might also be useful for the reassembly of individuals. Whilst untested, the total bone diameter seemed like a very stable variable over the same bone type, when the cortical indices were tested. Additions like this will hopefully, one day, give us the possibility of reassembling entire skeletons from commingled remains, helping us with researching past populations, but also giving us the possibility of laying the people from the past back to rest with a bit more respect.

6. Conclusion

When commingled remains are found in archaeological contexts, their study is often less detailed than those of assembled remains. This is because the interpretation is much more difficult due to their commingling. It is hard to say much about diseases, migration, and other phenomena if it is uncertain how many individuals are present and what bones belong to the same individual. Estimation techniques, like MNI, MLNI and MNE are often used to still be able to say some things about the commingled assemblage, but ideally, we would be able to reassemble the skeletons present amongst the commingled remains. This would provide more opportunities for studying the population represented in the commingled remains, but it would also give us the chance of paying more respect to the individuals present.

When a large number of skeletons from the Middenbeemster collection, was to be scanned in a CT-scanner and in a DEXA-scanner, the idea arose to see if these scans could be used to find a way of reassembling some of the bones of commingled individuals. The cortical bone thickness, recalculated as a cortical bone index and measured using the CT-scans, and the bone mineral densities that resulted from the DEXA-scans, were, therefore, used to try and reassociate the bones of these skeletons.

Firstly, in order to be able to match the bones, regression models were made. For many of the combinations of bones these regression models had moderate to high correlation coefficients. The data was recalculated for each combination, so that the values of one bone could be matched with those of another type of bone, but also the other way around.

The values and the recalculated values of different bones were placed in a neighbourhood analysis. This type of analysis looks at the difference between one bone and its nearest neighbour. These distances were compared to the difference between the bones of each individual to see if the bones of individuals were indeed closest to each other. When these neighbourhood analyses were performed on the total groups, the percentage of accurately reassociated bones was low. The total groups were, therefore, divided into smaller groups. Firstly, five groups of five were tested for each combination in both directions for each variable. The resulting percentages of accuracy that came out of these neighbourhood analyses were much better. It was decided that,

if a neighbourhood analyses did not result in accurate reassociations for at least one third of the individuals, the combination of bones would be excluded from neighbourhood analyses with larger groups. Some of the combinations of bones, were thus excluded, but for many combinations groups of ten were formed. The results of these neighbourhood analyses were accurate for more than a third of the individuals for the left to right femur combinations. All the other combinations of bones scored below the 33,33% accuracy. Groups of fifteen were formed for the combination of the left femur to the right femur, but the neighbourhood analyses performed on these groups also scored below the 33,33% accuracy.

In order to try and get better results, the two variables were combined. The distance to the nearest neighbour was measured in plots where both variables were mapped out with the use of a nearest neighbour analysis. Before this could be done, the two variables needed to be rescaled, so they could be properly compared. A scale of 0 to 100 was made for each variable for each bone. The distances that came out of these neighbourhood analyses were compared to the distances between the bones of an individual. In almost all cases, the resulting percentage of accuracy improved. The results for the total groups were still too low, but all the groups of five had a successful reassociation for more than one third of the individuals. Many combinations also had high enough accuracies for groups of ten and the femur-to-femur combinations even resulted in accuracies above the 33,33% for groups of fifteen.

Once all these neighbourhood analyses were performed, the results were plotted out to see if there were correlations between the accurately reassociated bones, the values of the bone and the distance between the bones of an individual. For many of the graphs, the inaccurately reassociated bones were mostly grouped around the average value of the bones. The accurately reassociated bones are also located around the average, but their differences to the other bone are much smaller. The accurately reassociated bones are also found further away from the average, where their difference to the other bone of the individual increases. This, basically, means that the further from the average a bone's value lays, the higher the chances of an accurate reassociation. For the individuals close to the average, a small difference between the bones of an individual is needed to accurately reassociate the bones.

Another set of graphs was made for the group sizes of combinations of bones that had accurately reassembled bones for over one third of the individuals. In these graphs the accurately reassociated bones, the values of the bone and the distance to their nearest neighbour were plotted out. These graphs showed a lot of overlap of distances for bones that were accurately and inaccurately reassembled. This means that if the bone mineral density or cortical index is applied for reassembly, then it will be hard to discern which bones actually belong together. However, for many of the plots the amount of false reassociations decreases as the value of the variable increases. It is, thus, way more likely that two bones belong together if they both lay further away from the average.

In some cases, the patterns described above are not present in the graphs. This happens in the graphs in which the bone mineral density is used in combination with the left humerus and in graphs where only the cortical index is used, and the accuracy is below 36%. For these combinations, it is less likely that bones are accurately reassociated when they are further away from the average, than for other combinations.

If someone wants to apply the bone mineral density and/or the cortical index to reassemble commingled remains, they should take the many limitations into account:

- The accuracy of the reassembly is very dependent on group size and the combination of bones.
- Not all bones can be measured for cortical indices and not all bones give results for the bone mineral density.
- The accuracy is very dependent on which variable is used.
- The applicability is highly dependent in the difference between the individuals that are present.

But, if a situation occurs, where these limitations are not preventing the neighbourhood analysis from being performed, then CT-scanning and DEXA-scanning can indeed be used to identify individuals from commingled archaeological remains.

The only things that are still needed is for this technique to be tested on different collections, to see how accurate the application is on different populations and on skeletons which endured different taphonomic processes. These applications will also

benefit from other variables, such as trabecular bone thickness and total bone diameter, being tested to see if they will improve the accuracy. Additions like this will hopefully, one day, give us the possibility of reassembling entire skeletons from commingled remains, helping us with researching past populations, but also giving us the possibility of laying the people from the past back to rest with a bit more respect.

Literature

Adams, B.J. and L.W. Konigsberg, 2004. Estimation of the most likely number of individuals from commingled human skeletal remains. *American Journal of Physical Anthropology: The Official Publication of the American Association of Physical Anthropologists*, *125*(2), 138-151.

Anstett, É. and J.M. Dreyfus, 2015. *Human remains and identification: mass violence, genocide and the 'forensic turn'*. Manchester University Press.

Bertsatos, A. and M. Chovalopoulou, 2019. Validation study of osteometric techniques for sorting commingled human skeletal remains in archaeological samples. *International Journal of Osteoarchaeology*, 29(2), 253-259.

Blake, G.M. and I. Fogelman, 2007. The role of DXA bone density scans in the diagnosis and treatment of osteoporosis. *Postgraduate medical journal*, *83*(982), 509-517.

Byrd, J.E. and C.B. LeGarde, 2014. *Commingled human remains: Methods in recovery, analysis, and identification*. Amsterdam, Elsevier.

Byrd, J.E. and C.B. LeGarde, 2018. Evaluation of method performance for osteometric sorting of commingled human remains. *Forensic Sciences Research, 3*(4), 343-349.

Croker, S.L., W. Reed and D. Donlon, 2009. The feasibility of using radiogrammetry in comparing cortical bone thickness in human and non-human tibiae. *Radiographer*, *56*(3),25-31.

Curate, F., A. Albuquerque and E.M. Cunha, 2013. Age at death estimation using bone densitometry: testing the Fernandez Castillo and Lopez Ruiz method in two documented skeletal samples from Portugal. *Forensic science international*, *226*(1-3), 296.e1-296.e6.

De Groote, I., K. Di Modica, A. Gregory, J.D. Irish, P. Crombe, H. Vandendriessche and D. Bonjean, 2020. Preliminary reports on the 2016-2017 excavation of the Neolithic ossuary and terrace. *Notae Praehistoricae*, *39*, 143-151.

Di Stefano, M., Boano, R., Rabino, E., Isaia, G.C. and Panattoni, G.L., 2012. Dual-energy X-ray absorptiometry (DXA): a non-destructive approach for the study of bone mass density in archaeological samples. *XIX Congress of Associazione Antropologica Italiana: 1961-2011: 50 years of congresses, past present and future of anthropology* ,85, No. 1, 232-233.

El Maghraoui, A. and C. Roux, 2008. DXA scanning in clinical practice. *QJM: An International Journal of Medicine*, *101*(8), 605-617.

Hakvoort, A., 2013. De begravingen bij de Keyserkerk te Middenbeemster. Zaandijk: Hollandia (reeks 464)

Harwood-Nash, D. C., 1979. Computed Tomography of Ancient Egyptian Mummies. *Journal of Computer Assisted Tomography, 3*(6), 768-773.

Herrmann, N.P. and J.B. Devlin, 2008. Assessment of Commingled Human Remains Using a GIS-

Based Approach, in Adams, B.J. and J.E. Byrd, eds., 2008. *Recovery, analysis, and identification of commingled human remains*. Springer Science & Business Media.

Hughes, S., 2011. CT scanning in archaeology. *Computed Tomography-Special Applications/Ed. L. Saba. InTech Europe*, 57-70.

Kendell, A. and P. Willey, 2013. Crow Creek Bone Bed Commingling: Relationship Between Bone Mineral Density and Minimum Number of Individuals and Its Effect on Paleodemographic Analyses, in Osterholtz, A.J., K.M. Baustian and D.L. Martin (eds), 2013. *Commingled and disarticulated human remains*. Springer.

Lütgert, S.A., 2000. Victims of the Great Famine and the Black Death?. *Hikuin*, *27*(27), 255-265.

Lyman, R.L., 1994. Relative abundances of skeletal specimens and taphonomic analysis of vertebrate remains. *Palaios*, *9*(3), 288-298.

Mays, S., B. Lees and J.C. Stevenson, 1998. Age-dependent bone loss in the femur in a medieval population. *International Journal of Osteoarchaeology*, *8*(2), 97-106.

Mays, S. A., 1999. Osteoporosis in Earlier Human Populations. *Journal of Clinical Densitometry, 2*(1), 71-78.

Mays, S., 2001. Effects of age and occupation on cortical bone in a group of 18th–19th century British men. *American Journal of Physical Anthropology: The Official Publication of the American Association of Physical Anthropologists*, *116*(1), 34-44.

McClanahan, B.S., K. Harmon-Clayton, K.D. Ward, R.C. Klesges, C.M. Vukadinovich and E.D. Cantler, 2002. Side-to-side comparisons of bone mineral density in upper and lower limbs of collegiate athletes. *Journal of strength and conditioning research*, *16*(4), 586-590.

Melton, L.J., 2001. The prevalence of osteoporosis: gender and racial comparison. *Calcified tissue international*, *69*(4), 179-181.

Mundorff, A.Z., 2008. Anthropologist-Directed Triage: Three Distinct Mass Fatality Events Involving Fragmentation of Human Remains, in Adams, B.J. and J.E. Byrd, eds., 2008. *Recovery, analysis, and identification of commingled human remains*. Springer Science & Business Media.

Murphy Jr, W.A., D.Z. Nedden, P. Gostner, R. Knapp, W. Recheis and H. Seidler, 2003. The iceman: discovery and imaging. *Radiology*, *226*(3), 614-629.

Nedden, D. zur, R. Knapp, K. Wicke, W. Judmaier, W.A. Murphy Jr, H. Seidler and W. Platzer, 1994. Skull of a 5,300-year-old mummy: reproduction and investigation with CT-guided stereolithography. *Radiology*, *193*(1), 269-272.

O'Donnell, C., M. Iino, K. Mansharan, J. Leditscke and N. Woodford, 2011. Contribution of postmortem multidetector CT scanning to identification of the deceased in a mass disaster: experience gained from the 2009 Victorian bushfires. *Forensic science international*, *205*(1-3), 15-28.

Osterholtz, A.J., K.M. Baustian and D.L. Martin (eds), 2013. *Commingled and disarticulated human remains*. Springer.

Osterholtz, A.J., K.M. Baustian, D.L. Martin and D.T. Potts, 2013a. Commingled Human Skeletal Assemblages: Integrative Techniques in Determination of the MNI/MNE, in Osterholtz, A.J., K.M. Baustian and D.L. Martin (eds), 2014. *Commingled and disarticulated human remains*. Springer.

Ortner, D., 2003. *Identification of pathological conditions in human skeletal remains* (2nd ed.). San Diego, CA [etc.]: Academic Press.

Primeau, C., P. Homøe and N. Lynnerup, 2019. Temporal changes in childhood health during the medieval Little Ice Age in Denmark. *International Journal of Paleopathology, 27*, 80-87.

Sullivan, L. P. and S.T. Childs, 2003. *Curating archaeological collections: From the field to the repository* (Vol. 6). New York: Altamira.

Ubelaker, D.H. and J.L. Rife, 2008. Approaches to Commingling Issues in Archeological Samples: A Case Study from Roman Era Tombs in Greece, in Adams, B.J. and J.E. Byrd, eds., 2008. *Recovery, analysis, and identification of commingled human remains*. Springer Science & Business Media.

Vickers, S., P.M. Lubinski, L. Henebry DeLeon and J.T. Bowen Jr, 2015. Proposed method for predicting pair matching of skeletal elements allows too many false rejections. *Journal of forensic sciences*, *60*(1), 102-106.

Walker, P.L., 2000. Bioarchaeological ethics: a historical perspective on the value of human remains. *Biological anthropology of the human skeleton*, *3*, 40.

List of figures

List of tables

Appendix 1: R-code and analytical steps

For a nndist function to be performed in R, an excel sheet needs to be made that contains a column with the values for the X-axis, a column with the values for the Y-axis (if only one variable was used, the Y-axis was 1 for each bone) and a column with the bone ID. This excel sheet needs to be uploaded in R. The excel sheet then needs to be turned into an object of ppp class. In this thesis, the following function was used:

```
PPPDATA <- ppp(Excelsheet$`Variable_x`, Excelsheet$`Variable_y`, c(0,100), c(0,100),
marks = Excelsheet$ID)
```

The following code can then be used to perform the nndist function:

```
nndist(PPPDATA$x, PPPDATA$y, k=1:2, by=as.factor(PPPDATA$marks))
```

This nndist code will give the distance to the nearest neighbour of each bone type based on the variables x and y.

To make the three dimensional scatterplots, another excel sheet was needed. This excel sheet needed to contain a column with the BMD value, a column with the cortical index and a column with the distance to the bone of the same individual or the distance to the nearest neighbour (depending on the graph). In this research another column was used that would give the colour to the plotted points (green for accurately reassociated and red for inaccurately reassociated). The code that was used was:

```
scatterplot3d(x=Excelsheet2$BMD, y=Excelsheet2$'cortical_index',
z=Excelsheet2$`distance-to-bone`, pch= 16, type="h", color =
factor(Excelsheet2$colour), xlab = 'BMD', ylab = 'Cortical index', zlab = 'Distance to bone'
)
```

Other aspects of the plot, like the scale of an axis, can also be changed with the help of the functions in the scatterplot3d function, but those were generally not used in this thesis.

Appendix 2: 2D plots of difference within an individual

This appendix contains the graphs that were plotted of the differences between bones that were accurately and inaccurately reassociated compared to the original values of the bone that was used for finding the associated bone.

The following properties apply to the graphs in this appendix:

- the X-axis presents the BMD-value or cortical index of the known bone
- the Y-axis presents the difference to the searched bone of the same skeleton
- green dots represent individuals whose own bone was reassociated
- red dots represent the individuals whose bones were reassociated with bones of a different individual

Left femur to right femur

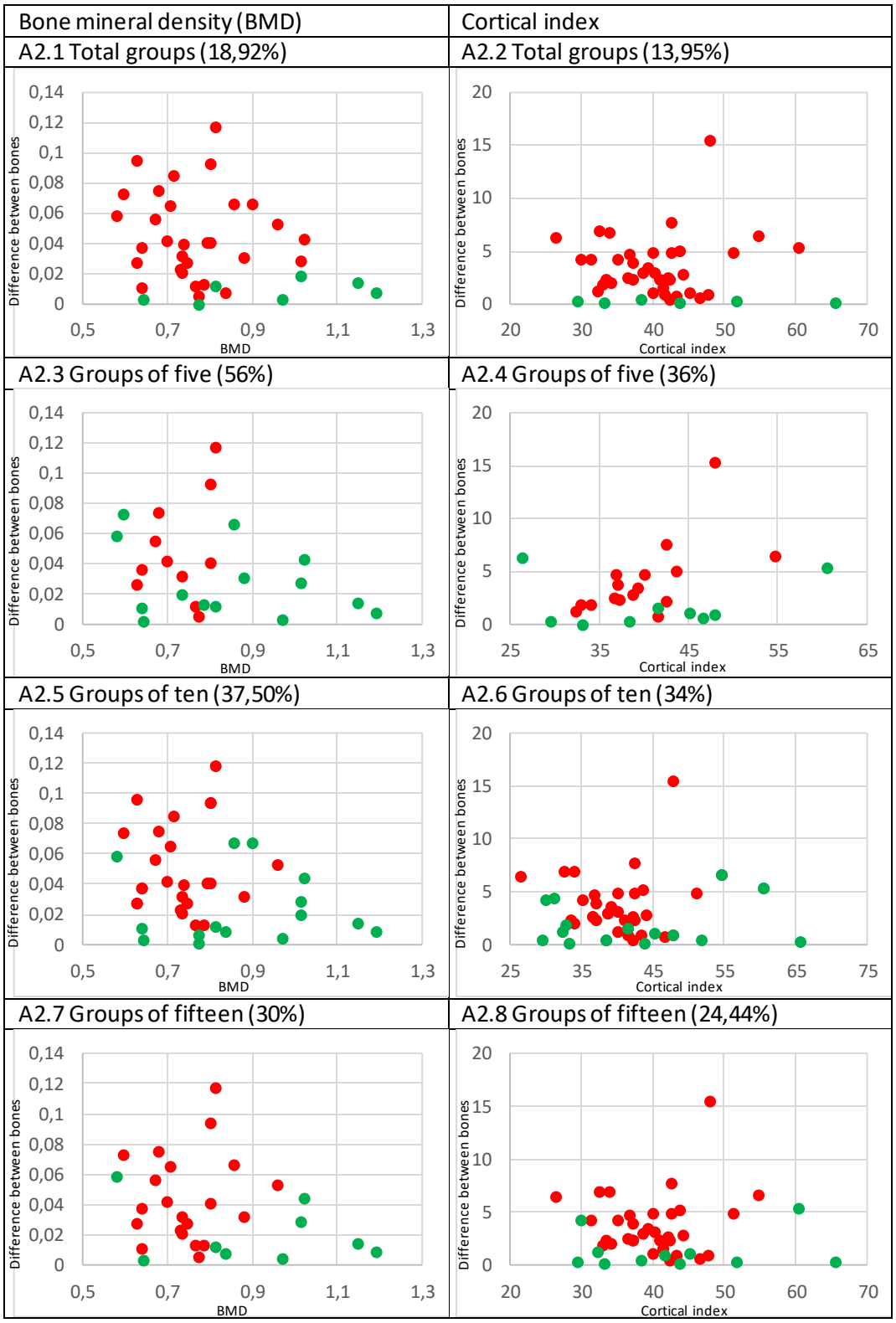

Figure A2.1 to A2.8: The difference between the BMD or cortical index of bones of an individual compared to their respective value.
Green dots: accurately reassociated individuals
Red dots: inaccurately reassociated individuals

Left femur to left humerus

Bone mineral density (BMD)	Cortical index
A2.9 Total groups (21,05%)	A2.10 Total groups (2,44%)
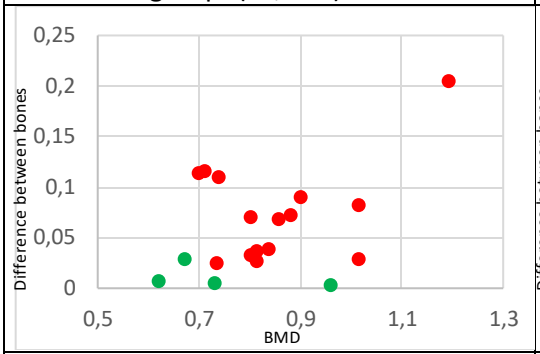	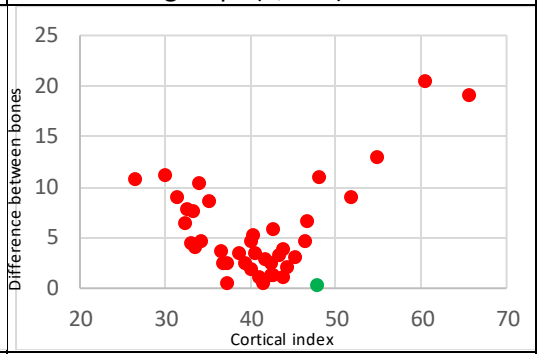
A2.11 Groups of five (28%)	A2.12 Groups of five (24%)
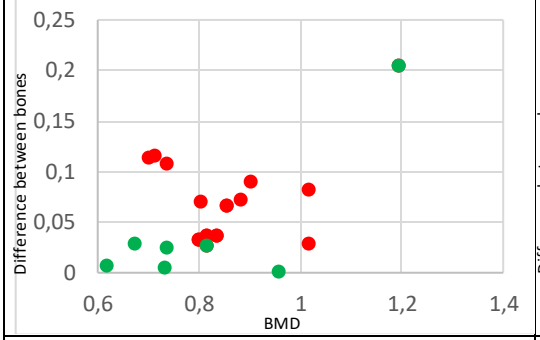	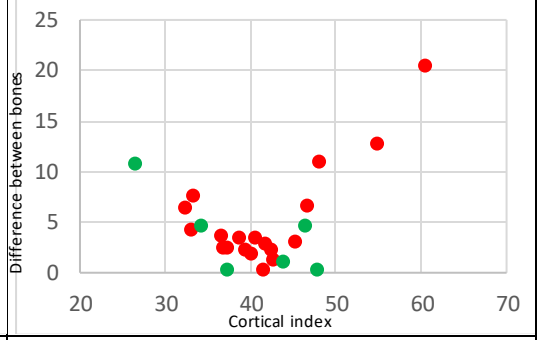
Groups of ten	Groups of ten
This neighbourhood analysis was not performed	This neighbourhood analysis was not performed
Groups of fifteen	Groups of fifteen
This neighbourhood analysis was not performed	This neighbourhood analysis was not performed

Figure A2.9 to A2.12: The difference between the BMD or cortical index of bones of an individual compared to their respective value.
Green dots: accurately reassociated individuals
Red dots: inaccurately reassociated individuals

Left femur to right humerus

Bone mineral density (BMD)	Cortical index
A2.13 Total groups (6,90%)	A2.14 Total groups (7,50%)
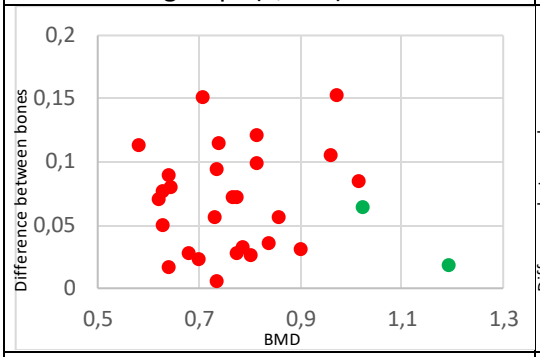	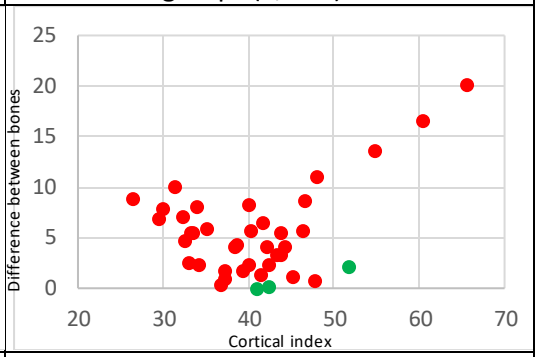
A2.15 Groups of five (40%)	A2.16 Groups of five (28%)
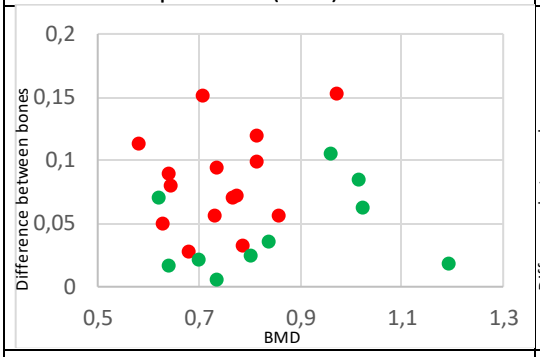	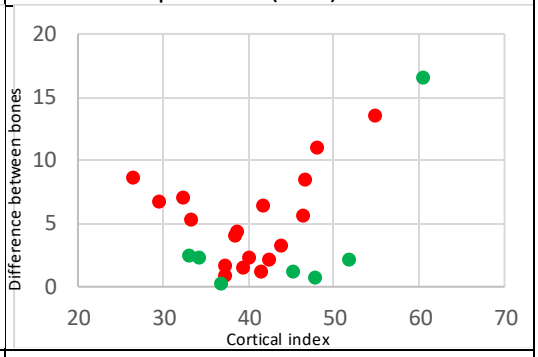
A2.17 Groups of ten (20%)	Groups of ten
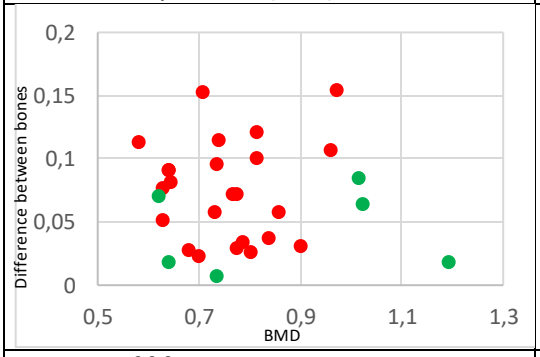	This neighbourhood analysis was not performed
Groups of fifteen	Groups of fifteen
This neighbourhood analysis was not performed	This neighbourhood analysis was not performed

Figure A2.13 to A2.17: The difference between the BMD or cortical index of bones of an individual compared to their respective value.
Green dots: accurately reassociated individuals
Red dots: inaccurately reassociated individuals

Right femur to left femur

Bone mineral density (BMD)	Cortical index
A2.18 Total groups (13,52%)	A2.19 Total groups (11,63%)
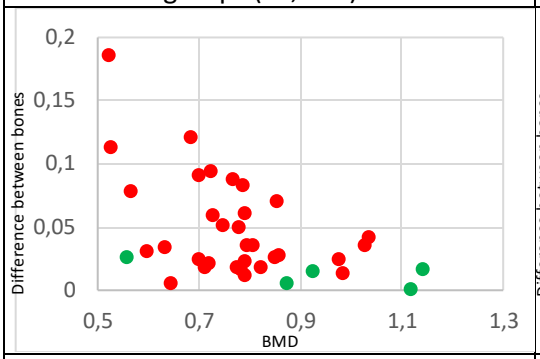	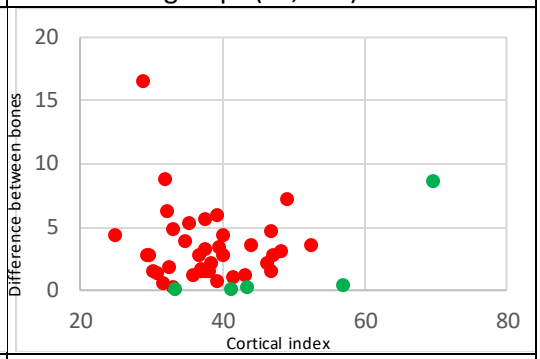
A2.20 Groups of five (68%)	A2.21 Groups of five (44%)
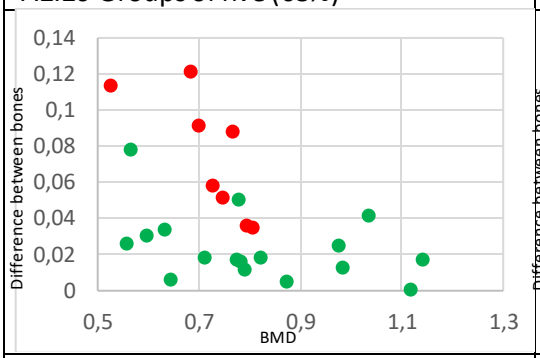	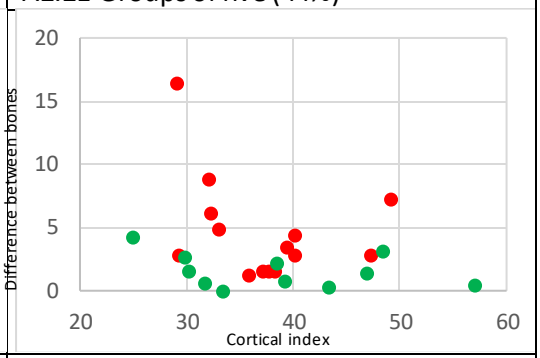
A2.22 Groups of ten (32,50%)	A2.23 Groups of ten (32%)
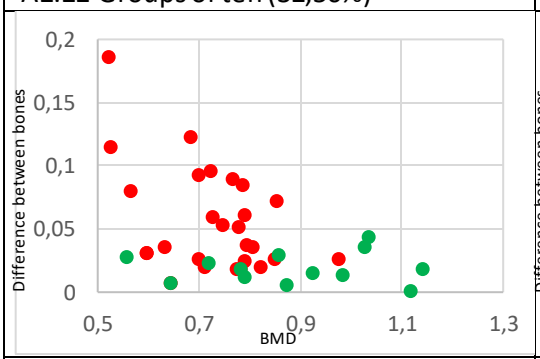	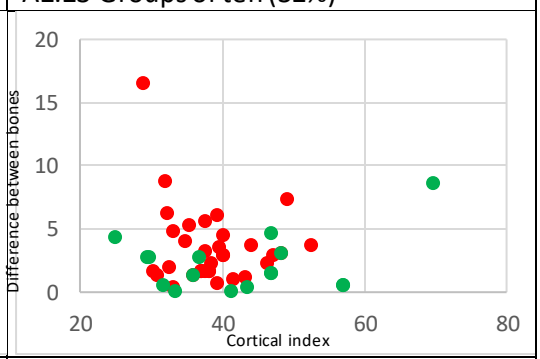
Groups of fifteen	Groups of fifteen
This neighbourhood analysis was not performed	This neighbourhood analysis was not performed

Figure A2.18 to A2.23: The difference between the BMD or cortical index of bones of an individual compared to their respective value.
Green dots: accurately reassociated individuals
Red dots: inaccurately reassociated individuals

Right femur to left humerus

Bone mineral density (BMD)	Cortical index
A2.24 Total groups (5,26%)	A2.25 Total groups (0%)
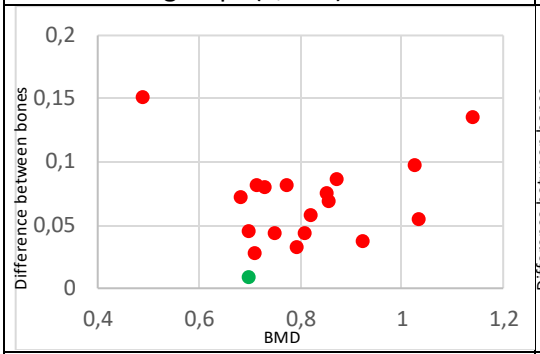	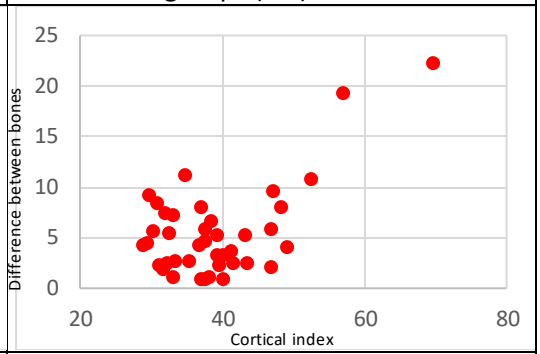
A2.26 Groups of five (40%)	A2.27 Groups of five (28%)
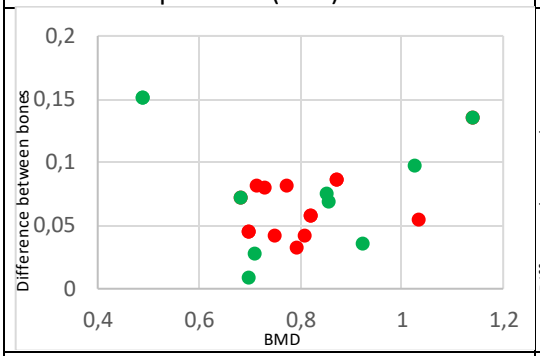	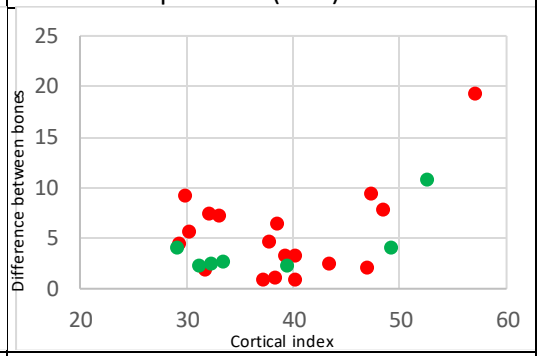
A2.28 Groups of ten (25%)	Groups of ten
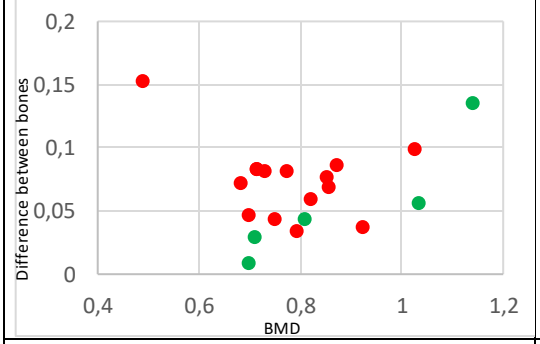	This neighbourhood analysis was not performed
Groups of fifteen	Groups of fifteen
This neighbourhood analysis was not performed	This neighbourhood analysis was not performed

Figure A2.24 to A2.28: The difference between the BMD or cortical index of bones of an individual compared to their respective value.
Green dots: accurately reassociated individuals
Red dots: inaccurately reassociated individuals

Right femur to right humerus

Bone mineral density (BMD)	Cortical index
A2.29 Total groups (13,79%)	A2.30 Total groups (7,50%)
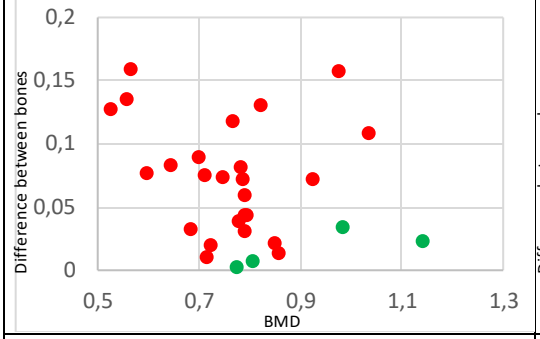	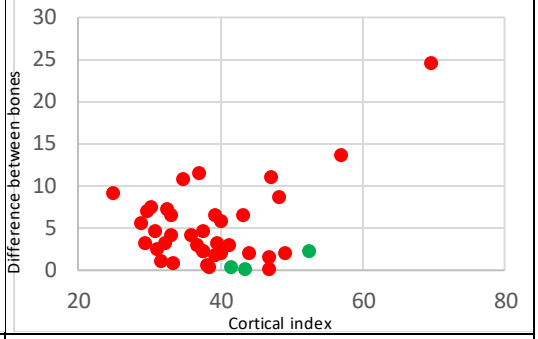
A2.31 Groups of five (44%)	A2.32 Groups of five (48%)
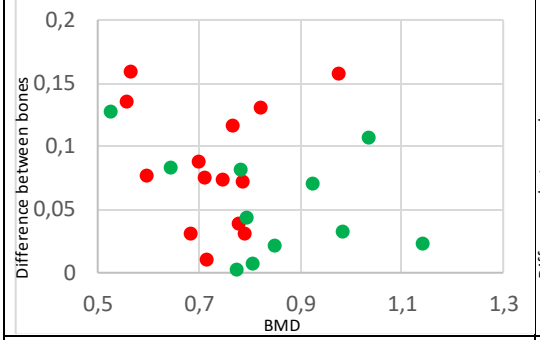	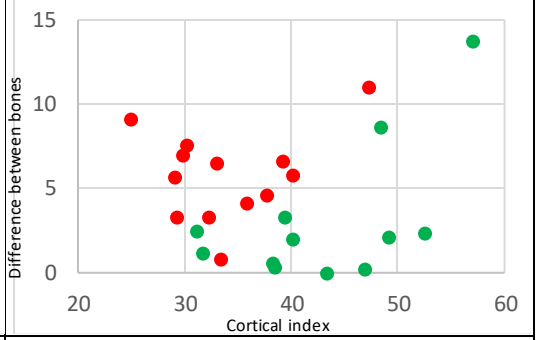
A2.33 Groups of ten (26,67%)	A2.34 Groups of ten (20%)
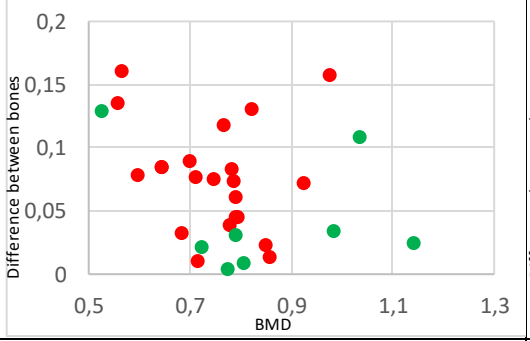	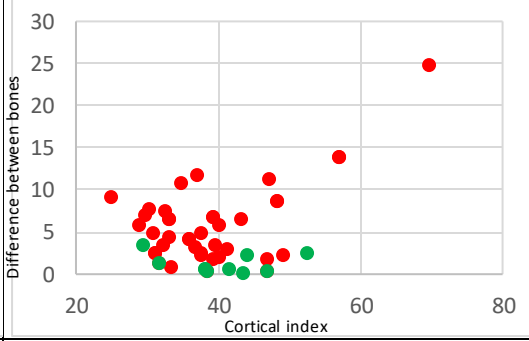
Groups of fifteen	Groups of fifteen
This neighbourhood analysis was not performed	This neighbourhood analysis was not performed

Figure A2.29 to A2.34: The difference between the BMD or cortical index of bones of an individual compared to their respective value.
Green dots: accurately reassociated individuals
Red dots: inaccurately reassociated individuals

Left humerus to left femur

Bone mineral density (BMD)	Cortical index
A2.35 Total groups (15,79%)	A2.36 Total groups (4,87%)
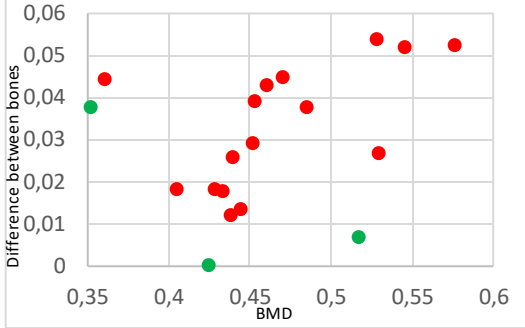	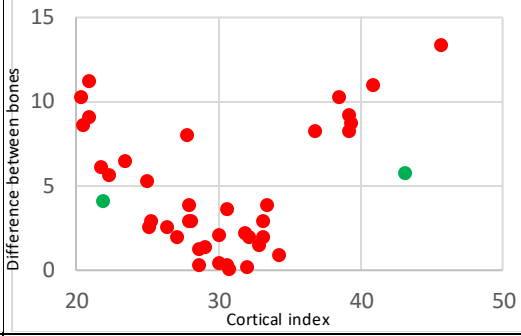
A2.37 Groups of five (20%)	A2.38 Groups of five (36%)
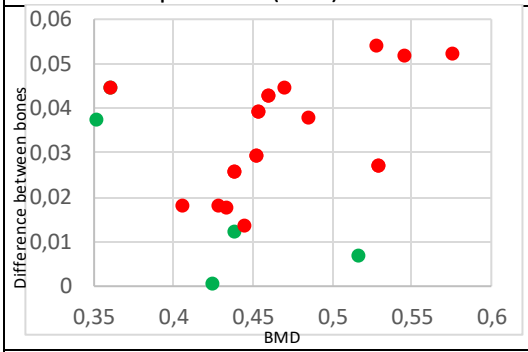	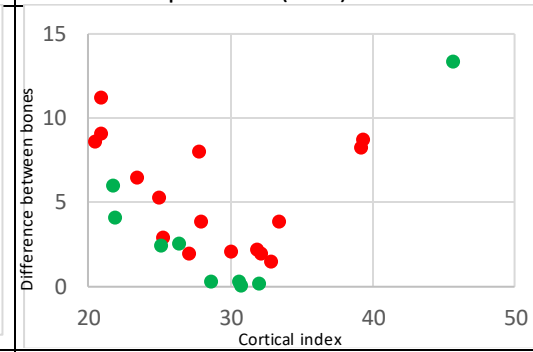
Groups of ten	A2.39 Groups of ten (20%)
This neighbourhood analysis was not performed	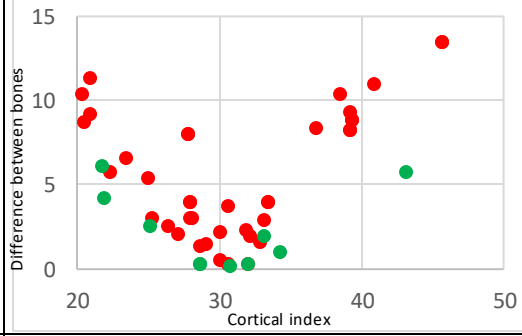
Groups of fifteen	Groups of fifteen
This neighbourhood analysis was not performed	This neighbourhood analysis was not performed

Figure A2.35 to A2.39: The difference between the BMD or cortical index of bones of an individual compared to their respective value.
Green dots: accurately reassociated individuals
Red dots: inaccurately reassociated individuals

Left humerus to right femur

Bone mineral density (BMD)	Cortical index
A2.40 Total groups (5,26%)	A2.41 Total groups (7,50%)
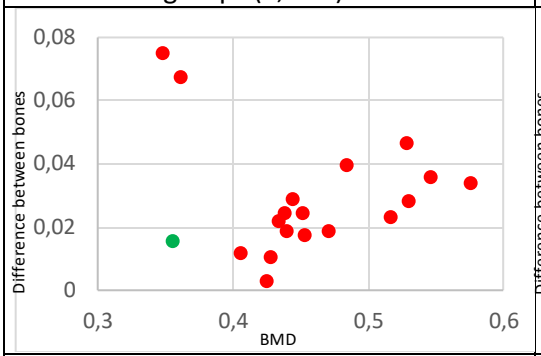	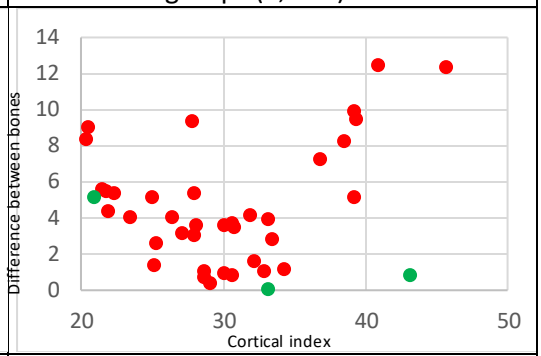
A2.42 Groups of five (40%)	A2.43 Groups of five (28%)
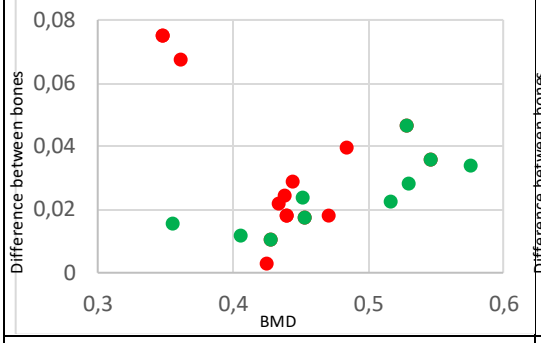	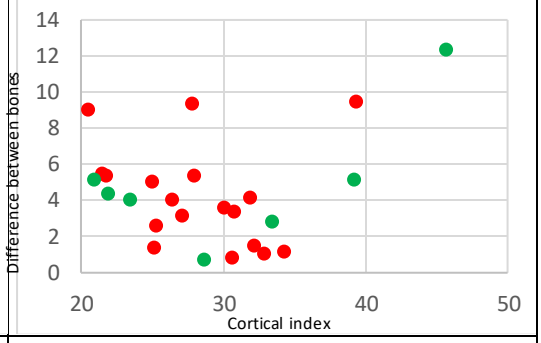
A2.44 Groups of ten (20%)	Groups of ten
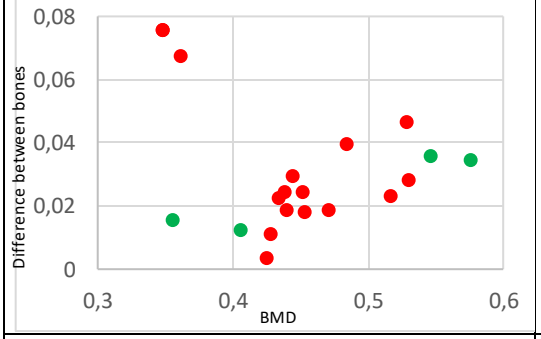	This neighbourhood analysis was not performed
Groups of fifteen	Groups of fifteen
This neighbourhood analysis was not performed	This neighbourhood analysis was not performed

Figure A2.40 to A2.44: The difference between the BMD or cortical index of bones of an individual compared to their respective value.
Green dots: accurately reassociated individuals
Red dots: inaccurately reassociated individuals

Left humerus to right humerus

Bone mineral density (BMD)	Cortical index
A2.45 Total groups (20%)	A2.46 Total groups (5%)
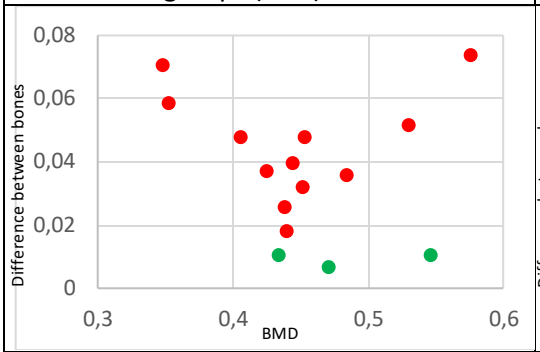	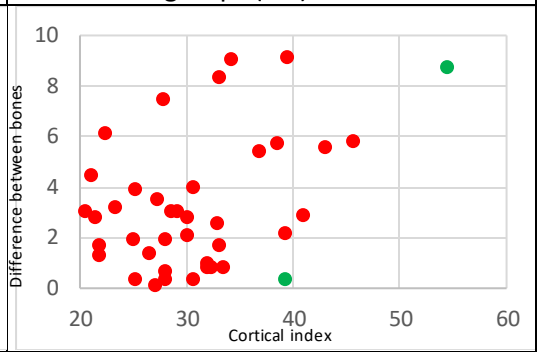
A2.47 Groups of five (32%)	A2.48 Groups of five (56%)
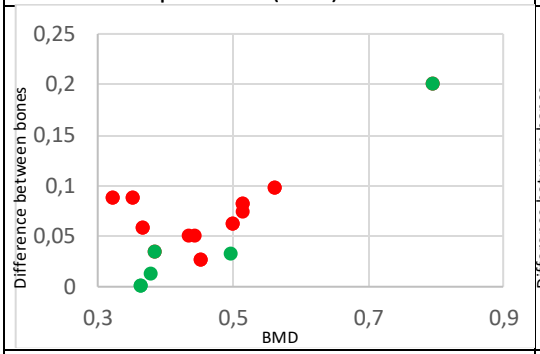	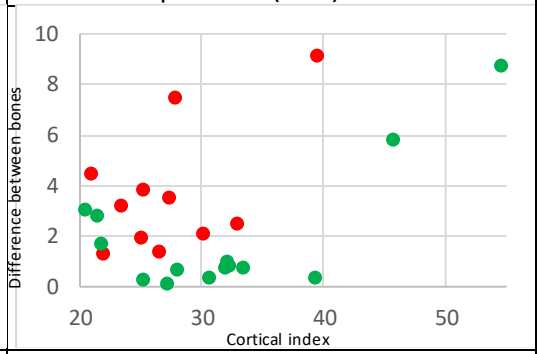
Groups of ten	A2.49 Groups of ten (32%)
This neighbourhood analysis was not performed	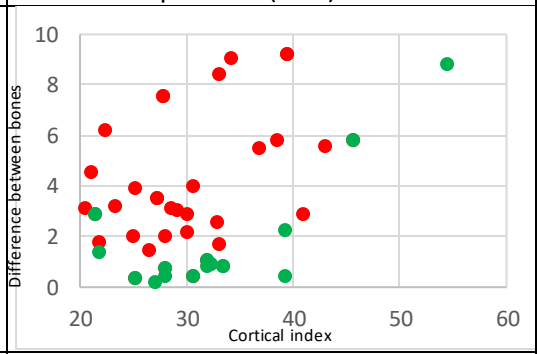
Groups of fifteen	Groups of fifteen
This neighbourhood analysis was not performed	This neighbourhood analysis was not performed

Figure A2.45 to A2.49: The difference between the BMD or cortical index of bones of an individual compared to their respective value.
Green dots: accurately reassociated individuals
Red dots: inaccurately reassociated individuals

Right humerus to left femur

Bone mineral density (BMD)	Cortical index
A2.50 Total groups (17,24%)	A2.51 Total groups (2,50%)
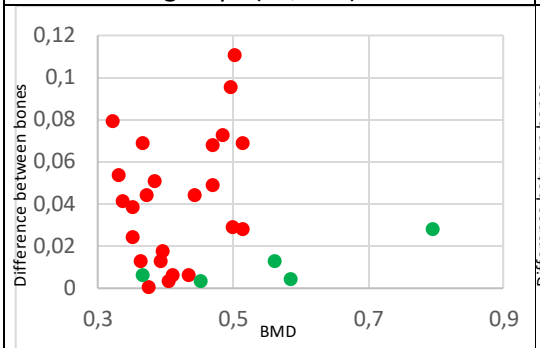	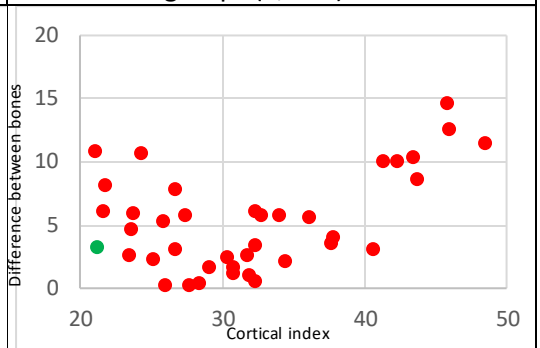
A2.52 Groups of five (40%)	A2.53 Groups of five (32%)
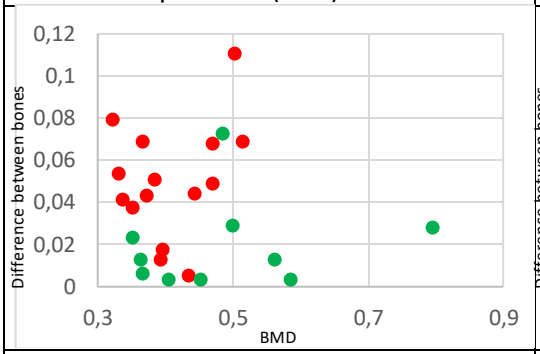	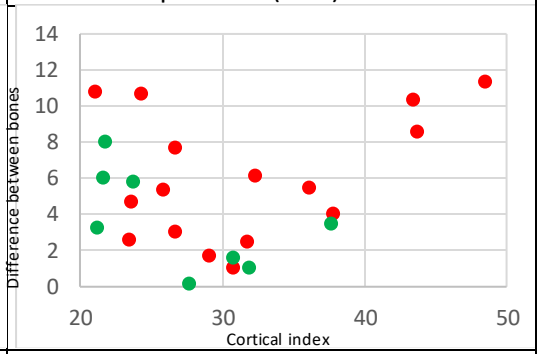
A2.54 Groups of ten (30%)	Groups of ten
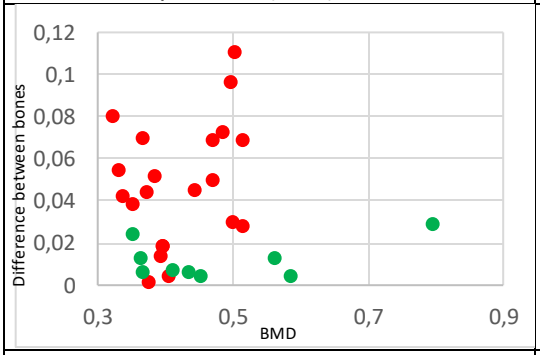	This neighbourhood analysis was not performed
Groups of fifteen	Groups of fifteen
This neighbourhood analysis was not performed	This neighbourhood analysis was not performed

Figure A2.50 to A2.54: The difference between the BMD or cortical index of bones of an individual compared to their respective value.
Green dots: accurately reassociated individuals
Red dots: inaccurately reassociated individuals

Right humerus to right femur

Bone mineral density (BMD)	Cortical index
A2.55 Total groups (10,34%)	A2.56 Total groups (5%)
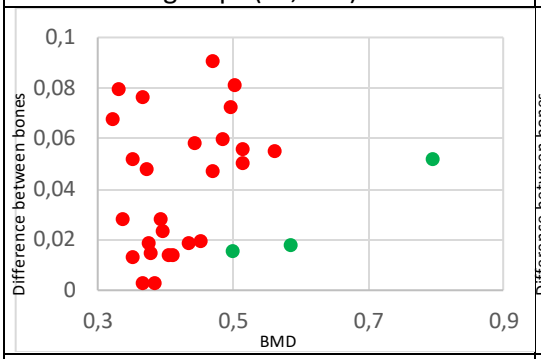	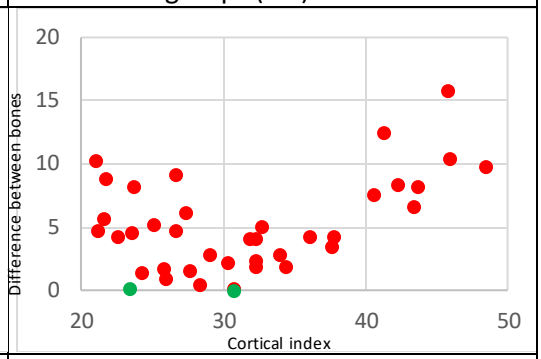
A2.57 Groups of five (36%)	A2.58 Groups of five (40%)
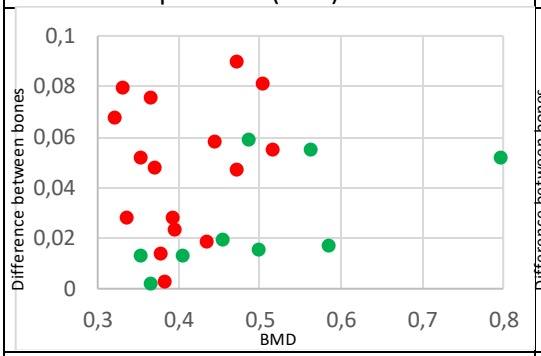	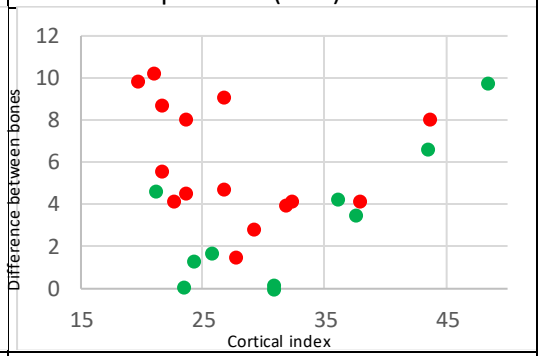
A2.59 Groups of ten (23,33%)	A2.60 Groups of ten (26%)
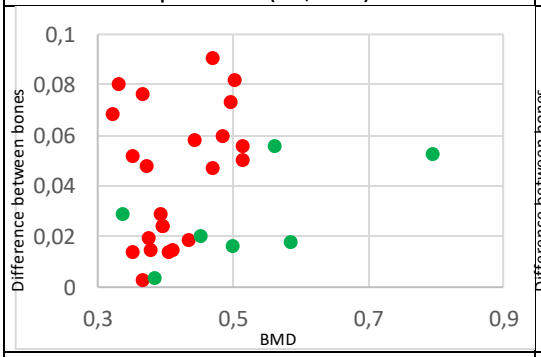	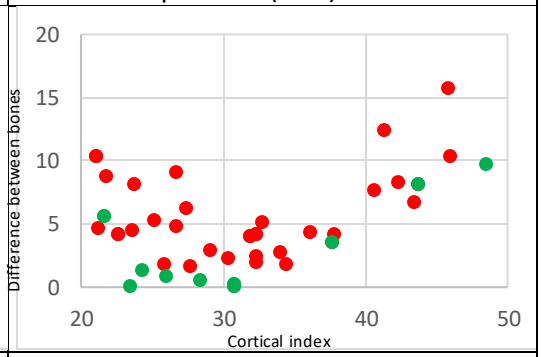
Groups of fifteen	Groups of fifteen
This neighbourhood analysis was not performed	This neighbourhood analysis was not performed

Figure A2.55 to A2.60: The difference between the BMD or cortical index of bones of an individual compared to their respective value.
Green dots: accurately reassociated individuals
Red dots: inaccurately reassociated individuals

Right humerus to left humerus

Bone mineral density (BMD)	Cortical index
A2.61 Total groups (0%)	A2.62 Total groups (7,69%)
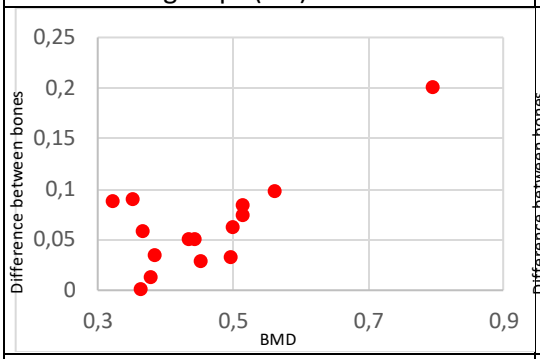	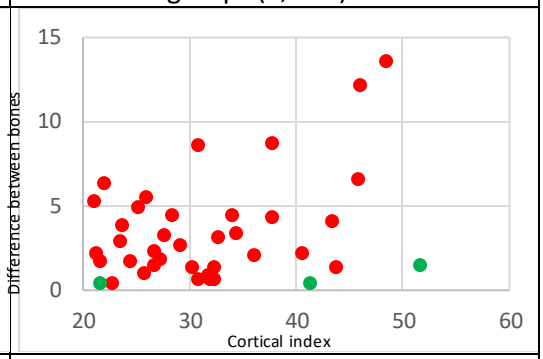
A2.63 Groups of five (24%)	A2.64 Groups of five (52%)
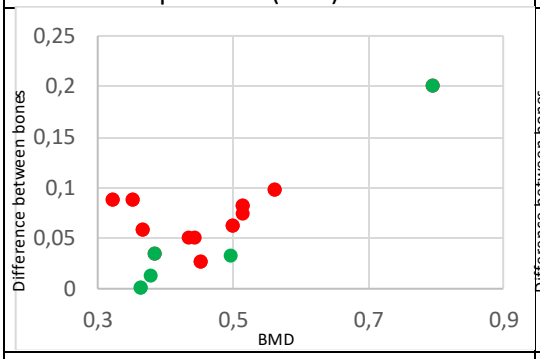	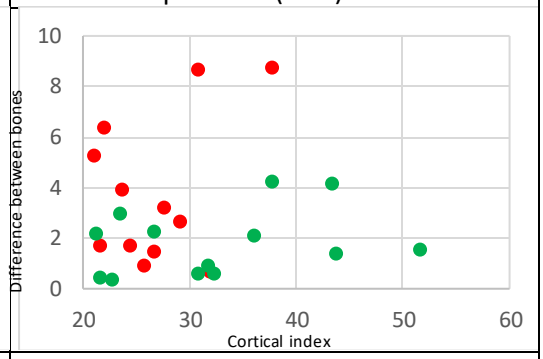
Groups of ten	A2.65 Groups of ten (28%)
This neighbourhood analysis was not performed	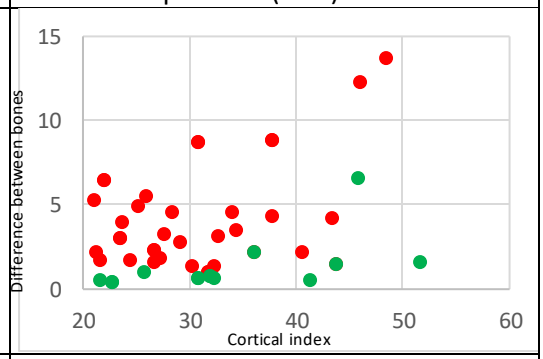
Groups of fifteen	Groups of fifteen
This neighbourhood analysis was not performed	This neighbourhood analysis was not performed

Figure A2.61 to A2.65: The difference between the BMD or cortical index of bones of an individual compared to their respective value.
Green dots: accurately reassociated individuals
Red dots: inaccurately reassociated individuals

Appendix 3: 3D plots of difference within an individual

This appendix contains the 3D graphs that were plotted of the differences between bones that were accurately and inaccurately reassociated using both variables compared to the original values of the bone that was used for finding the associated bone.

The following properties apply to the graphs in this appendix:

- the X-axis presents the BMD-value of the known bone
- the Y-axis presents the cortical index of the known bone
- the Z-axis presents the difference between the known bone and the searched bone of that individual
- green dots represent individuals whose own bone was reassociated
- red dots represent the individuals whose bones were reassociated with bones of a different individual

Left femur to right femur

Bone mineral density (BMD) and cortical index

A3.1 Total groups (22,86%)

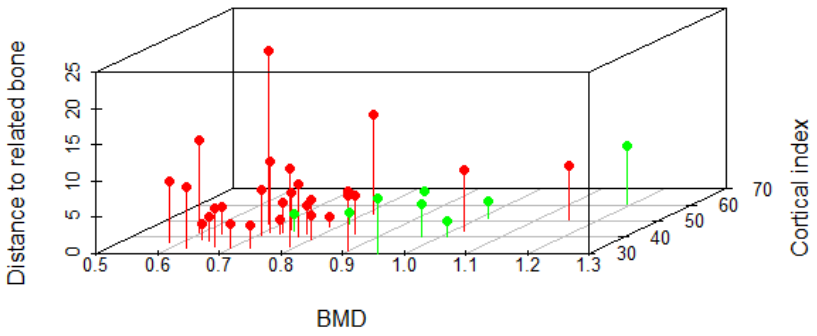

A3.2 Groups of five (76%)

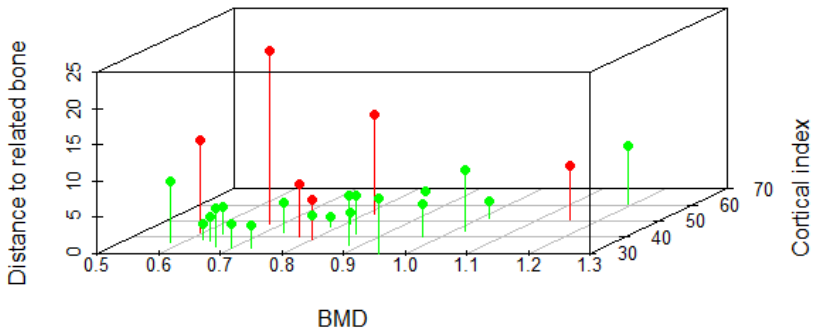

Figure A3.1 and A3.2: The difference between the BMD and cortical index of bones of an individual compared to their respective values.
Green dots: accurately reassociated individuals
Red dots: inaccurately reassociated individuals

A3.3 Groups of ten (47,50%)

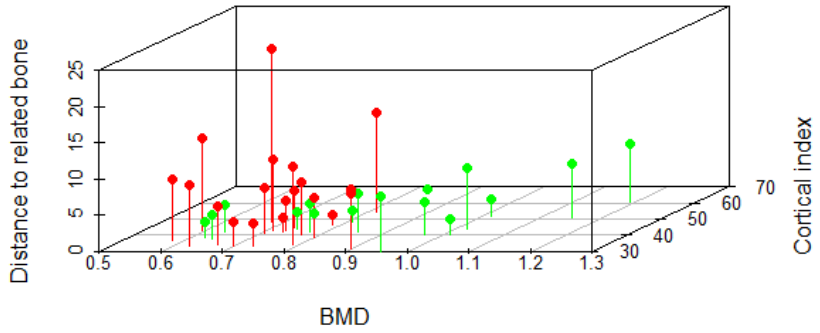

A3.4 Groups of fifteen (43,33%)

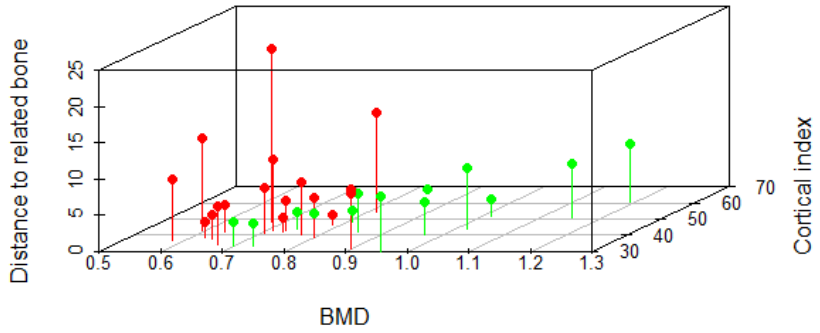

Figure A3.3 and A3.4: The difference between the BMD and cortical index of bones of an individual compared to their respective values.
Green dots: accurately reassociated individuals
Red dots: inaccurately reassociated individuals

A3.5 Groups of twenty (30%)

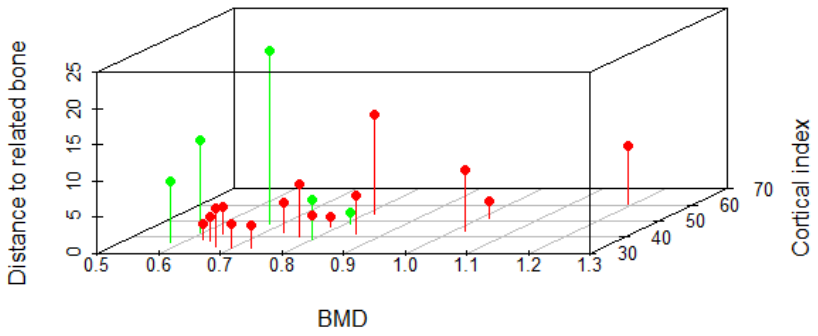

Figure A3.5: The difference between the BMD and cortical index of bones of an individual compared to their respective values.
Green dots: accurately reassociated individuals
Red dots: inaccurately reassociated individuals

Left femur to left humerus

Bone mineral density (BMD) and cortical index

A3.6 Total groups (26,32%)

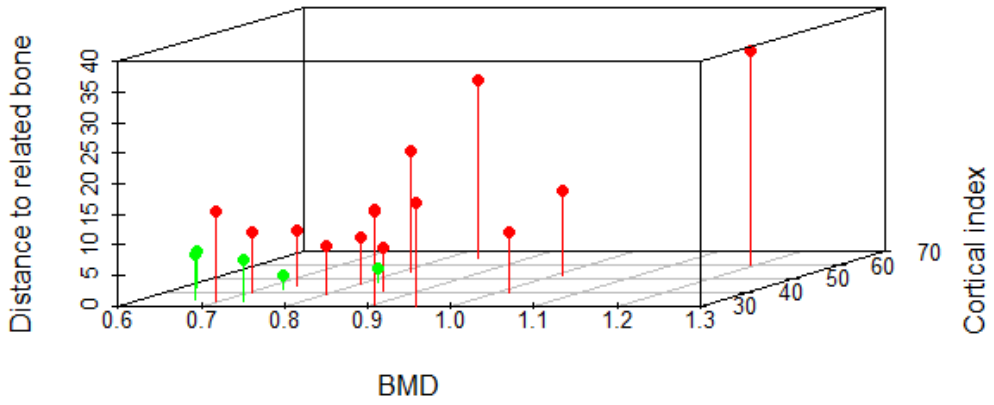

A3.7 Groups of five (44%)

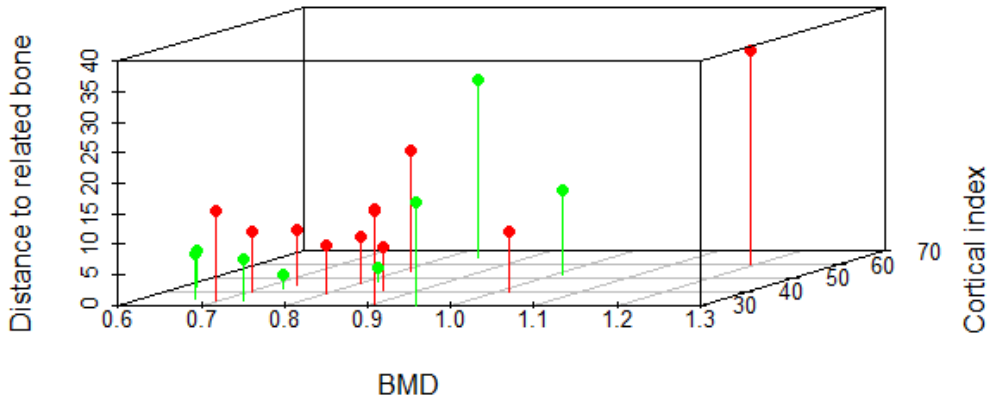

Figure A3.6 and A3.7: The difference between the BMD and cortical index of bones of an individual compared to their respective values.
Green dots: accurately reassociated individuals
Red dots: inaccurately reassociated individuals

A3.8 Groups of ten (35%)

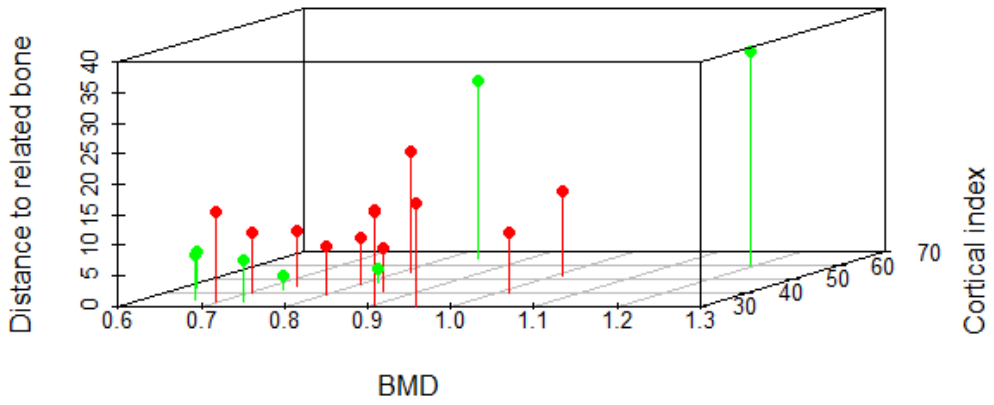

A3.9 Groups of fifteen (26,67%)

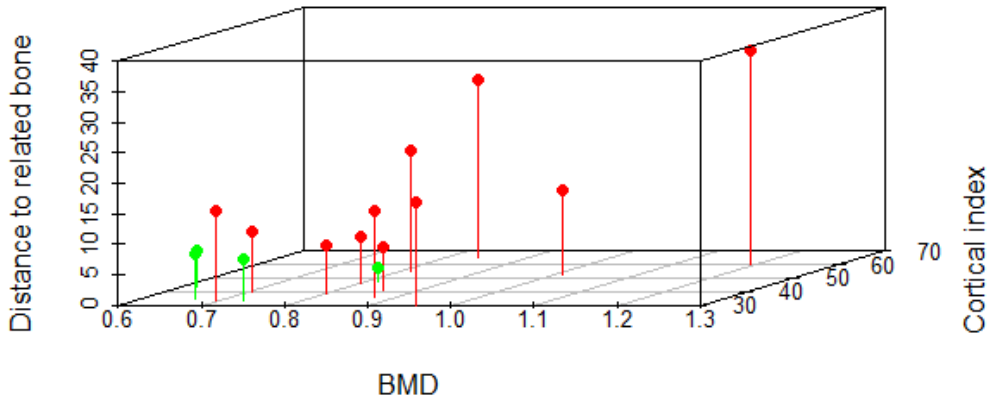

Figure A3.8 and A3.9: The difference between the BMD and cortical index of bones of an individual compared to their respective values.
Green dots: accurately reassociated individuals
Red dots: inaccurately reassociated individuals

Left femur to right humerus

Bone mineral density (BMD) and cortical index

A3.10 Total groups (14,29%)

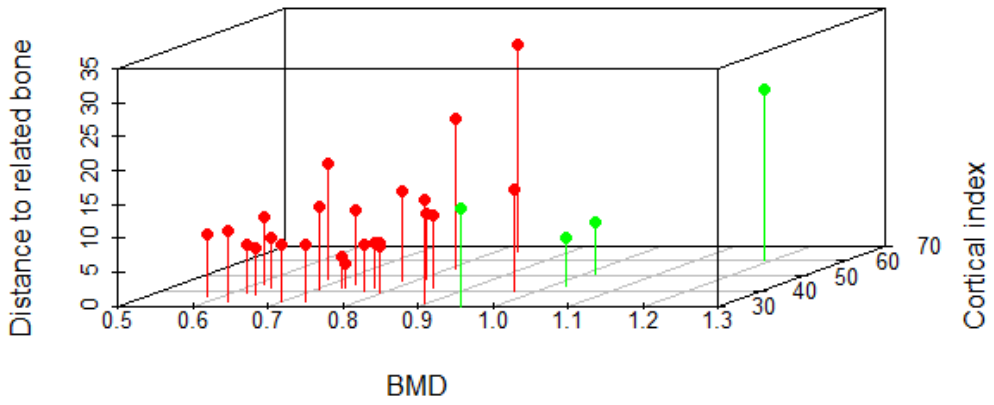

A3.11 Groups of five (36%)

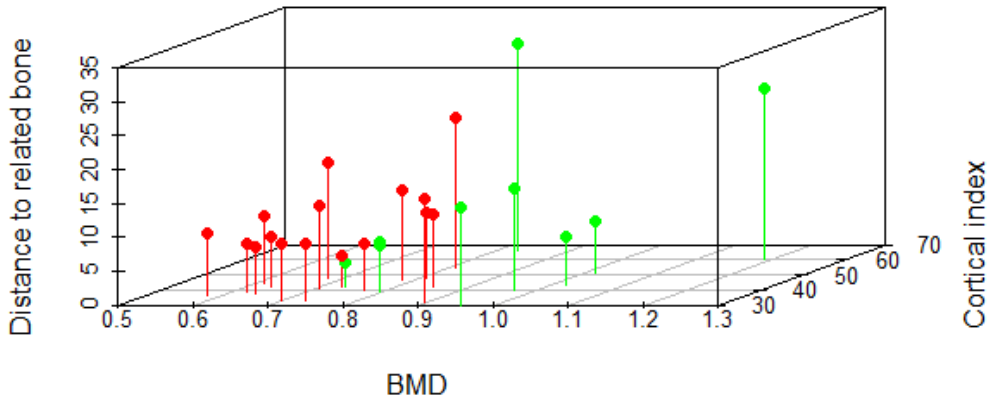

Figure A3.10 and A3.11: The difference between the BMD and cortical index of bones of an individual compared to their respective values.
Green dots: accurately reassociated individuals
Red dots: inaccurately reassociated individuals

A3.12 Groups of ten (23,33%)

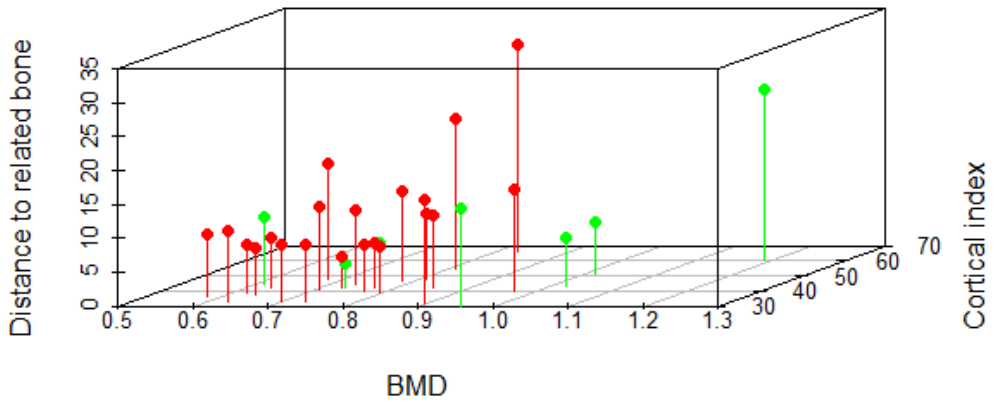

Figure A3.12: The difference between the BMD and cortical index of bones of an individual compared to their respective values.
Green dots: accurately reassociated individuals
Red dots: inaccurately reassociated individuals

Right femur to left femur

Bone mineral density (BMD) and cortical index

A3.13 Total groups (22,86%)

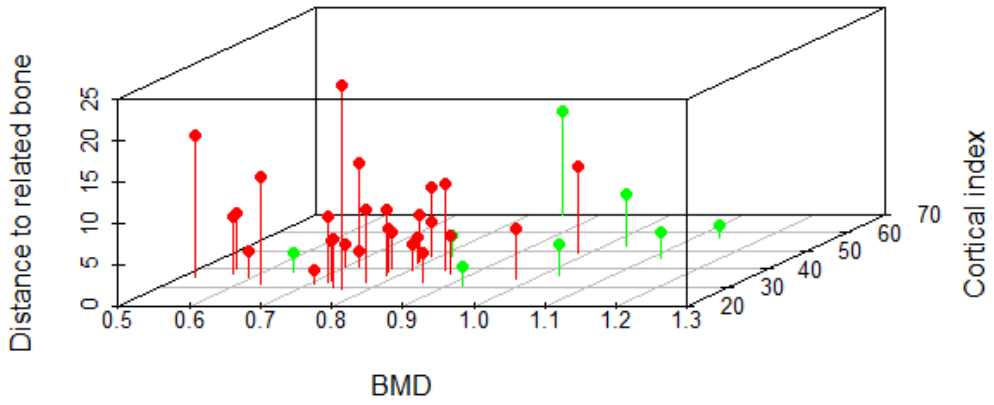

A3.14 Groups of five (76%)

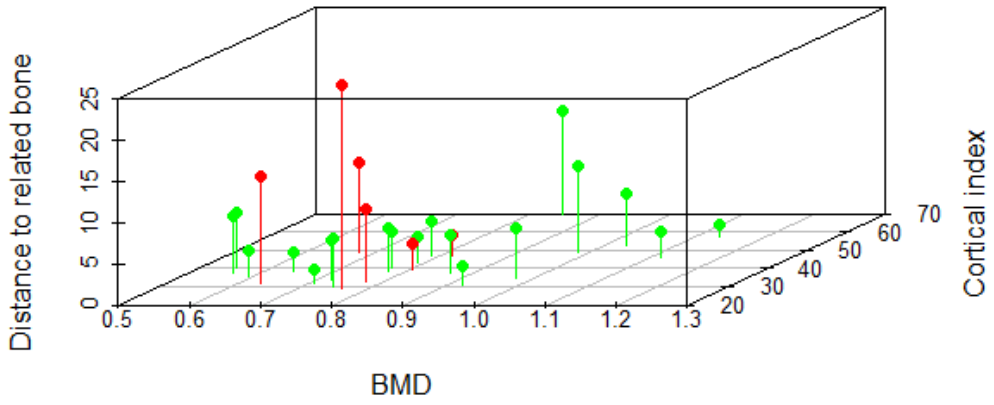

Figure A3.13 and A3.14: The difference between the BMD and cortical index of bones of an individual compared to their respective values.
Green dots: accurately reassociated individuals
Red dots: inaccurately reassociated individuals

A3.15 Groups of ten (47,50%)

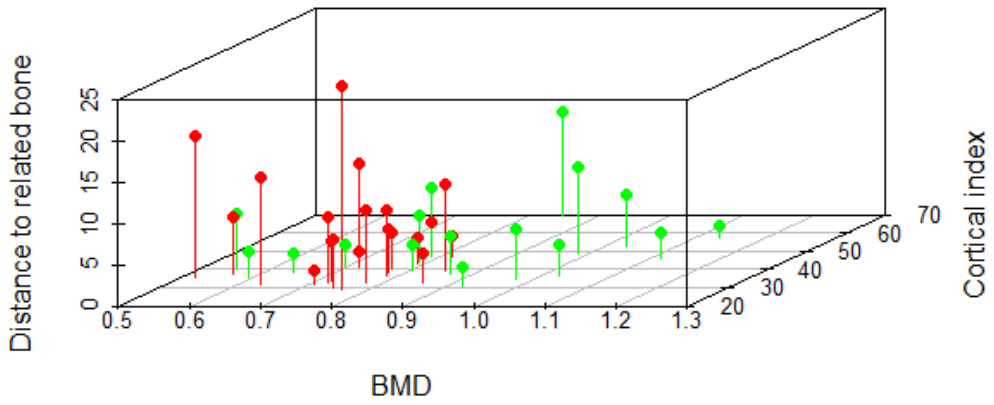

A3.16 Groups of fifteen (36,67%)

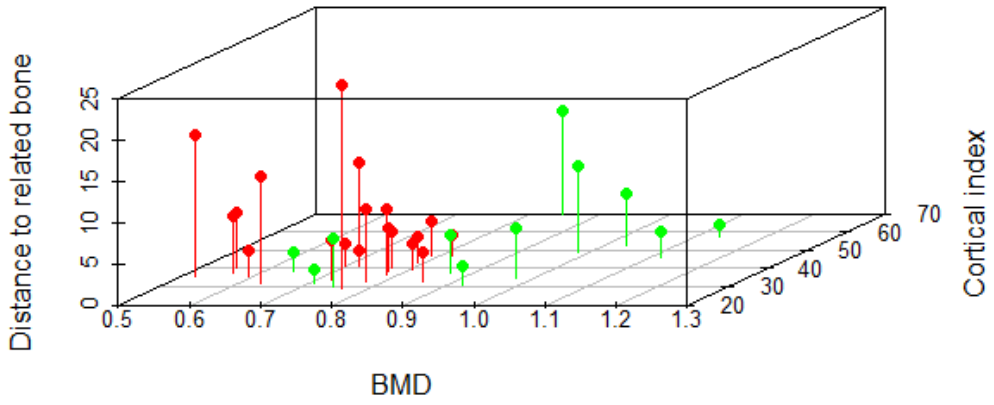

Figure A3.15 and A3.16: The difference between the BMD and cortical index of bones of an individual compared to their respective values.
Green dots: accurately reassociated individuals
Red dots: inaccurately reassociated individuals

A3.17 Groups of twenty (20%)

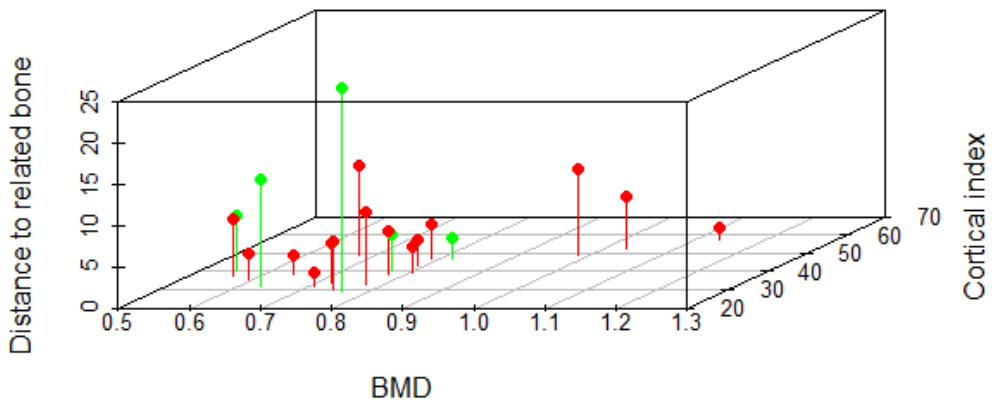

Figure A3.17: The difference between the BMD and cortical index of bones of an individual compared to their respective values.
Green dots: accurately reassociated individuals
Red dots: inaccurately reassociated individuals

Right femur to left humerus

Bone mineral density (BMD) and cortical index

A3.18 Total groups (11,11%)

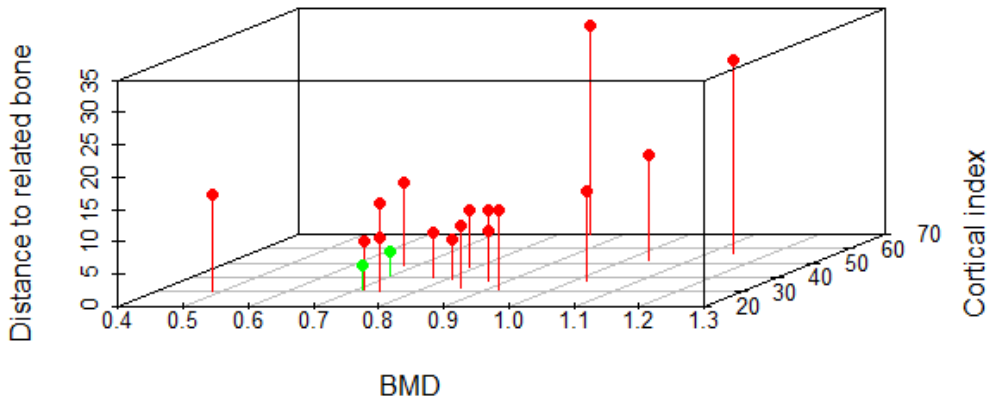

A3.19 Groups of five (52%)

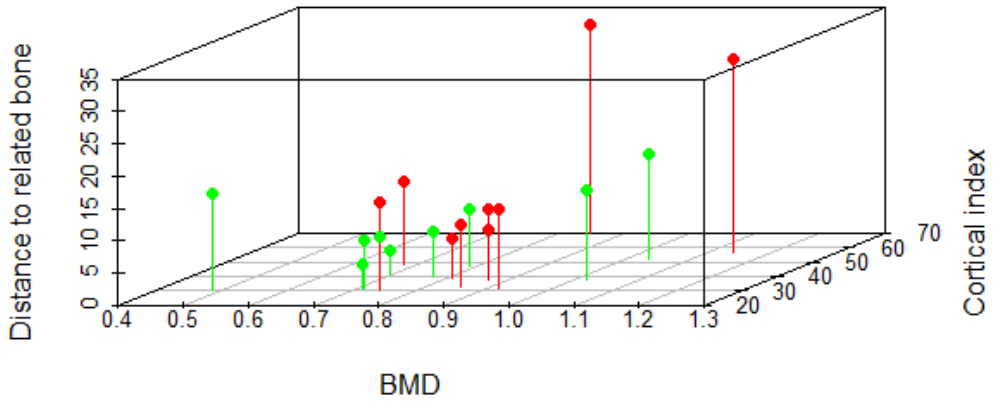

Figure A3.18 and A3.19: The difference between the BMD and cortical index of bones of an individual compared to their respective values.
Green dots: accurately reassociated individuals
Red dots: inaccurately reassociated individuals

A3.20 Groups of ten (35%)

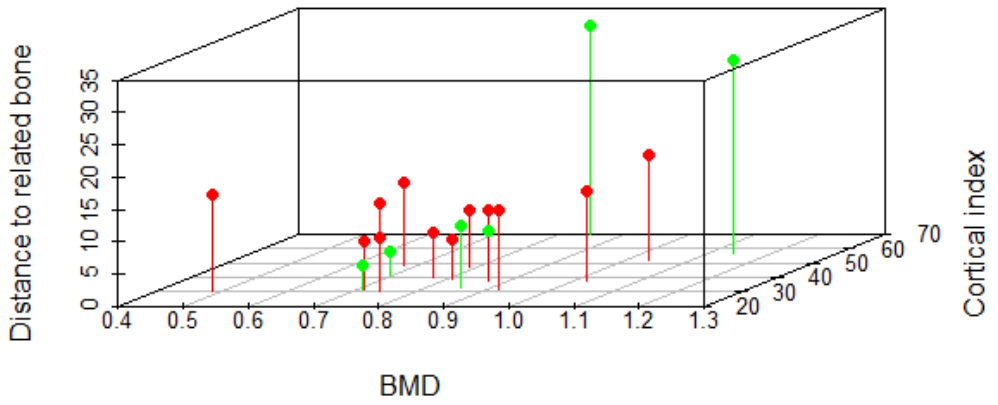

A3.21 Groups of fifteen (13,33%)

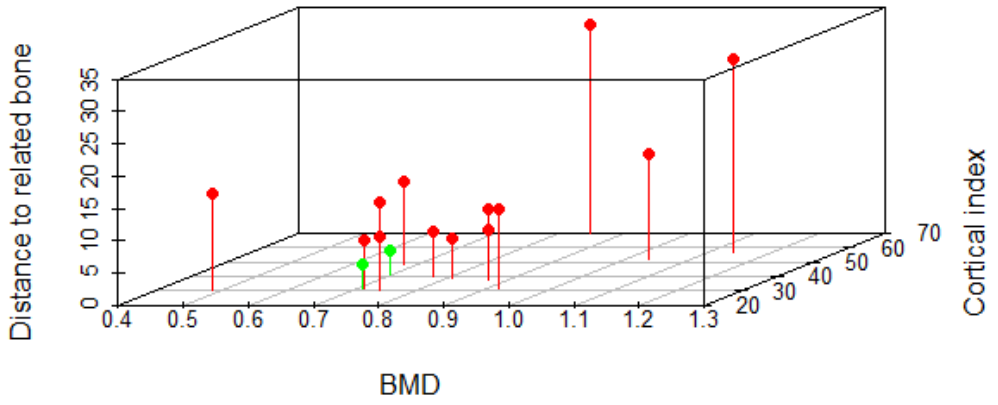

Figure A3.20 and A3.21: The difference between the BMD and cortical index of bones of an individual compared to their respective values.
Green dots: accurately reassociated individuals
Red dots: inaccurately reassociated individuals

Right femur to right humerus

Bone mineral density (BMD) and cortical index

A3.22 Total groups (17,86%)

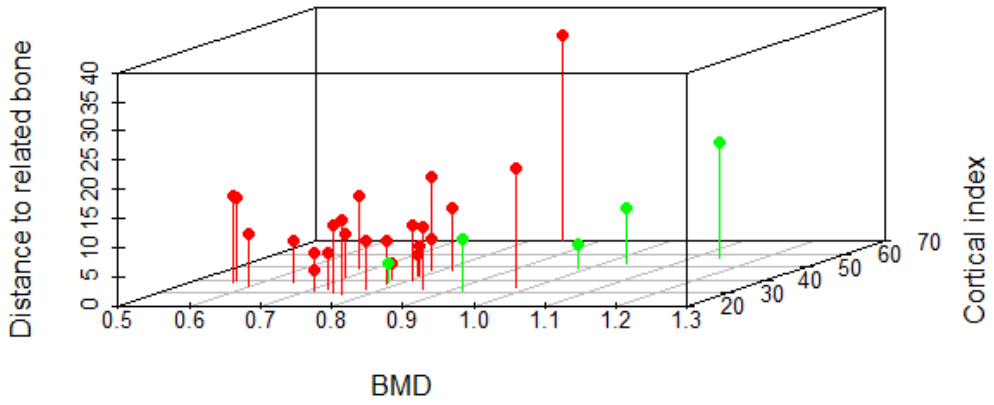

A3.23 Groups of five (36%)

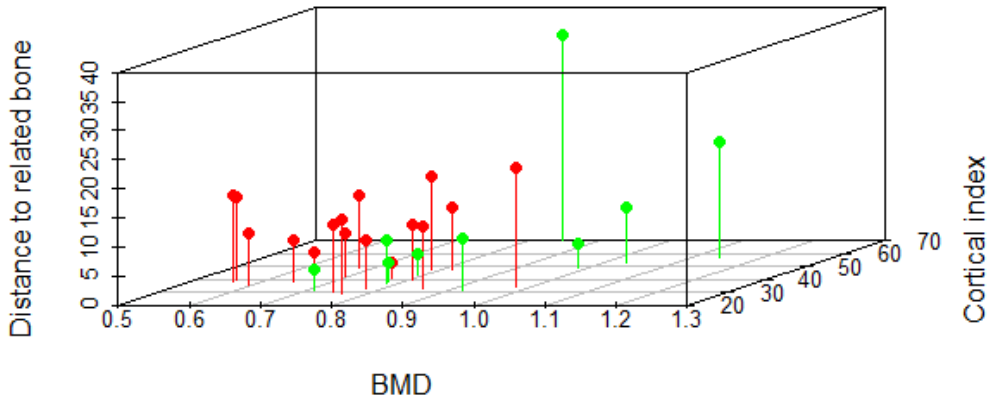

Figure A3.22 and A3.23: The difference between the BMD and cortical index of bones of an individual compared to their respective values.
Green dots: accurately reassociated individuals
Red dots: inaccurately reassociated individuals

A3.24 Groups of ten (33,33%)

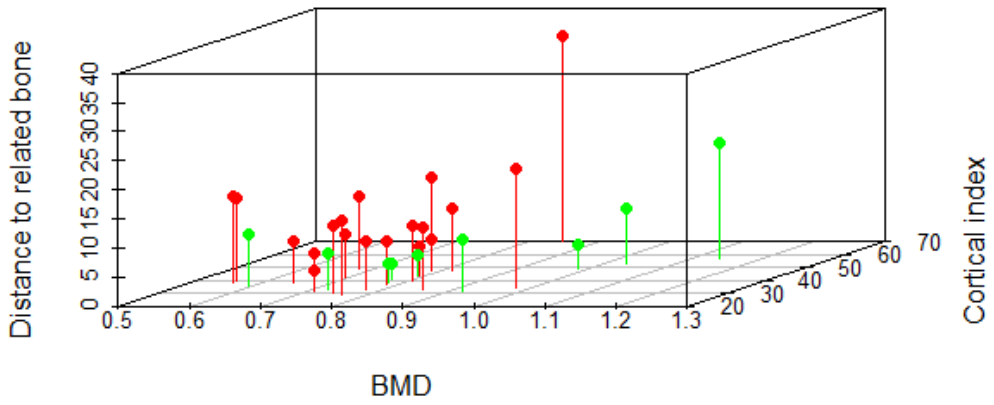

A3.25 Groups of fifteen (20%)

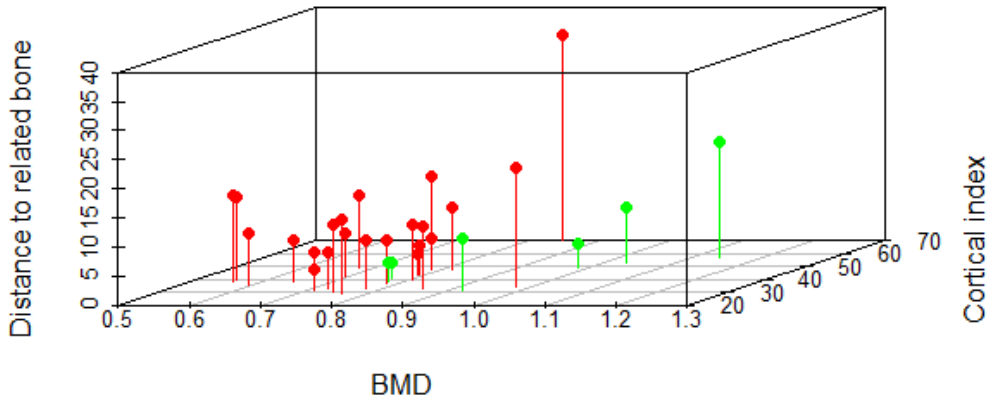

Figure A3.24 and A3.25: The difference between the BMD and cortical index of bones of an individual compared to their respective values.
Green dots: accurately reassociated individuals
Red dots: inaccurately reassociated individuals

Left humerus to left femur

Bone mineral density (BMD) and cortical index

A3.26 Total groups (21,05%)

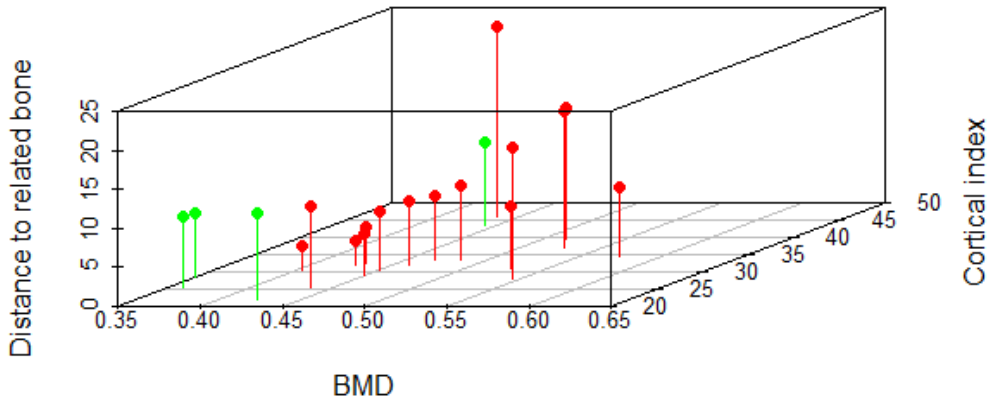

A3.27 Groups of five (44%)

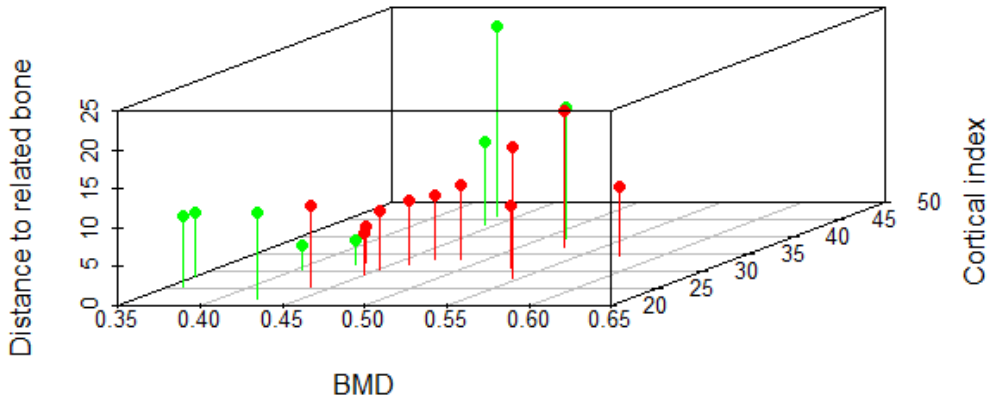

Figure A3.26 and A3.27: The difference between the BMD and cortical index of bones of an individual compared to their respective values.
Green dots: accurately reassociated individuals
Red dots: inaccurately reassociated individuals

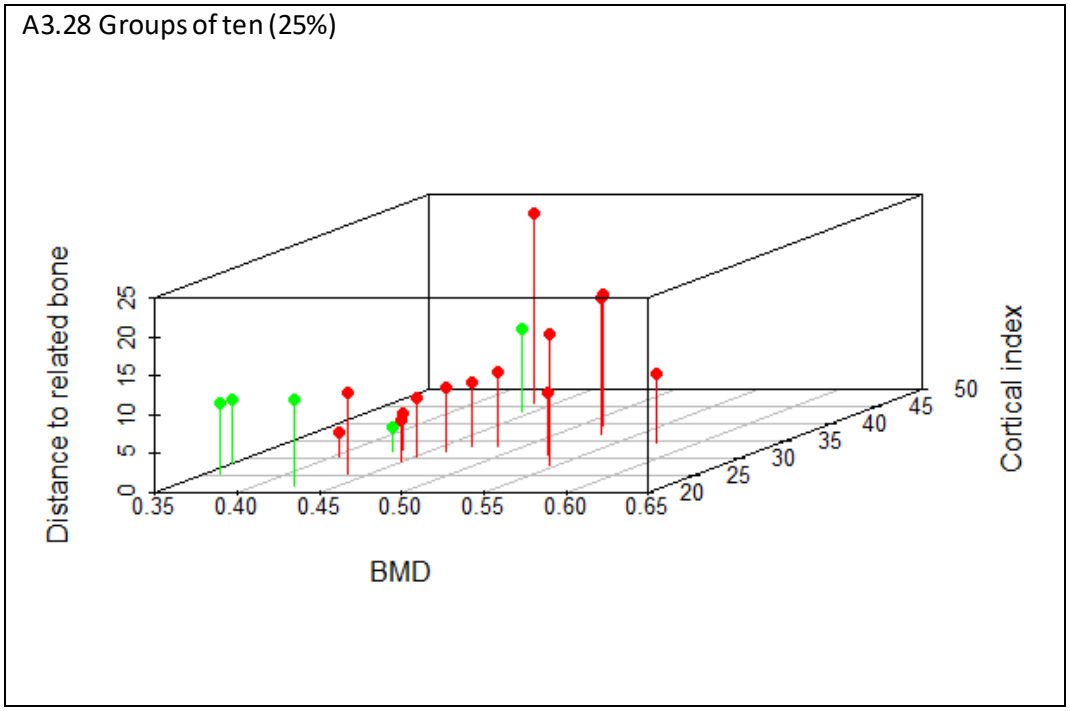

Figure A3.28: The difference between the BMD and cortical index of bones of an individual compared to their respective values.
Green dots: accurately reassociated individuals
Red dots: inaccurately reassociated individuals

Left humerus to right femur

Bone mineral density (BMD) and cortical index

A3.29 Total groups (16,67%)

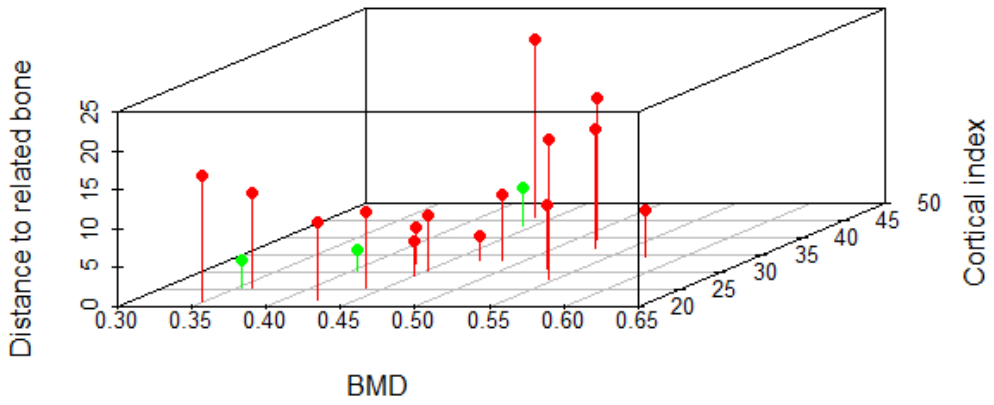

A3.30 Groups of five (40%)

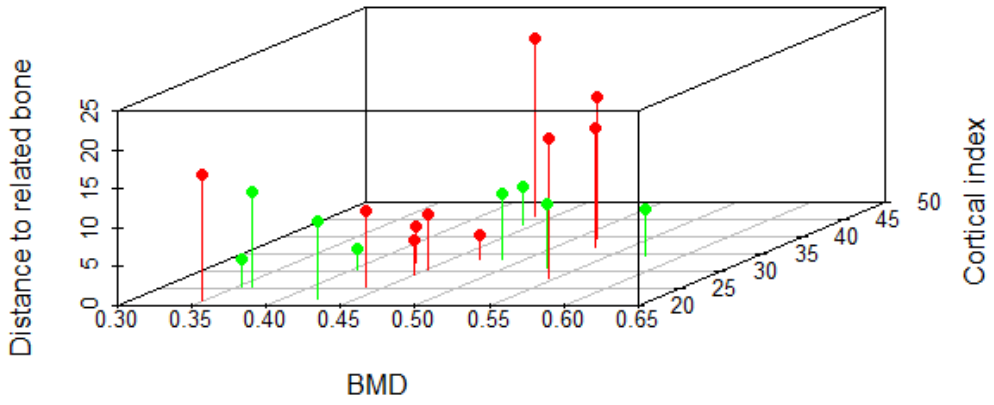

Figure A3.29 and A3.30: The difference between the BMD and cortical index of bones of an individual compared to their respective values.
Green dots: accurately reassociated individuals
Red dots: inaccurately reassociated individuals

A3.31 Groups of ten (25%)

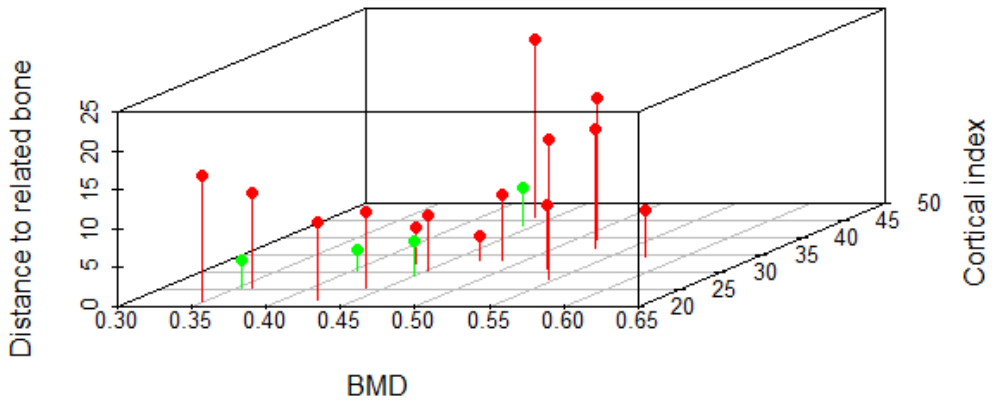

Figure A3.31: The difference between the BMD and cortical index of bones of an individual compared to their respective values.
Green dots: accurately reassociated individuals
Red dots: inaccurately reassociated individuals

Left humerus to right humerus

Bone mineral density (BMD) and cortical index

A3.32 Total groups (6,67%)

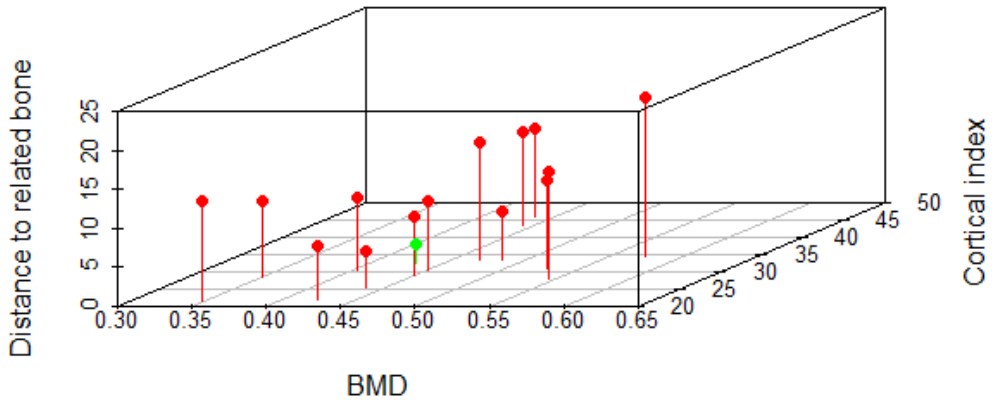

A3.33 Groups of five (40%)

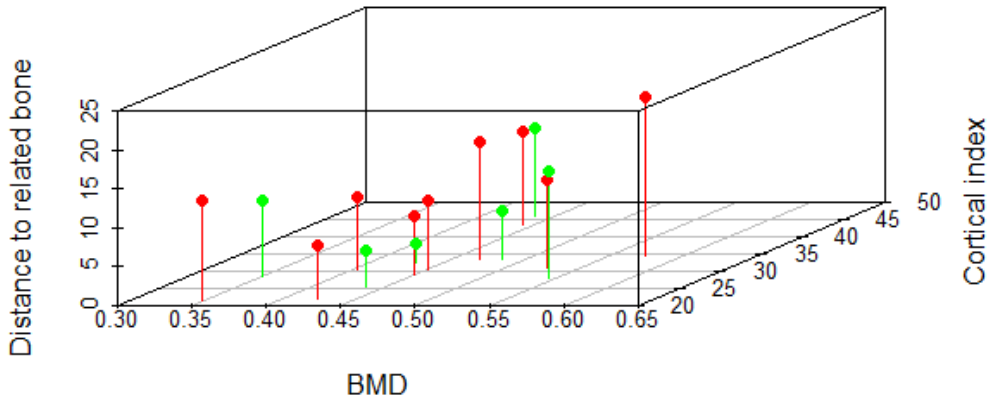

Figure A3.32 and A3.33: The difference between the BMD and cortical index of bones of an individual compared to their respective values.
Green dots: accurately reassociated individuals
Red dots: inaccurately reassociated individuals

A3.34 Groups of ten (40%)

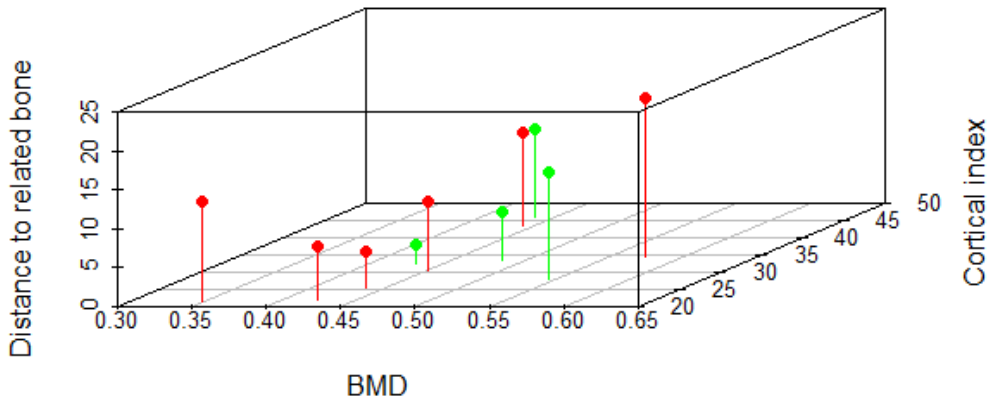

A3.35 Groups of fifteen (6,67%)

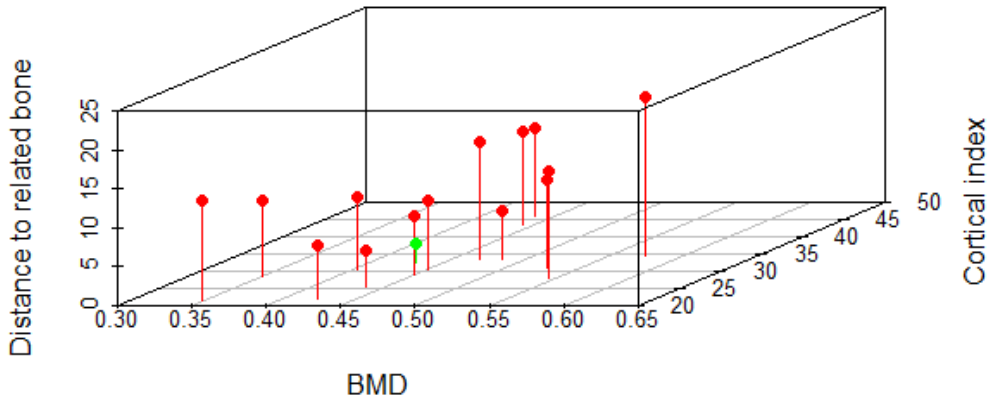

Figure A3.34 and A3.35: The difference between the BMD and cortical index of bones of an individual compared to their respective values.
Green dots: accurately reassociated individuals
Red dots: inaccurately reassociated individuals

Right humerus to left femur

Bone mineral density (BMD) and cortical index

A3.36 Total groups (7,41%)

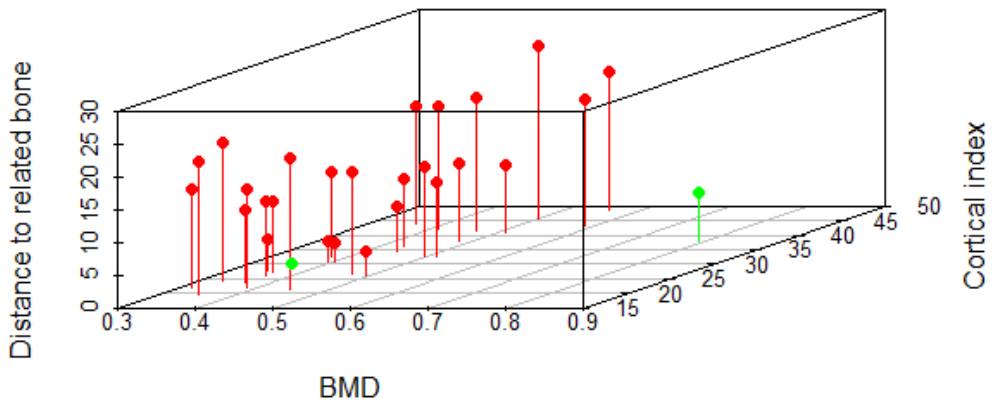

A3.37 Groups of five (48%)

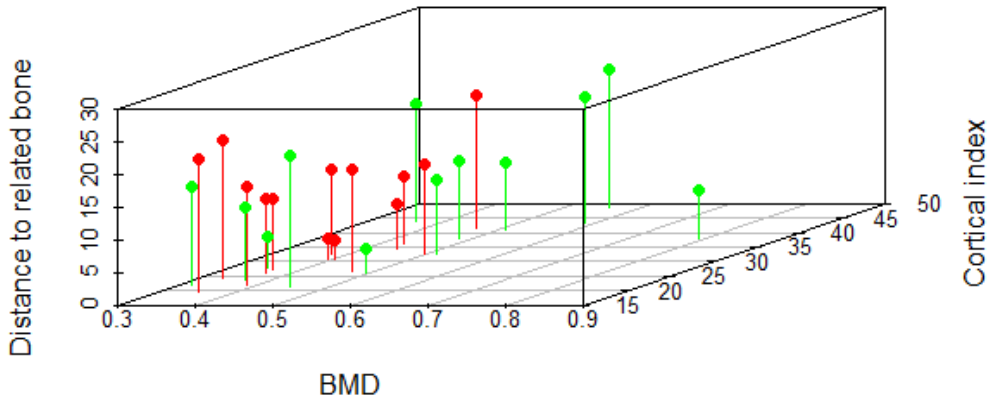

Figure A3.36 and A3.37: The difference between the BMD and cortical index of bones of an individual compared to their respective values.
Green dots: accurately reassociated individuals
Red dots: inaccurately reassociated individuals

A3.38 Groups of ten (20%)

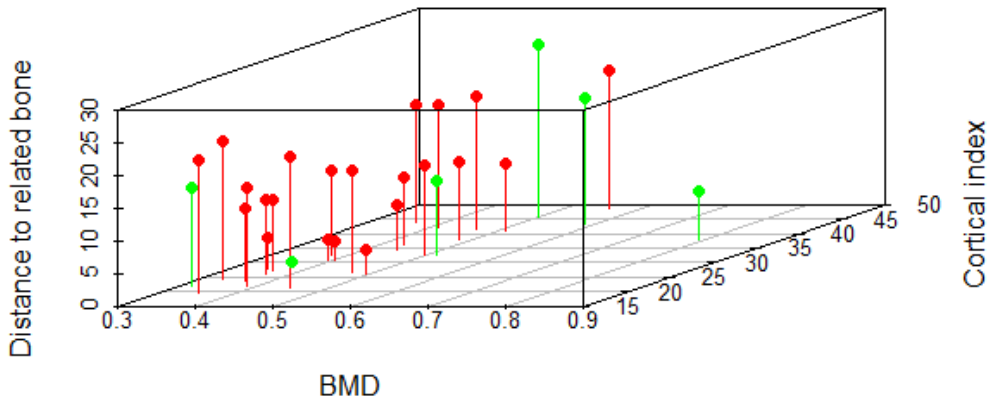

Figure A3.38: The difference between the BMD and cortical index of bones of an individual compared to their respective values.
Green dots: accurately reassociated individuals
Red dots: inaccurately reassociated individuals

Right humerus to right femur

Bone mineral density (BMD) and cortical index

A3.39 Total groups (10,71%)

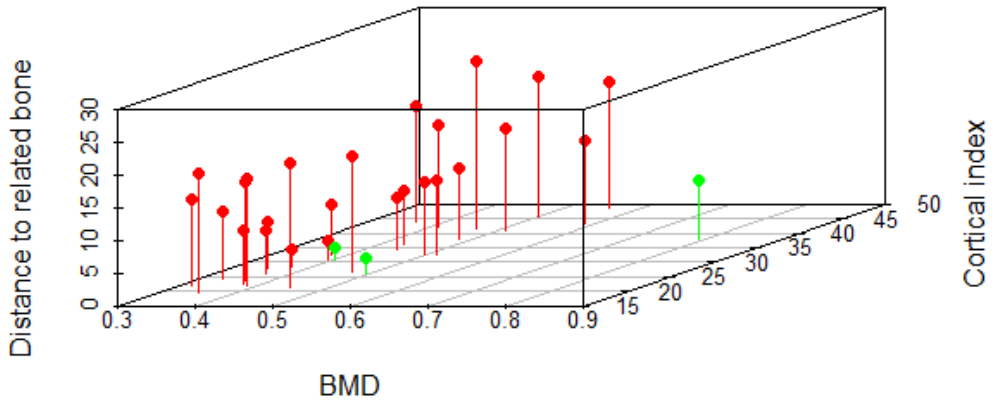

A3.40 Groups of five (36%)

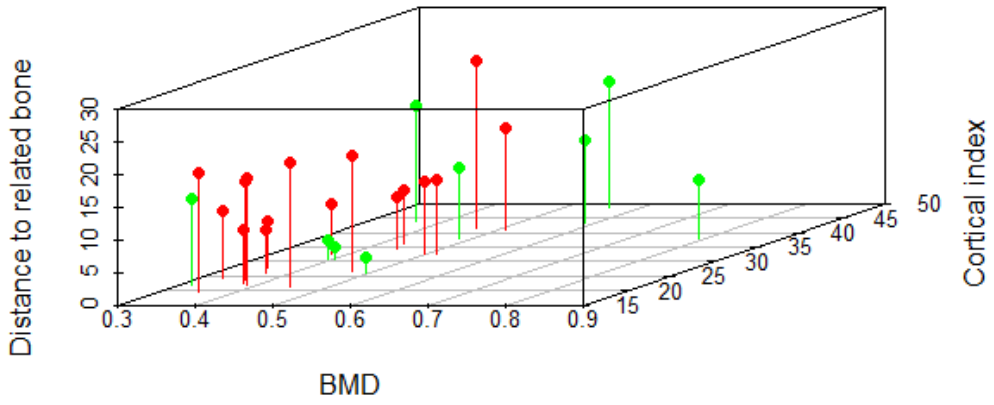

Figure A3.39 and A3.40: The difference between the BMD and cortical index of bones of an individual compared to their respective values.
Green dots: accurately reassociated individuals
Red dots: inaccurately reassociated individuals

A3.41 Groups of ten (36,67%)

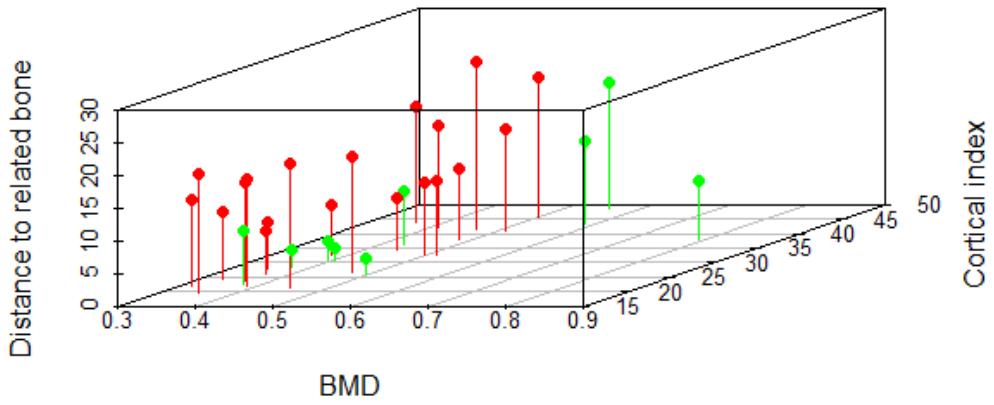

A3.42 Groups of fifteen (20%)

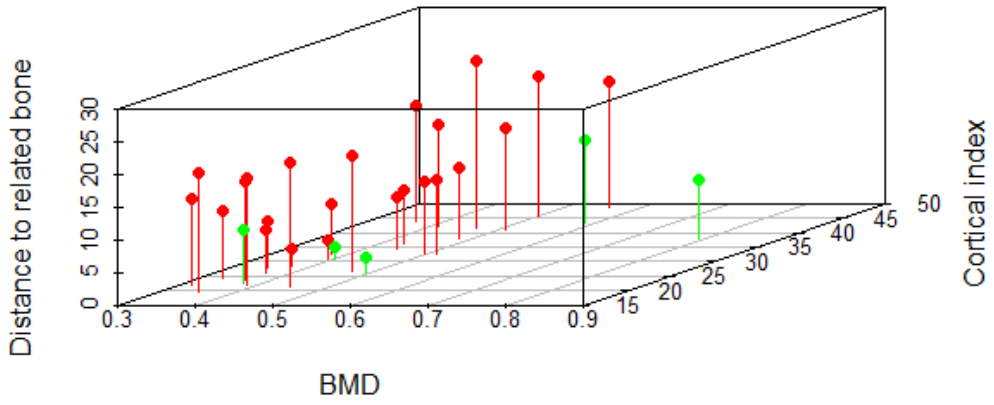

Figure A3.41 and A3.42: The difference between the BMD and cortical index of bones of an individual compared to their respective values.
Green dots: accurately reassociated individuals
Red dots: inaccurately reassociated individuals

Right humerus to left humerus

Bone mineral density (BMD) and cortical index

A3.43 Total groups (26,67%)

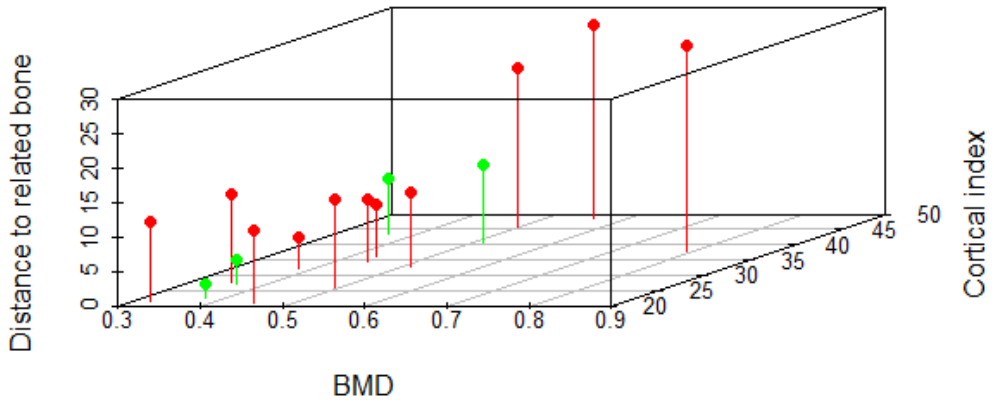

A3.44 Groups of five (52%)

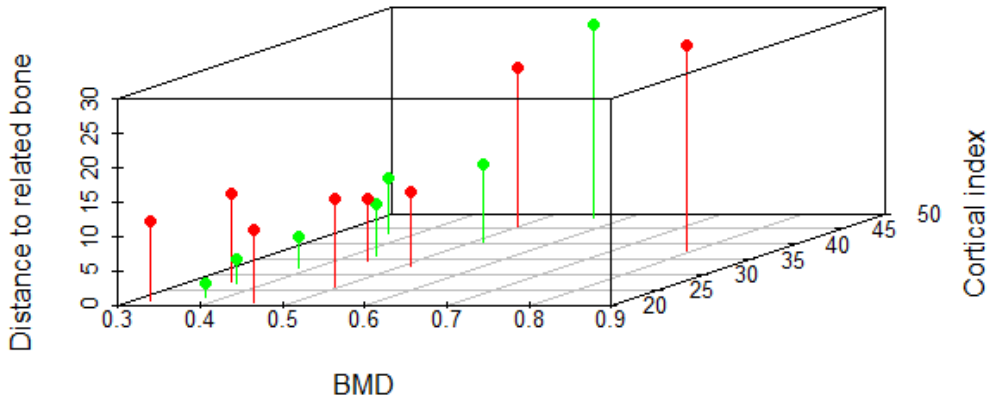

Figure A3.43 and A3.44: The difference between the BMD and cortical index of bones of an individual compared to their respective values.
Green dots: accurately reassociated individuals
Red dots: inaccurately reassociated individuals

A3.45 Groups of ten (40%)

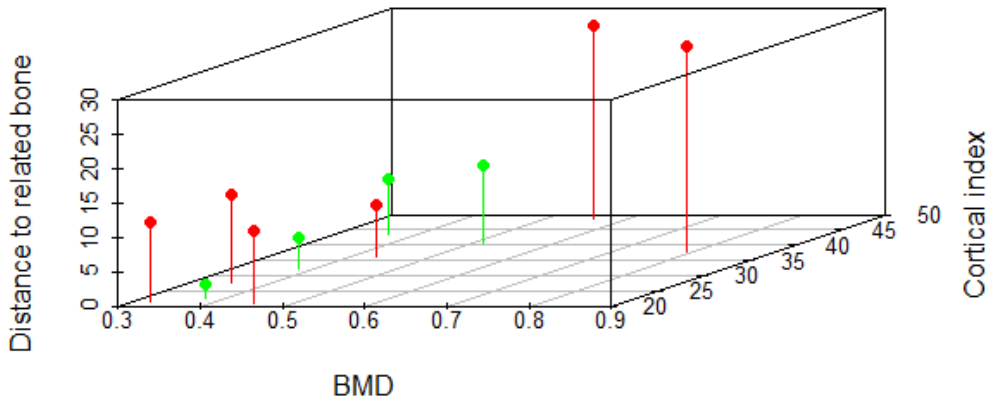

A3.46 Groups of fifteen (26,67%)

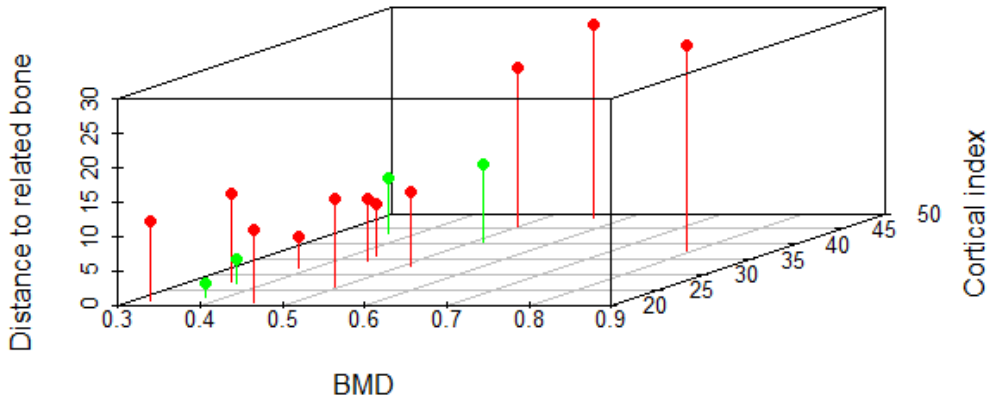

Figure A3.45 and A3.46: The difference between the BMD and cortical index of bones of an individual compared to their respective values.
Green dots: accurately reassociated individuals
Red dots: inaccurately reassociated individuals

Appendix 4: plots of difference to nearest neighbour

This appendix contains the (3D) graphs that were plotted of the differences between bones and their nearest neighbours, that were accurately and inaccurately reassociated using both variables compared to the original values of the bone that was used for finding the associated bone.

The following properties apply to the 2D-graphs in this appendix:

- the X-axis presents the BMD-value or cortical index of the known bone
- the Y-axis presents the difference to the searched bone of the same skeleton
- green dots represent individuals whose own bone was reassociated
- red dots represent the individuals whose bones were reassociated with bones of a different individual

The following properties apply to the 3D-graphs in this appendix:

- the X-axis presents the BMD-value of the known bone
- the Y-axis presents the cortical index of the known bone
- the Z-axis presents the difference between the known bone and the searched bone of that individual
- green dots represent individuals whose own bone was reassociated
- red dots represent the individuals whose bones were reassociated with bones of a different individual

Bone mineral density (BMD) - groups of five

A4.1 Left femur to right femur (56%)

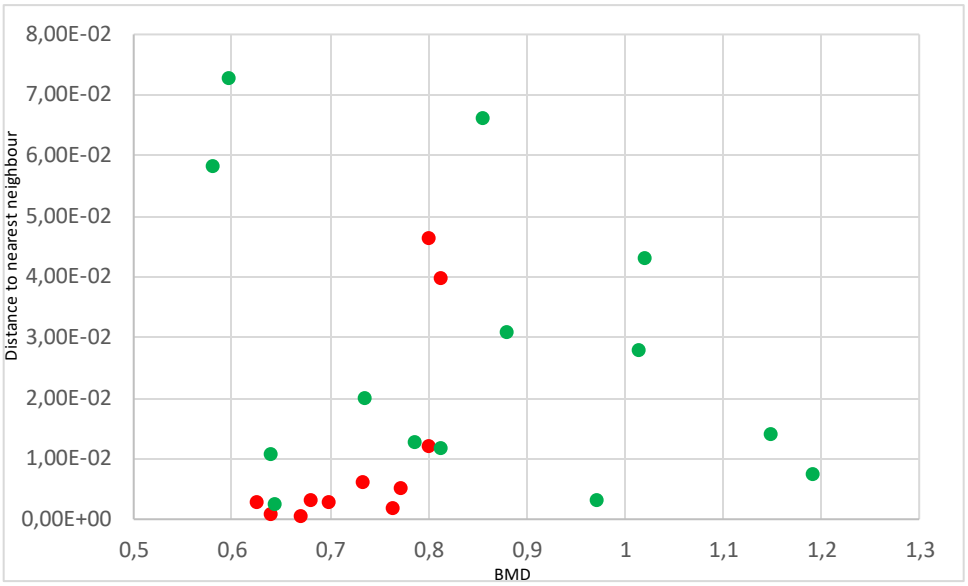

A4.2 Left femur to right humerus (40%)

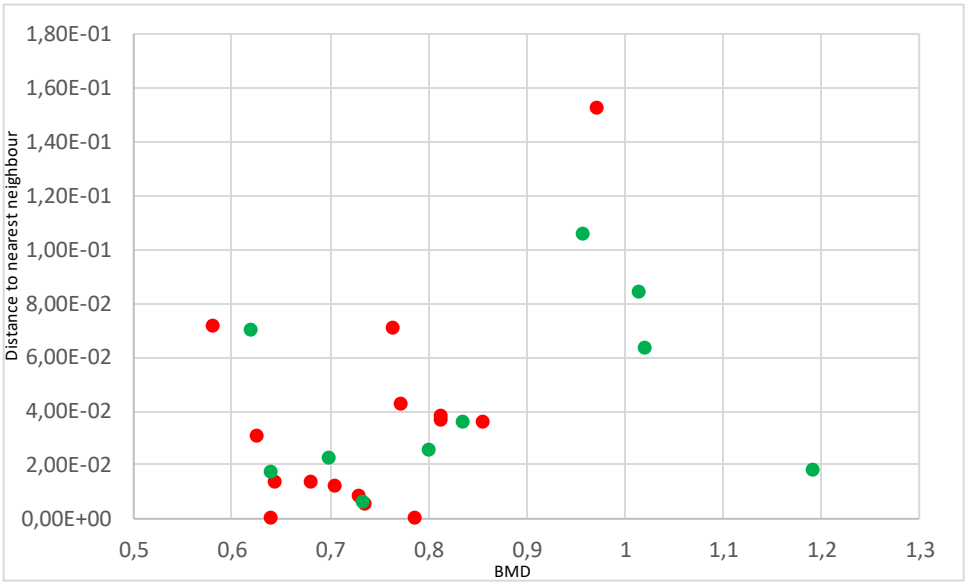

Figure A4.1 and A4.2: The distance from the BMD of a bone to the nearest neighbouring bone.
Green dots: accurately reassociated individuals
Red dots: inaccurately reassociated individuals

A4.3 Right femur to left femur (68%)

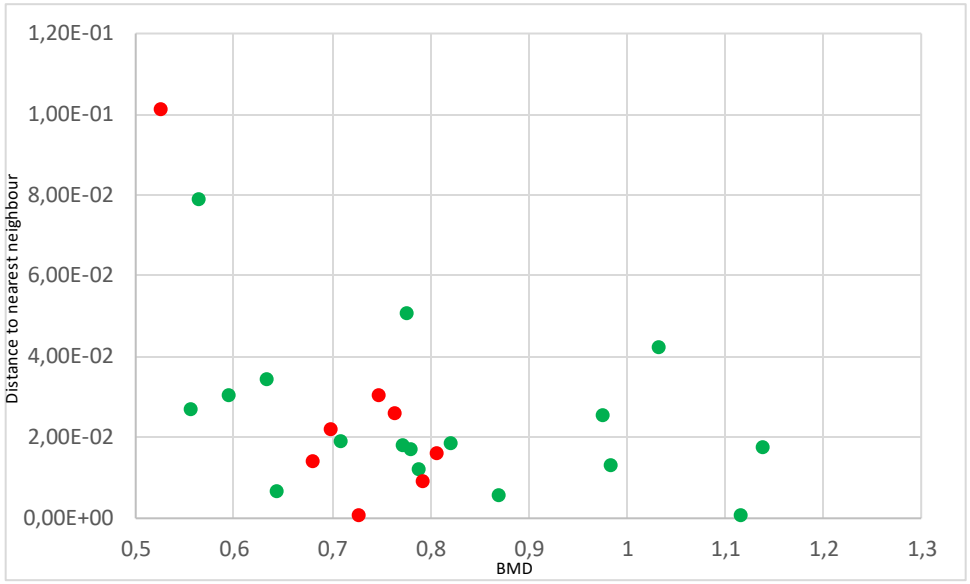

A4.4 Right femur to left humerus (40%)

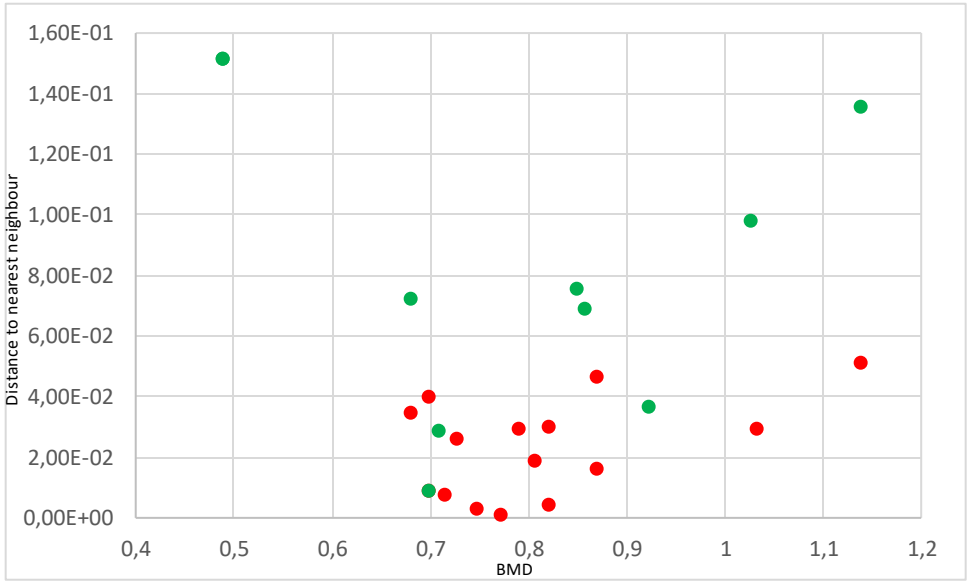

Figure A4.3 and A4.4: The distance from the BMD of a bone to the nearest neighbouring bone.
Green dots: accurately reassociated individuals
Red dots: inaccurately reassociated individuals

A4.5 Right femur to right humerus (44%)

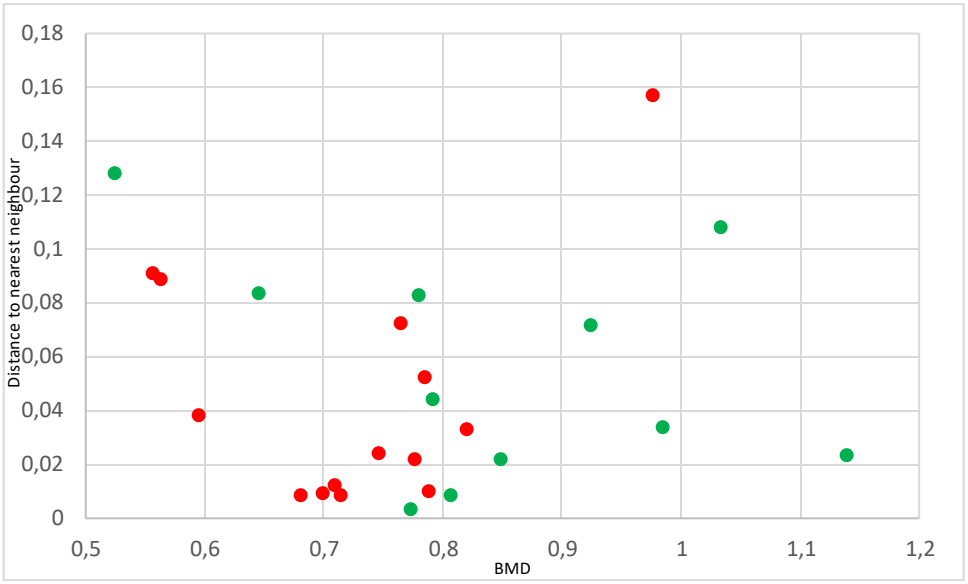

A4.6 Left humerus to right femur (40%)

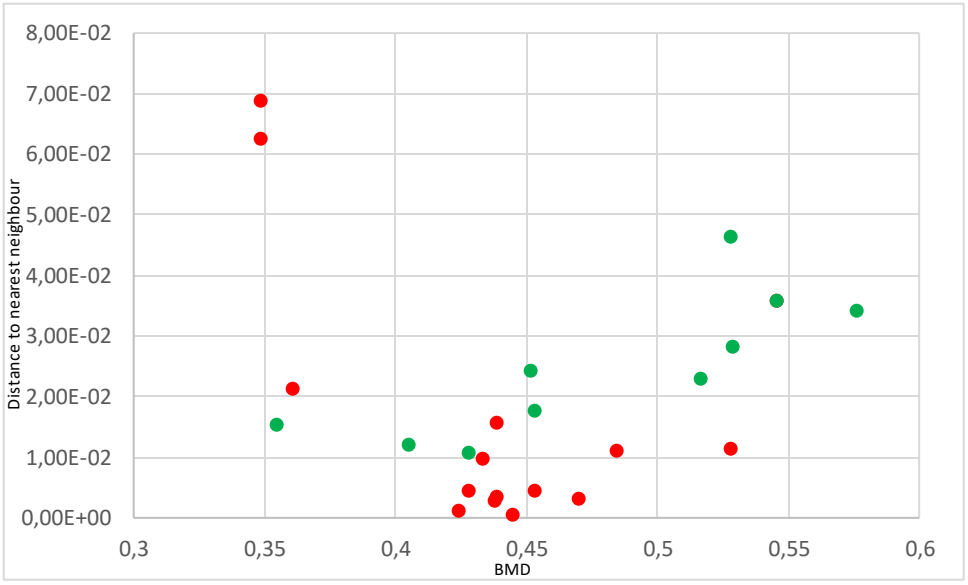

Figure A4.5 and A4.6: The distance from the BMD of a bone to the nearest neighbouring bone.
Green dots: accurately reassociated individuals
Red dots: inaccurately reassociated individuals

A4.7 Right humerus to left femur (40%)

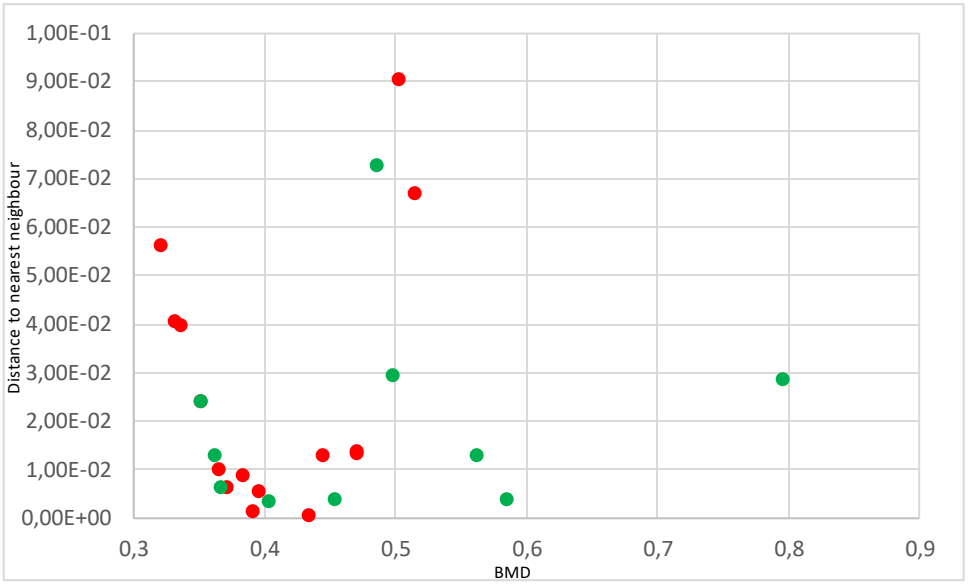

A4.8 Right humerus to right femur (36%)

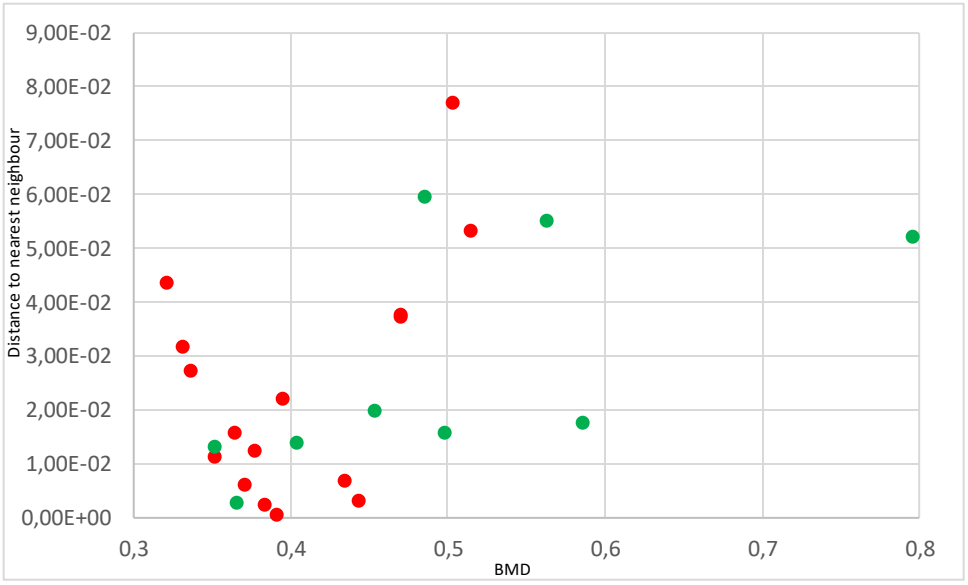

Figure A4.7 and A4.8: The distance from the BMD of a bone to the nearest neighbouring bone.
Green dots: accurately reassociated individuals
Red dots: inaccurately reassociated individuals

Cortical index - groups of five

A4.9 Left femur to right femur (36%)

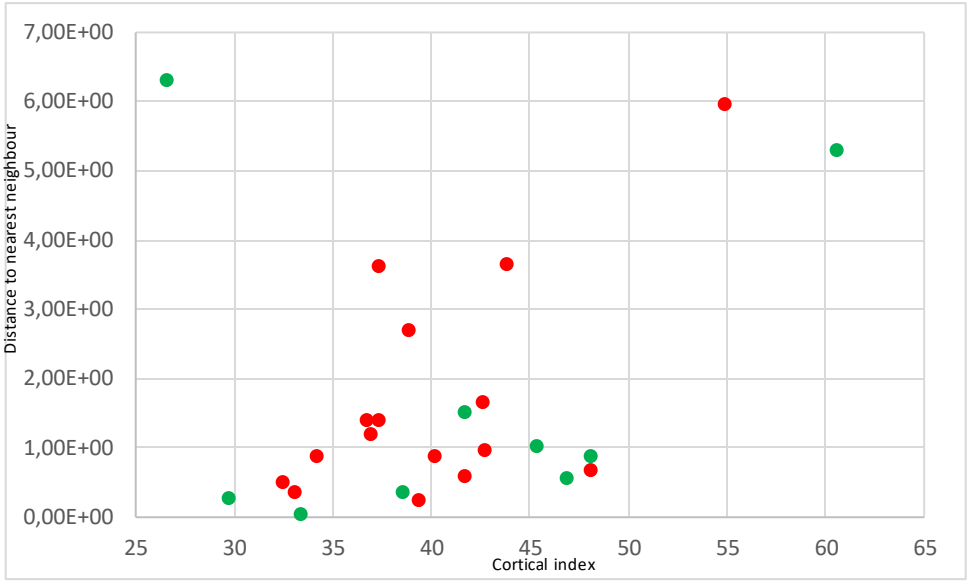

A4.10 Right femur to left femur (44%)

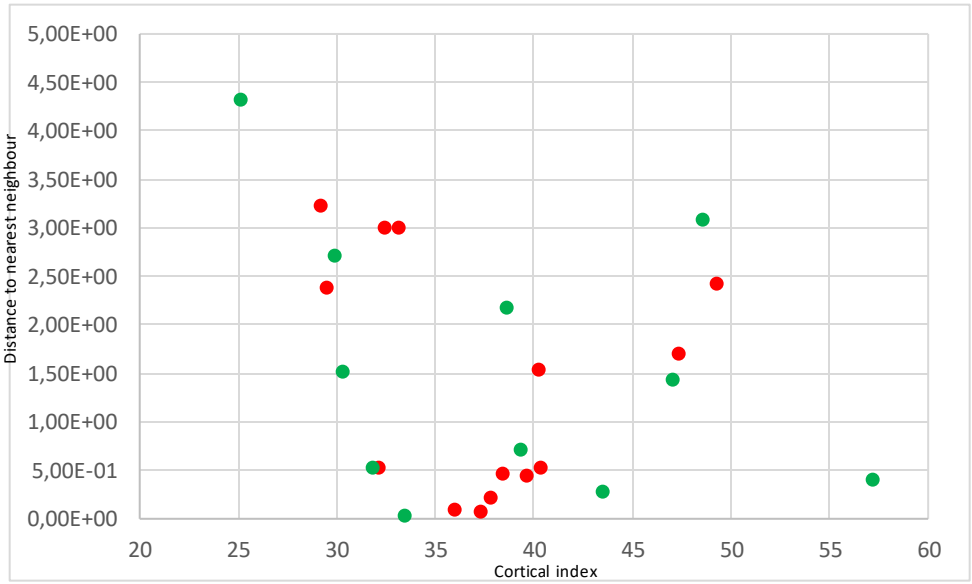

Figure A4.9 and A4.10: The distance from the cortical index of a bone to the nearest neighbouring bone.
Green dots: accurately reassociated individuals
Red dots: inaccurately reassociated individuals

A4.11 Right femur to right humerus (48%)

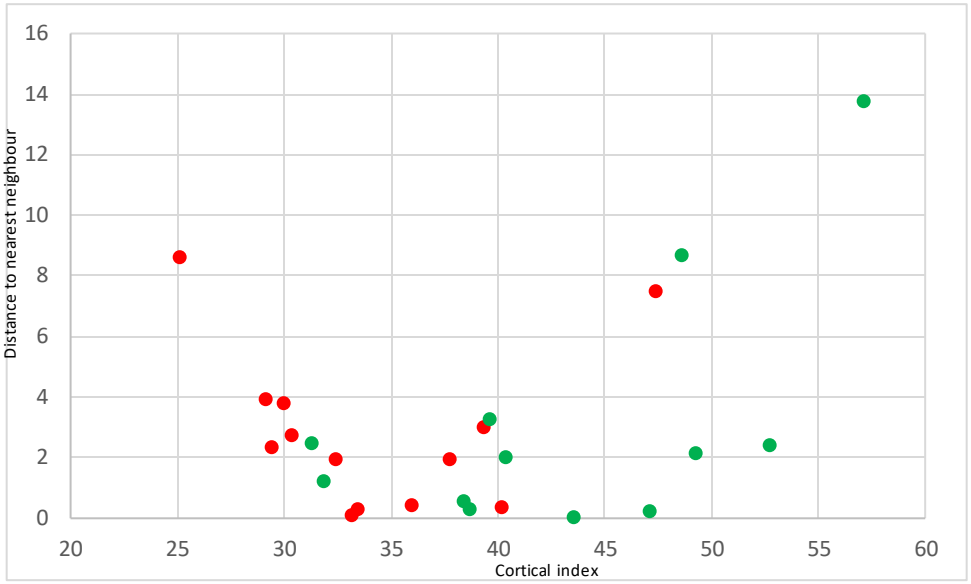

A4.12 Left humerus to left femur (36%)

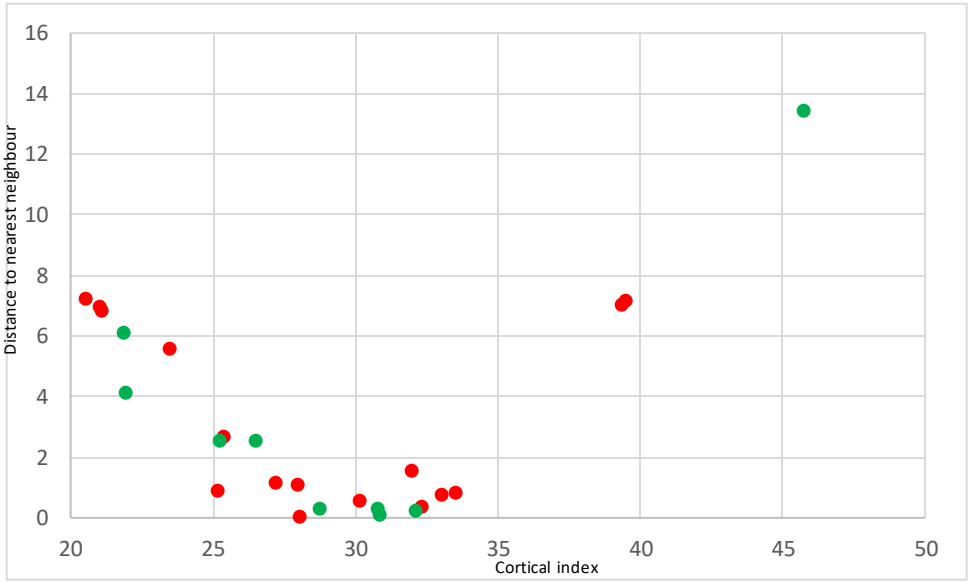

Figure A4.11 and A4.12: The distance from the cortical index of a bone to the nearest neighbouring bone.
Green dots: accurately reassociated individuals
Red dots: inaccurately reassociated individuals

A4.13 Left humerus to right humerus (56%)

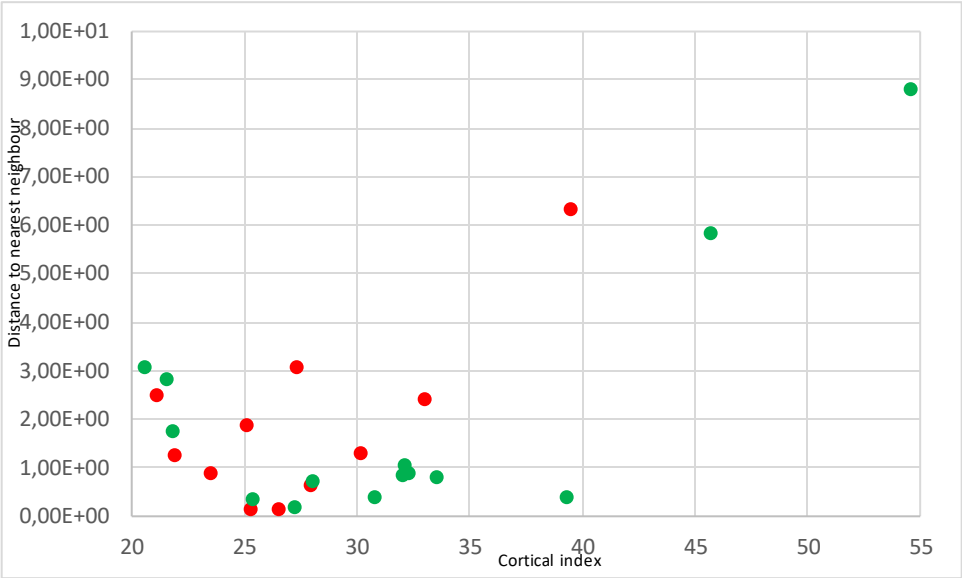

A4.14 Right humerus to right femur (40%)

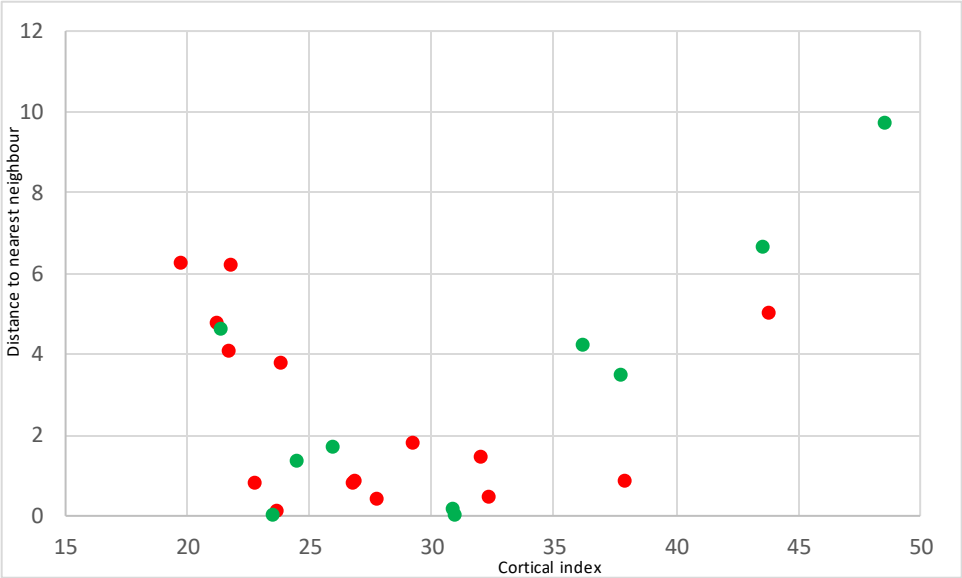

Figure A4.13 and A4.14: The distance from the cortical index of a bone to the nearest neighbouring bone.
Green dots: accurately reassociated individuals
Red dots: inaccurately reassociated individuals

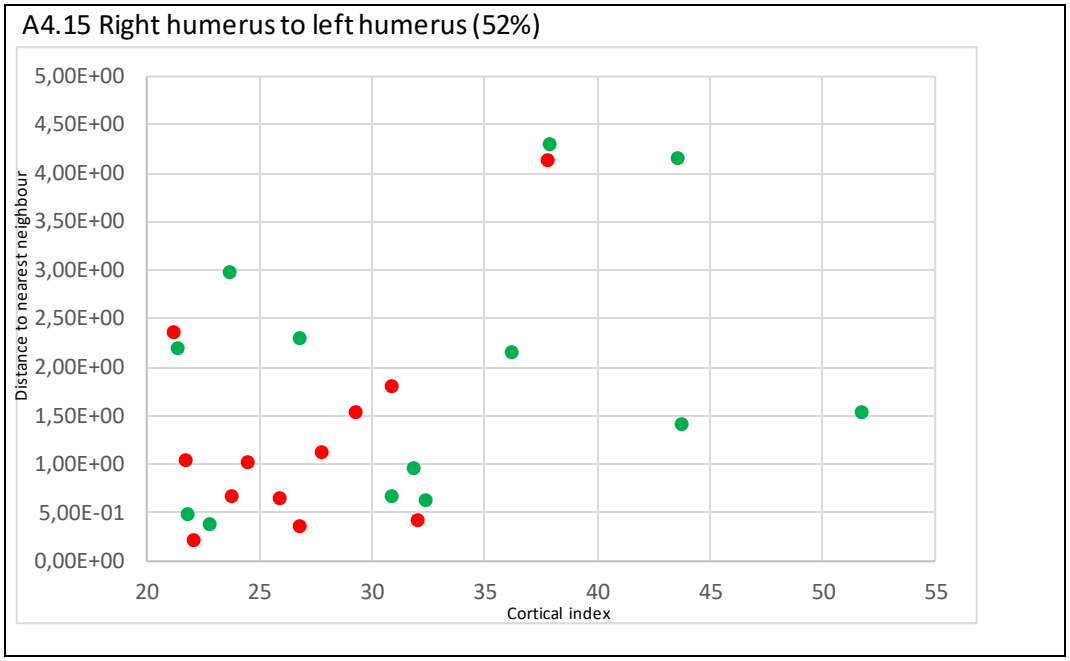

Figure A4.15: The distance from the cortical index of a bone to the nearest neighbouring bone.
Green dots: accurately reassociated individuals
Red dots: inaccurately reassociated individuals

The BMD and cortical index combined- groups of five

A4.16 Left femur to right femur (76%)

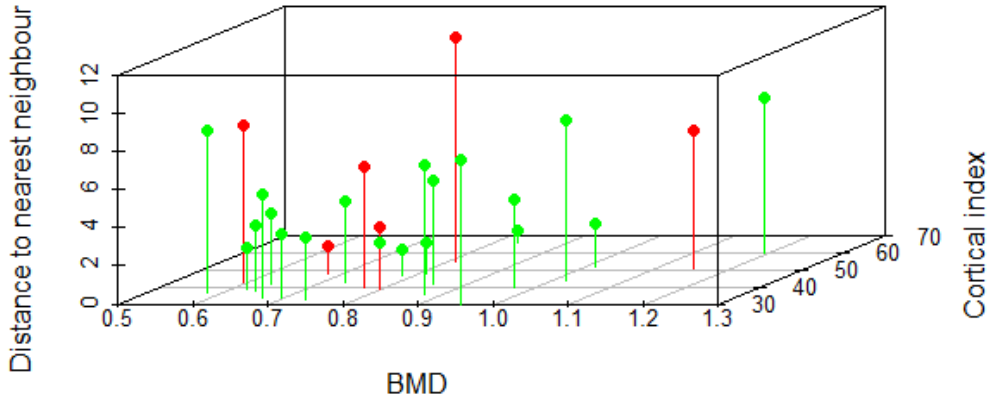

A4.17 Left femur to left humerus (44%)

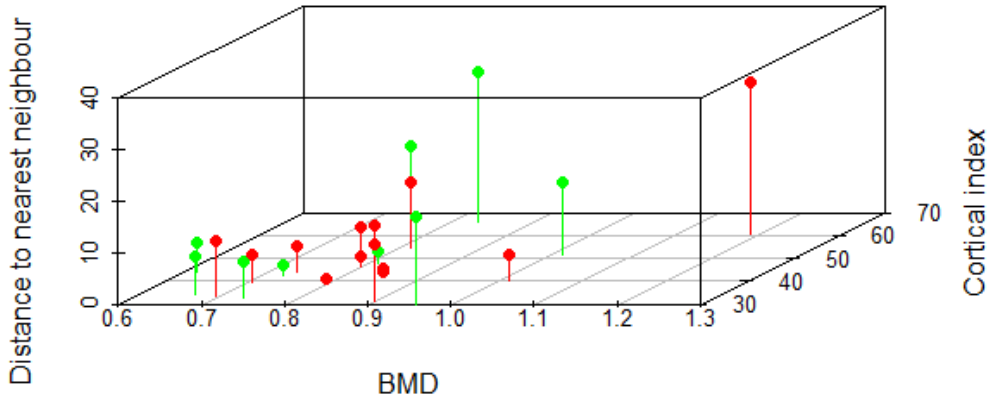

Figure A4.16 and A4.17: The distance from the BMD and cortical index of a bone to the nearest neighbouring bone.
Green dots: accurately reassociated individuals
Red dots: inaccurately reassociated individuals

A4.18 Left femur to right humerus (36%)

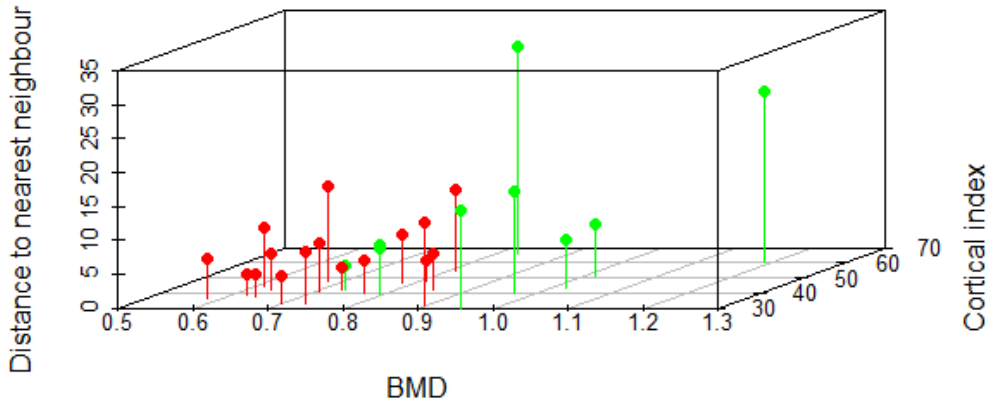

A4.19 Right femur to left femur (76%)

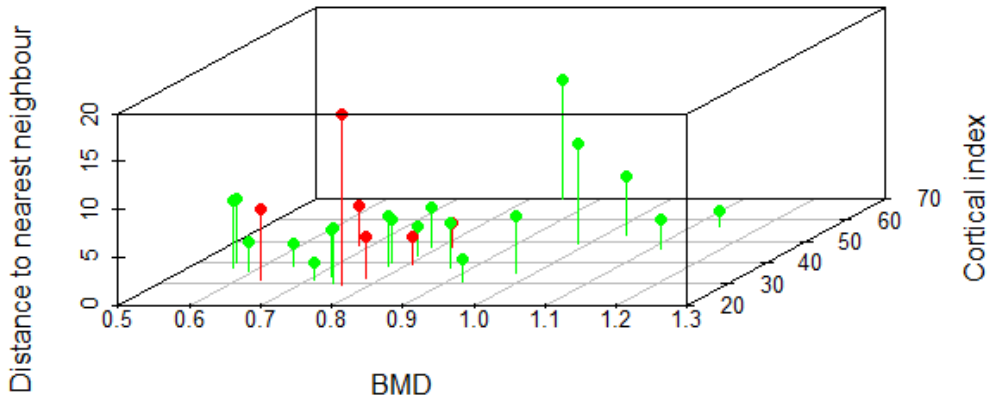

Figure A4.18 and A4.19: The distance from the BMD and cortical index of a bone to the nearest neighbouring bone.
Green dots: accurately reassociated individuals
Red dots: inaccurately reassociated individuals

A4.20 Right femur to left humerus (52%)

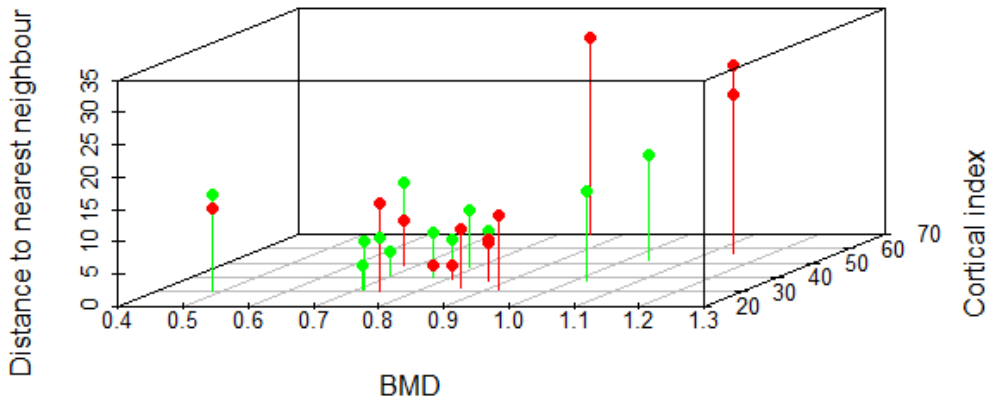

A4.21 Right femur to right humerus (36%)

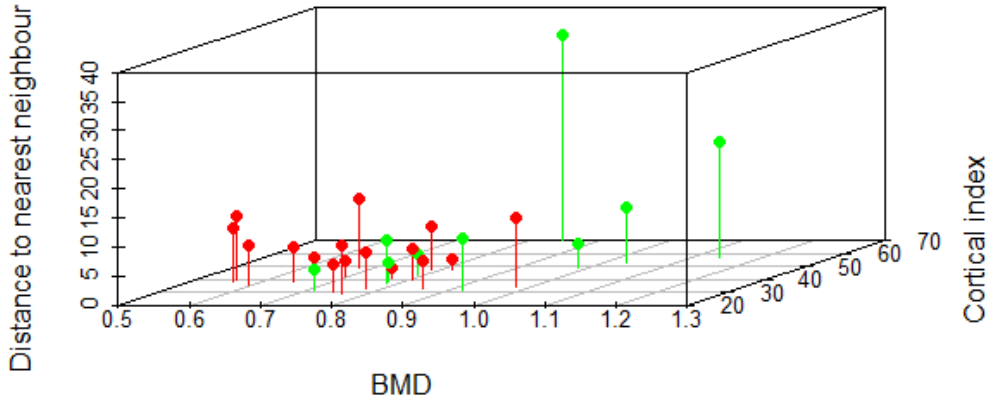

Figure A4.20 and A4.21: The distance from the BMD and cortical index of a bone to the nearest neighbouring bone.
Green dots: accurately reassociated individuals
Red dots: inaccurately reassociated individuals

A4.22 Left humerus to left femur (44%)

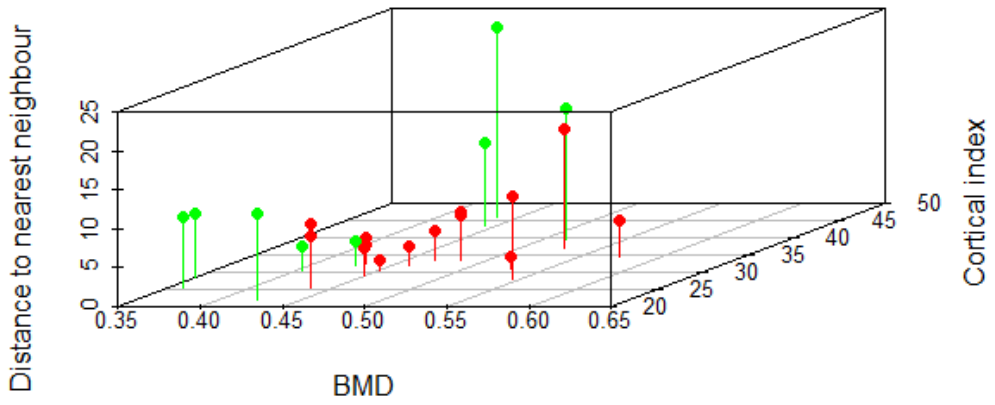

A4.23 Left humerus to right femur (40%)

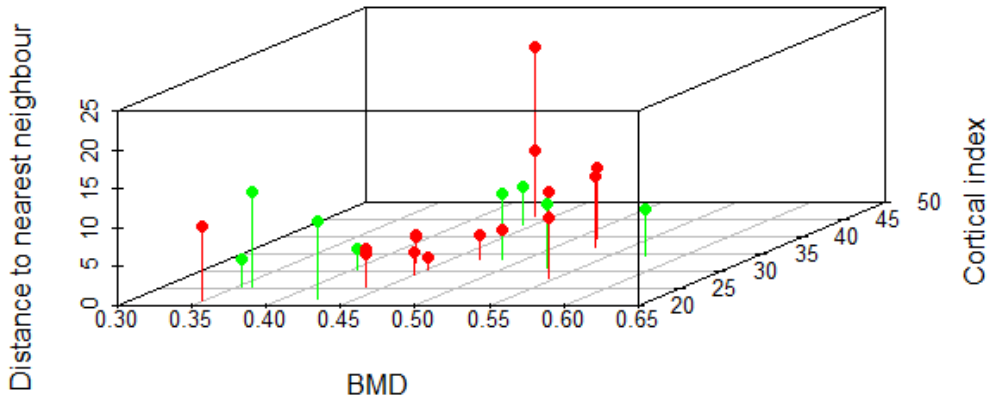

Figure A4.22 and A4.23: The distance from the BMD and cortical index of a bone to the nearest neighbouring bone.
Green dots: accurately reassociated individuals
Red dots: inaccurately reassociated individuals

A4.24 Left humerus to right humerus (40%)

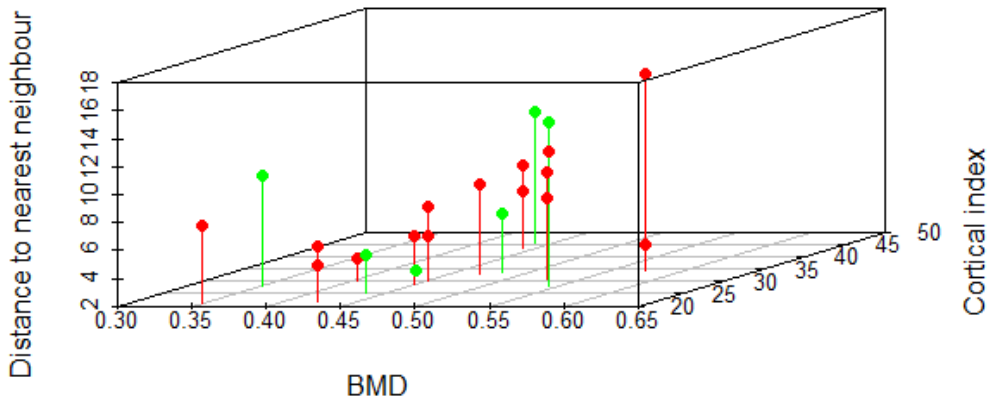

A4.25 Right humerus to left femur (48%)

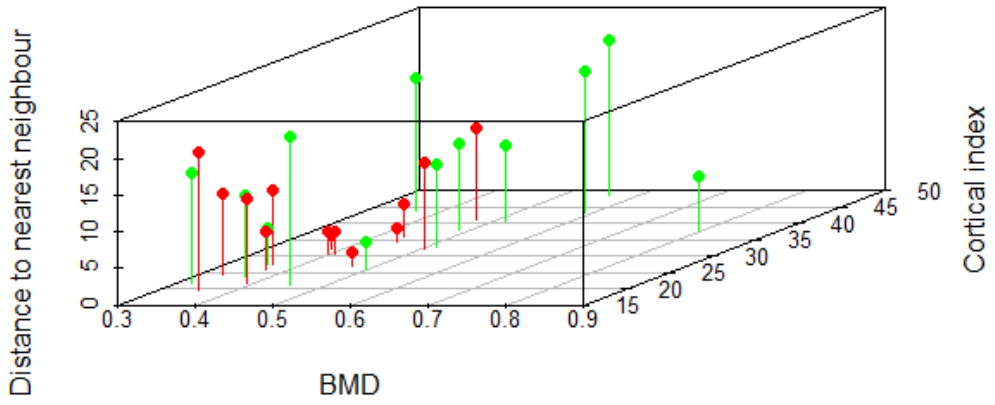

Figure A4.24 and A4.25: The distance from the BMD and cortical index of a bone to the nearest neighbouring bone.
Green dots: accurately reassociated individuals
Red dots: inaccurately reassociated individuals

A4.26 Right humerus to right femur (36%)

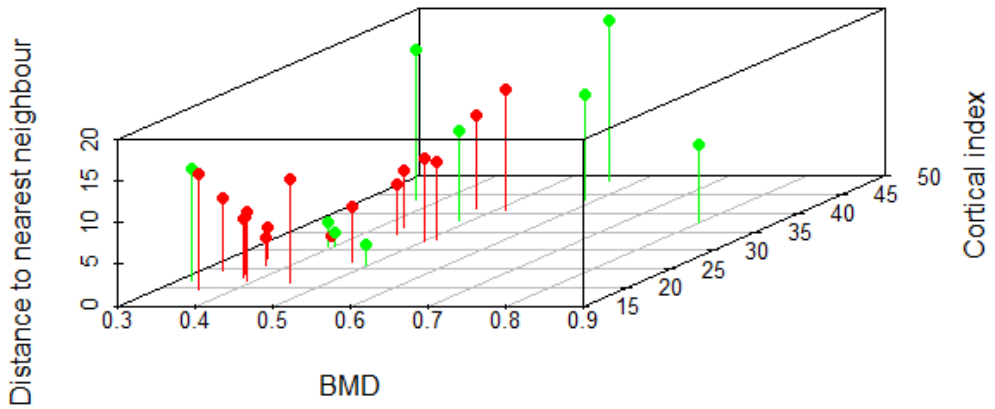

A4.27 Right humerus to left humerus (52%)

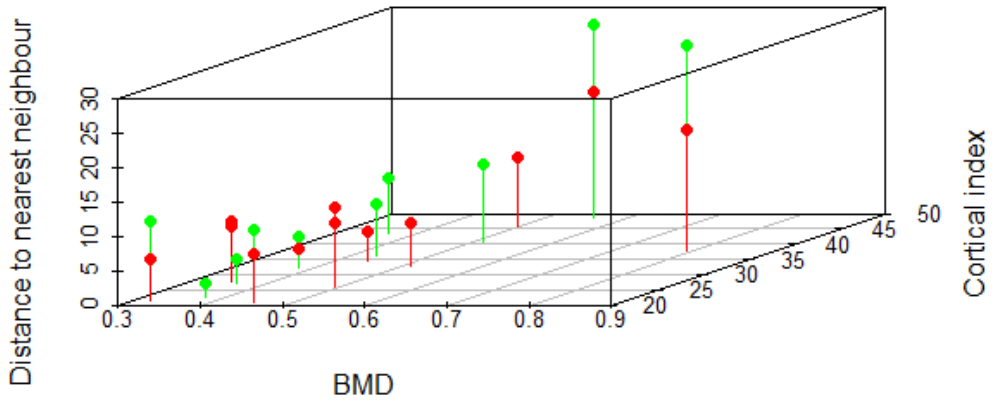

Figure A4.26 and A4.27: The distance from the BMD and cortical index of a bone to the nearest neighbouring bone.
Green dots: accurately reassociated individuals
Red dots: inaccurately reassociated individuals

Bone mineral density (BMD) - groups of ten

A4.28 Left femur to right femur (37,50%)

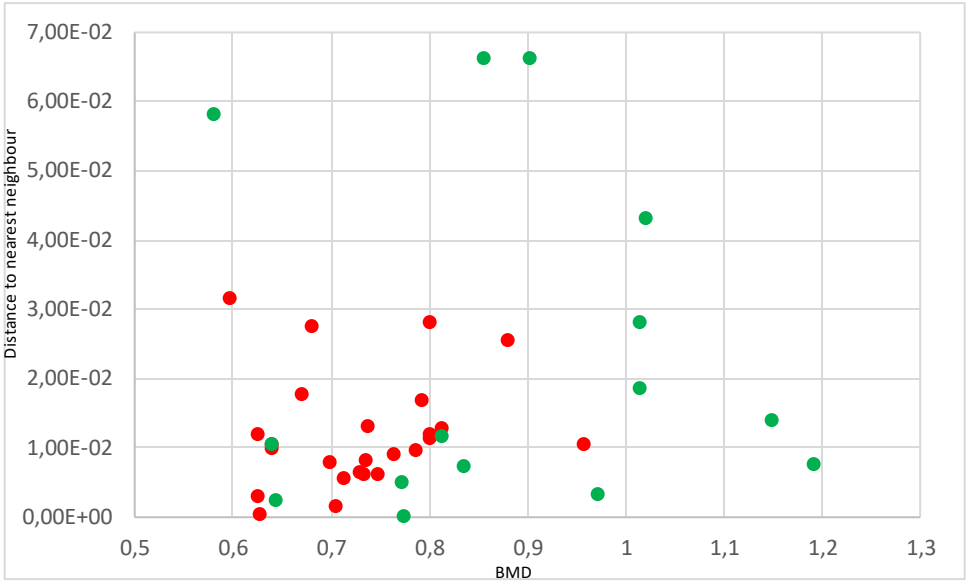

Figure A4.28: The distance from the BMD of a bone to the nearest neighbouring bone.
Green dots: accurately reassociated individuals
Red dots: inaccurately reassociated individuals

Cortical index - groups of ten

A4.29 Left femur to right femur (34%)

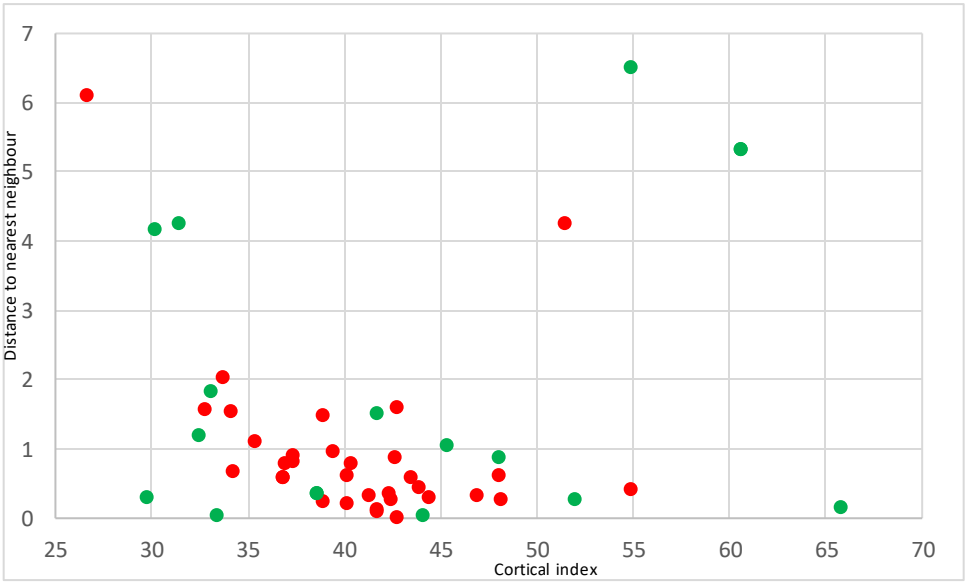

Figure A4.29: The distance from the cortical index of a bone to the nearest neighbouring bone.
Green dots: accurately reassociated individuals
Red dots: inaccurately reassociated individuals

The BMD and cortical index combined- groups of ten

A4.30 Left femur to right femur (47,50%)

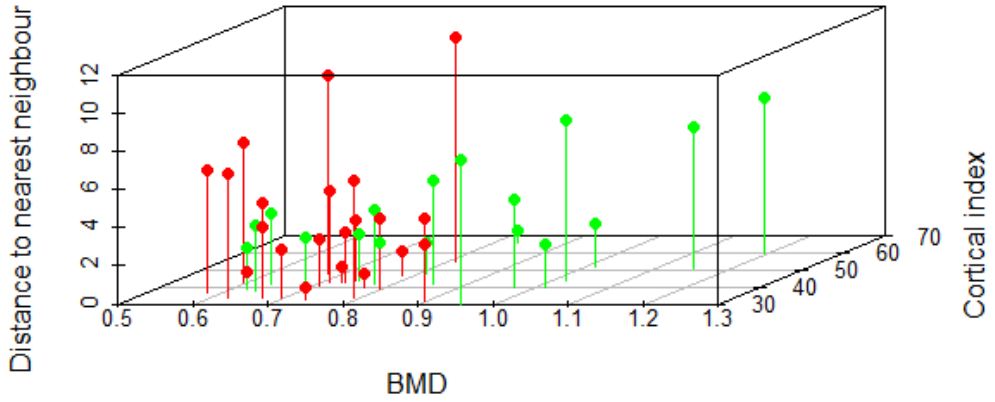

A4.31 Left femur to left humerus (35%)

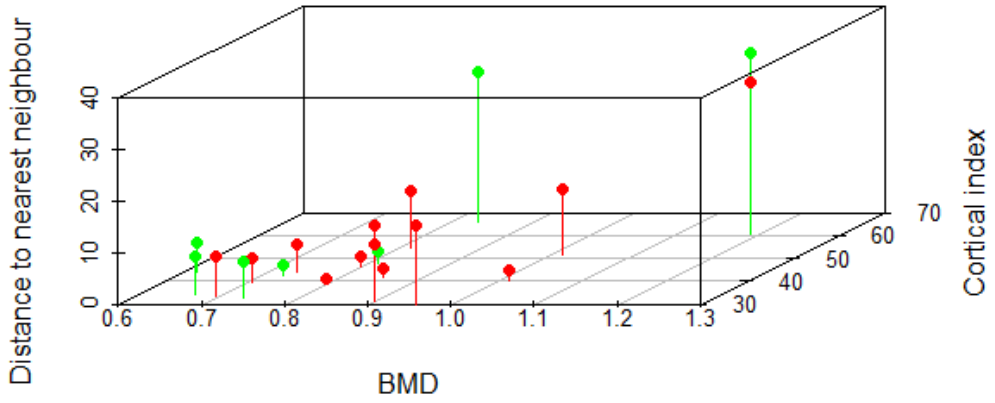

Figure A4.30 and A4.31: The distance from the BMD and cortical index of a bone to the nearest neighbouring bone.
Green dots: accurately reassociated individuals
Red dots: inaccurately reassociated individuals

A4.32 Right femur to left femur (47,5%)

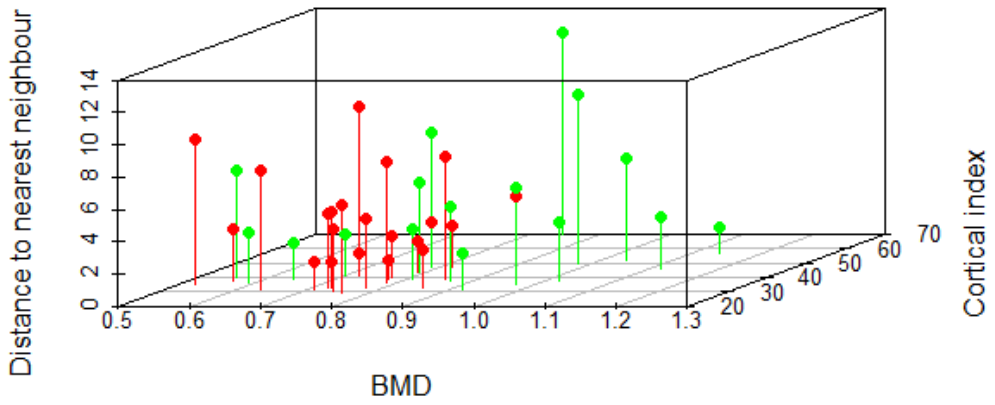

A4.33 Right femur to left humerus (35%)

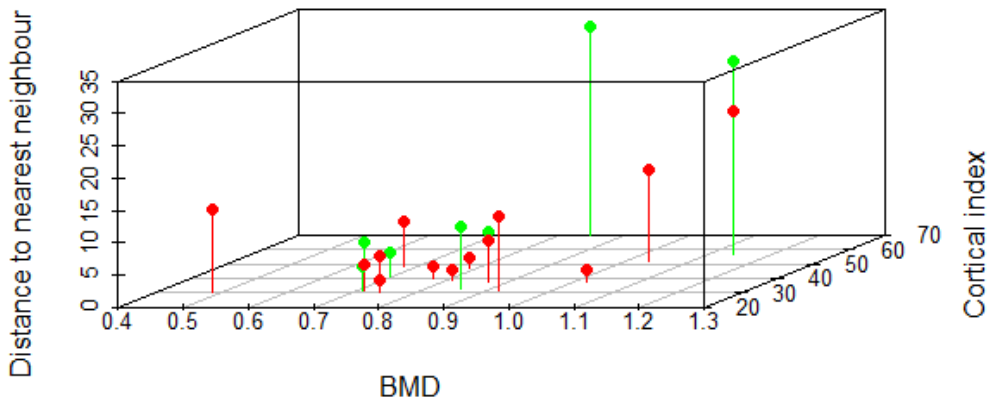

Figure A4.32 and A4.33: The distance from the BMD and cortical index of a bone to the nearest neighbouring bone.
Green dots: accurately reassociated individuals
Red dots: inaccurately reassociated individuals

A4.34 Right femur to right humerus (33,33%)

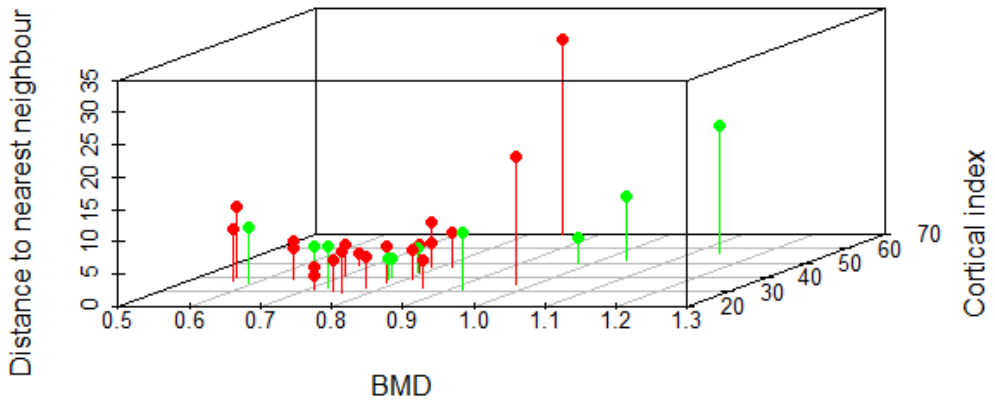

A4.35 Left humerus to right humerus (40%)

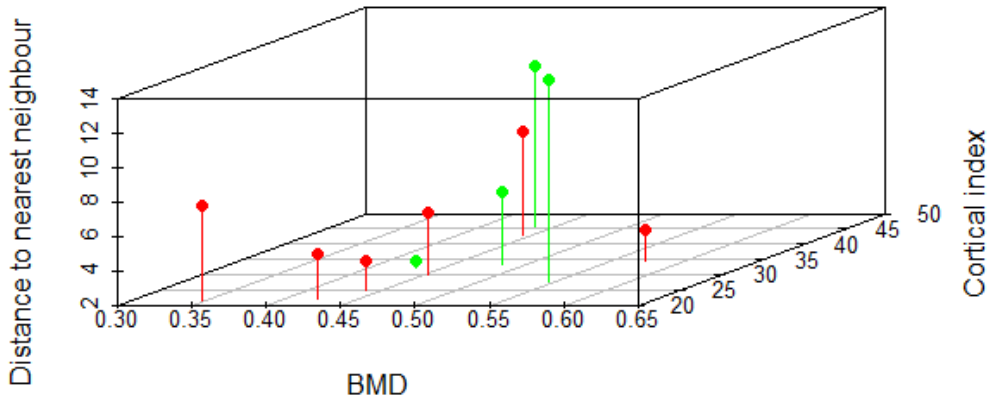

Figure A4.34 and A4.35: The distance from the BMD and cortical index of a bone to the nearest neighbouring bone.
Green dots: accurately reassociated individuals
Red dots: inaccurately reassociated individuals

A4.36 Right humerus to right femur (36,67%)

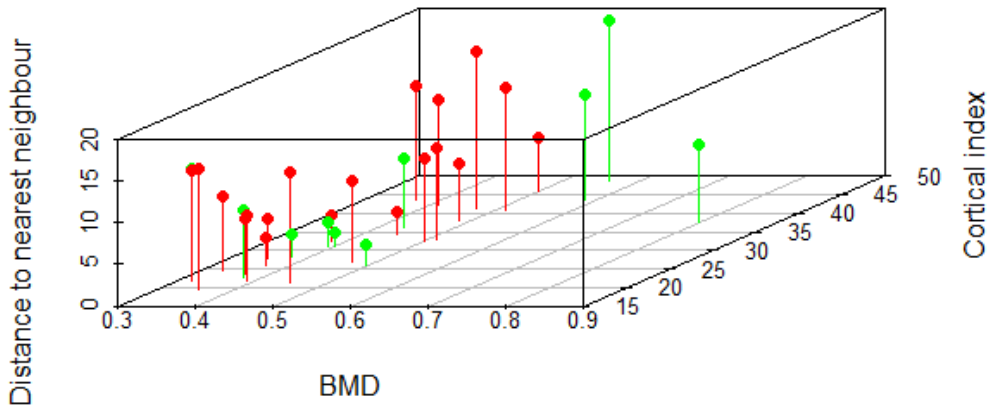

A4.37 Right humerus to left humerus (40%)

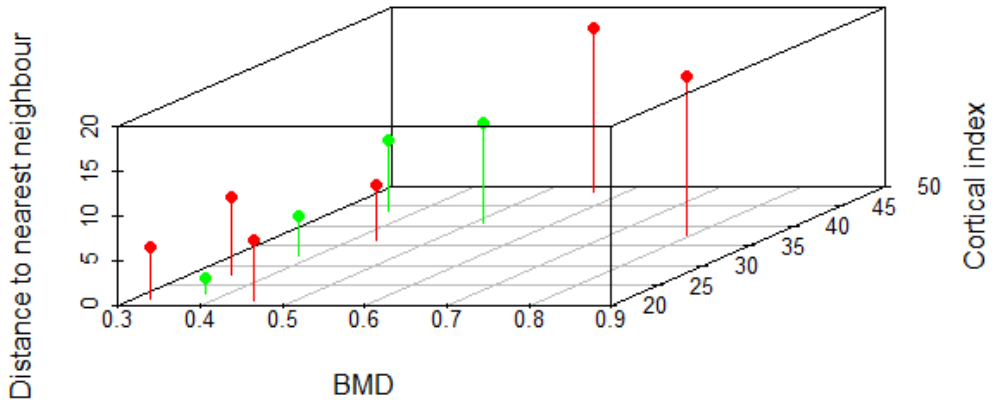

Figure A4.36 and A4.37: The distance from the BMD and cortical index of a bone to the nearest neighbouring bone.
Green dots: accurately reassociated individuals
Red dots: inaccurately reassociated individuals

The BMD and cortical index combined- groups of fifteen

A4.38 Left femur to right femur (43,33%)

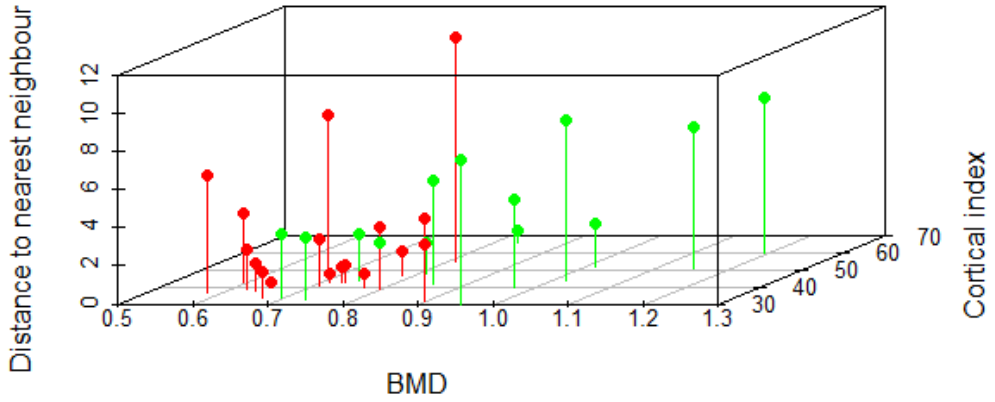

A4.39 Right femur to left femur (36,67%)

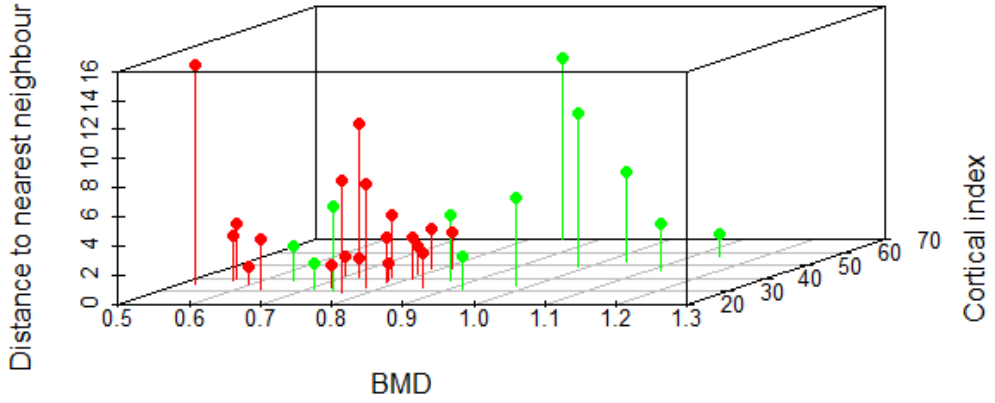

Figure A4.38 and A4.39: The distance from the BMD and cortical index of a bone to the nearest neighbouring bone.
Green dots: accurately reassociated individuals
Red dots: inaccurately reassociated individuals